University of Stavanger

Faculty of Science and Technology

MASTER'S THESIS

Study program/ Specialization: Offshore Technology-Marine and Subsea Technology	Spring semester, 2015 Restricted access
Writer: Karar Abu Kalal	…………………………………………. (Writer's signature)
Faculty supervisor: Adjunct Professor Ljiljana D. Oosterkamp External supervisor(s): Redion Kajolli, Wood Group Kenny Norge AS	
Thesis title: Structural integrity assessment of shackle in subsea tether arrangements	
Credits (ECTS):30	
Key words: Structural Analysis Corrosion on Shackle Finite element Fatigue Analysis	Pages: … 72………… + Appendix: 69…… Stavanger,15.06.2015………….. Date/year

ABSTRACT

Inspection images gives an impression that the H-link shackles are subjected to a combination of pitting, crevice and fretting corrosion. All these relate to localized corrosion. There are several coating breakdowns areas and which might be experiencing severe corrosion. However the difficulty of detecting material degradation and uncertainty/variance of corrosion pattern proves difficult for providing a generalized guideline for the integrity assessment of similar types of systems

The overall goal of this study was to find out how corrosion effect the structural integrity if the shackle connected to a tether system. The theory part of the report includes a study of basic different types of corrosion, contact mechanism, and detecting yielding and fatigue under different corrosion condition. This was done by drawing a first model represent the fabricated shackle .This model is used to observe how the shackle react to the forces prior of any corrosion. The method used to simulate the corrosion was to change the dimension of the shackle according to the amount of material lost. A third model was made to demonstrate the effect local corrosion combined with uniform corrosion. A numerical and analytical analysis was done to compare the results.

The crack formation is the most critical one, showing that the number of cycles to failure is greatly reduced and the pin loses 90 percent of its capacity. This means that if the shackle in field is design to withstand 20 year in service life. The shackle can fail in 2 year in presence if cracks according to the results obtained in this work

PREFACE

This master thesis is written by Karar A. Kalal during the spring of 2015 at the University of Stavanger. In November 2015 .I contacted Associate Professor Sudath C. Siriwardane who works at University of Stavanger and asked if they had any subjects I could look into for my thesis. We had a meeting where we discussed possible subjects and came to the conclusion that a study how corrosion can affect the integrity of the structure. The title of the master thesis became “Structural Integrity Assessment of Components in Subsea Tether Arrangement”. The purpose of the study is to assess the structural integrity of the tether shackles utilized in subsea environment and subjected to material degradation/corrosion. The tool used for the thesis was ANSYS v15 that is widely used in the industry, thus it was a good opportunity to get familiar with such tool. In the start a lot of time was spent to get familiar with the program learning tutorials online. Before starting, I had to read and learn how to model and preform structural analysis on Ansys. The well-known “trial and error method” was frequently used. Although most of the results were incorrect in the beginning I learned a lot from it. Different model were used to reach the final result. I would like to give a special thanks to Adjunct Professor Ljiljana D. Oosterkamp and my Associate Professor Sudath C. Siriwardane .Another person that deserves acknowledgement is Redion Kajolli for guiding trough the thesis and Josip Dragan Bogdanovic for helping me with ANSYS and the thesis in general.

TABLE OF CONTENTS

List of tables viii

List of figures x

List of symbols xii

1 Introduction 1

1.1 Objective 1

1.2 Limitation 2

2 Problem statement 3

2.1 Corrosion 3

2.2 Why metal corrodes 3

2.3 Electro-Chemical corrosion in water: 4

2.4 Recognizing the forms of corrosion 6

2.4.1 Uniform corrosion 6

2.4.2 Pitting corrosion 6

2.4.3 Crevice corrosion 7

2.4.4 Fretting corrosion 9

2.4.5 Corrosion fatigue 9

2.5 Mitigation 10

2.5.1 Pitting corrosion 10

2.5.2 Crevice corrosion 10

2.5.3 Fretting corrosion 11

2.5.4 Corrosion fatigue 11

3 THEORIES OF FAILURE 12

3.1 Elasticity/Yielding 12

3.2 Failure criterions 13

3.3 Ductile failure 13

3.3.1 Max shear stress yielding criterion 13

3.3.2 Von Mises Criterion 14

3.4 Brittle material 14

3.4.1 Maximum stress Theory: 14

4 Finite element method 15

4.1 General stress analysis 15

4.1 Solids element 17

5 Fatigue 18

5.1 Constant Amplitude 18

5.2 Fatigue analysis based on SN-Data 19

5.3 Stress concentration 20

5.4 Mean stress effect 21

5.5 Contact fatigue 22

5.5.1 Effect of corrosion on SN-curve 22

6 Fracture mechanics 23

6.1 Stress Analysis for crack 23

6.2 Crack tip plasticity 26
7 Static Analysis 28
7.1 Pin 28
7.2 Padeye 29
7.3 Herzian contact stress 29
7.4 General case of contact of two solids 30
8 Analysis setup in Ansys 32
8.1 Definition of the system 32
8.2 Engineering data 33
8.3 Model description 34
8.3.1 General 34
8.3.2 Models description 34
8.4 Surface Contact Modelling IN ANSYS 36
8.5 Pin and the Pad-eye 37
8.5.1 Pin-head and the pad-eye 37
8.5.2 Mesh 38
8.5.3 Load and boundary condition 39
9 Design basis 40
9.1 Action factors 40
9.1.1 Ultimate limit state 40
9.1.2 Fatigue limit state 40

9.2 Acceptance criteria 41

9.2.1 Yielding 41

10 Result 42

10.1 Verification of the FE model and analysis procedure 42

10.1.1 Pin 42

10.1.2 Padeye 44

10.1.3 Contact area 46

10.2 ULS calculation 47

10.2.1 Model 1 47

10.2.2 Model 2 48

10.2.3 Model 3 49

10.3 Fatigue calculation 49

10.3.1 Pin 50

10.3.2 Padeye 50

10.3.3 Model 1 51

10.3.4 Model 2 58

10.3.5 Model 3 62

11 Discussion of the results 63

11.1 ULS check 63

11.2 Fatigue analysis 65

11.2.1 Analytical Analysis 65

11.2.2 Numerical Analysis 66

11.2.3 Comparison of numerical and analytical results: 67

11.2.4 Load 68

11.3 SN-curve 68

12 Conclusion 69

13 Further work 70

14 Reference 71

Appendix A 1

Appendix B 2

B1 Verification Model 2 2

Appendix C 5

C1 Model 1 5

C2 Model 2 6

C3 Model 3 7

LIST OF TABLES

Table 2-1 Corrosion group 6

Table 8-1 Material properties required for different grade 33

Table 8-2 Corrosion allowance for chain from DNV-OS-E301 35

Table 8-3 Different load cases 39

Table 9-1 Action factor from Norsok N-001 40

Table 9-2 Design fatigue factor 40

Table 10-1 Normal stress for the contact area and pin 46

Table 10-2 Von Mises stress on model 1 47

Table 10-3 Von Mises stress on model 2 48

Table 10-4 Von Mises stress for model 3 49

Table 10-5 Fatigue calculation based on contact shear stress for model 1 52

Table 10-6 Stress ratio between max shear stress and yielding stress 53

Table 10-7 Fatigue calculation based on FEA stress for model 1 54

Table 10-8 Calculation based on concentrated stress near the hole on padeye for model 1 56

Table 10-9 Max principal stress on padeye for model 1 57

Table 10-10 Fatigue analysis based on max principal stress for model 1 58

Table 10-11 Fatigue analysis based on contact shear stress for model 2 58

Table 10-12 Fatigue analysis based on contact shear stress for model 2 59

Table 10-13 Fatigue analysis based on FE max shear stress for model 2 59

Table 10-14 Fatigue analysis based concentrated stress near the hole on padeye for model 2 60

Table 10-15 Max principal stress on padeye for model 2 60

Table 10-16 Fatigue analysis based on max principal stress for model 61

Table 10-17 stress ratio between max shear stress and yielding stress for model 3 62

Table 10-18 Fatigue analysis based on FE max shear stress for model 3 63

LIST OF FIGURES

Figure 2-1 Energy required to convert metal to oxide (Roberge, 2008) 4

Figure 2-2 Reaction of iron in water 5

Figure 2-3 Different pitting corrosion shape (NACE, 2015c) 7

Figure 2-4 Crevice corrosion mechanism (Ahmad & Institution of Chemical, 2006) 8

Figure 3-1 stress strain curve for steel 12

Figure 5-1 Constant amplitude loading (Pook, 2007) 18

Figure 5-2 SN-curve for different environment 20

Figure 5-3 Corrosion effect on the SN-curve 22

Figure 6-1 Different crack mode 23

Figure 6-2 Stresses near the crack (Hearn, 1997) 24

Figure 6-3 Geometry factor Y for different load case(Hearn, 1997) 25

Figure 6-4 Photoelastic fringes for an edge crack(Hearn, 1997) 25

Figure 6-5 plastic zone region in crack (Hearn, 1997) 27

Figure 7-1 Static system for pin 28

Figure 7-2 Herzian contact model (Hearn, 1997) 30

Figure 7-3 Contact geometry for different values of α(Hearn, 1997) 31

Figure 8-1 System description 32

Figure 8-2 Contact between pin and padeye 37

Figure 8-3 Contact between pinhead and padeye 38

Figure 8-4 FE mesh of the shackle 38

Figure 8-5 Load and boundary condition 39

Figure 10-1 Normal stress in x-direction 43

Figure 10-2 Total deformation on the shackle 43

Figure 10-3 Stresses near the hole on padeye 44

Figure 10-4 Contact pressure on the padeye 45

Figure 11-1 Von Mises stress accumulations for different model 64

Figure 11-2 Number of cycles to failure for normal operation in model 1 and 2 66

Figure 11-3 Number of cycles to failure for normal operation 67

LIST OF SYMBOLS

DNV- Det Norske Veritas

FEA –Finite Element Analysis

FE = Finite Element

MBL = Minimum breaking load

C = Perpendicular distance from the natural axis to a point farthest away from the natural axix

E = Modulus of elasticity

F = System load factor

I = Moment of Inertia

K = Intensity factor

K^e= Element stiffness matrix

K^T= System stiffness matrix

L = Length of the pin

M_i = Moment in i position

N = Number of cycles to failure for stress range

N_j = Interpolation functions

P = Load from Chain

R_i = Reaction force in i position

U= System displacement vector

W = Un-cracked specimen width

Y = geometric correction factor

a = length of crack

ā = Intercept of the design S-N-curve with the log (N) axis

f = Nodal displacement vector of the element load vector

j = Ranges over the element's nodes

m = Negative inverse slope of the design S-N-curve

p_o = Maximum contact stress

t = Thickness

u = Nodal displacement of the element

u_j= Node displacement

v = Poisson's ratio

ε = Engineering strain

σ_1 = Maximum principal stress

σ_2 = Minimum principal stress

σ_{ys} = Yield strength

σ_u =Ultimate strenth

$\Delta\sigma$ = The stress range

σ_{max} = Maximum principal stress

σ_{min} = Minimum principal stress

σ_a = Amplitude stress

σ_m = Means stress

σ_{SCF} = Concentrated stress

σ_{yy} = Normal stress in the y direction

σ_{xx} = Normal stress in the x direction

τ_{xy} = Shear stress in x-y plane

σ_{yd} = Design Yield strength

1 INTRODUCTION

The purpose of a Lazy S configured Mid Water Arch is to provide structural support to flexible riser and umbilical's through the use of a cylindrical tank filled with nitrogen to provide buoyancy. The Mid Water Ach system usually consists of a buoyancy tank, steel riser trays, 2 steel chain tethers and a gravity-based anchor structure. The riser trays on top of the buoyancy tank provide support for the riser during operation. The trays are designed so that the minimum bending radius of the riser is never violated, taking spatial bending into consideration. Under the buoyancy tank there are two hinged tether connections that act as bridles. A triangular tether connection frame connects the buoyancy tank to the tether chains, which again are connected to the anchor structure via H-link shackles and a delta-plate. The tethers are prevented from having electrical contact with the buoyancy tank and the anchor structure by bushings in tether connection frame (at mid waters) and in the pad eyes (at the anchor base). The tether components are designed with corrosion allowance. Inspection images gives an impression that the H-link shackles are subjected to a combination of pitting, crevice and fretting corrosion. There are several coating breakdowns areas which might be experiencing severe corrosion. However the difficulty of detecting material degradation and uncertainty/variance of corrosion pattern proves difficult for providing a generalized guideline for the integrity assessment of similar types of systems

1.1 OBJECTIVE

The objective of this thesis is to look at the structural integrity of the tether shackle in the subsea environmental and subjected to material corrosion. It is important to estimate remaining load capacity and the service life of the tether shackles. The design consists of stress analysis (yielding) and evaluation of the design life, fatigue. The Fatigue life is checked by using DNV-RP-203 in combination with a given design load spectrum. Based on their boundary condition and assumption, calculation of yielding and fatigue will be performed on the shackle. Another purpose of this thesis was to be familiar with finite element software and to understand the structural analysis and design methodology.

1.2 LIMITATION

The main uncertainty if the model is that it is uniform and based on the particular size of crack. It does not take into account the progression of the corrosion processes .the same is for crack extension and wear between the contact surfaces. To take all these effects into account some of these conditions, the life of the shackle should be determined taking into account not only SN-curve but fracture mechanics. The purpose of such analysis is to document, by means of calculations, that fatigue cracks, which might occur during service life, will not exceed the crack size corresponding to unstable fracture. DNV-RP-C203 has guideline such as using Paris equations to determine the life of the component with crack initiation .This method take into account the crack expanding during service life unlike model 3 where we assumed a particular size of crack.

The university license have a restricted number of mesh in the model, which makes it difficult to do the sensitivity analysis due change in stresses as a function of mesh density. There are some function named inflation on Ansys making the contact results more accurate. But it required a dens mesh making it not possible to use. This leads us to presume that the model is right, and the stresses is precise

2 PROBLEM STATEMENT

2.1 CORROSION

Corrosion has a highly damaging effect on the integrity and the fatigue strength of the structure mainly because of the progressive metal loss. Uniformly corroded surface areas are taken care of by a corrosion allowance or coating in the design of structural components. However, it is the concentrated corrosion like pits, crevice and fretting with more severe metal loss that are more critical when it comes to fatigue. The rough shape of corrosion damage and the stress concentration may lead to very critical stress due to the stress concentration (Roberge, 2008).

The definition of corrosion is deterioration of material by chemical reactions with the environment. A process produces a less desirable material from its origin and can damage the functionality of the component or system. The term is most commonly used for iron as production of rust witch form on the surface of steel. Another form of corrosion can have no sign of the deterioration, however properties change which can lead to material failure.(Roberge, 2008).Corrosion is a vast of the problems in the offshore industry, and large sums of money each year is set for inspections and repairs because of corrosion. As metals are always searching back to a smaller energy state, the corrosion product can be a combination of oxides and salts of the original metal (Szary, 2006).

2.2 WHY METAL CORRODES

The driving force causing the metal to corrode is the consequence of their existence in oxide form. To create metals, providing their existence as minerals and ions with a certain amount of energy is necessary. In steel production, iron is separated from its associated oxygen in the blast furnace, a process which needs a huge amount of energy which is shown in Figure 2-1 .When steel rusts, energy is released and the metal returns to its natural state (oxide) and the cycle is complete. When iron is in a metal state it can therefore be consider as being in a metastable state and has a desire to lose its energy to convert back to its original states.

The energy required varies from metal to metal, for metals such as magnesium, aluminum and iron the levels are very high(Roberge, 2008).Figure 2-1 illustrate the amount of energy required to convert them from their oxides to metal.

	Metal	Oxide	Energy (MJ kg^{-1})
Highest energy	Li	Li_2O	40.94
	Al	Al_2O_3	29.44
	Mg	MgO	23.52
	Ti	TiO_2	18.66
	Cr	Cr_2O_3	10.24
	Na	Na_2O	8.32
	Fe	Fe_2O_3	6.71
	Zn	ZnO	4.93
	K	K_2O	4.17
	Ni	NiO	3.65
	Cu	Cu_2O	1.18
	Pb	PbO	0.92
	Pt	PtO_2	0.44
	Ag	Ag_2O	0.06
Lowest energy	Au	Au_2O_3	-0.18

Figure 2-1 Energy required to convert metal to oxide (Roberge, 2008)

2.3 ELECTRO-CHEMICAL CORROSION IN WATER:

Electrochemical reaction is defined as a chemical reaction which contains transportations of electrons. An electro chemical reaction includes an oxidation and reduction. At the anode, the reaction which take place is oxidation of the area where the metal is lost. Typical for the anode is the entry of metal ion into the solution and release of electrons which flow through the metal to react at the cathode area(Ahmad & Institution of Chemical, 2006). Electrons are exposed to the environment where they restore the electrical balance and are removed from the metal. The reaction rate at the anode and cathode must be equivalent according to faraday law, which is called corrosion current , Ia = I c (Roberge, 2008).The following is a simplified mechanism of corrosion in water:

Anode reaction:

$$Fe = Fe^{2+} + 2e \qquad \text{Eq. 2-1}$$

Water itself dissolves to produce equal quantities of H^+ and OH^- ions displayed in the following equilibrium:

$$H_2O \rightleftarrows H^+ + OH^- \qquad \text{Eq. 2-2}$$

Cathode reaction:

$$2H^{+} + 2e \rightarrow H_2 \qquad \text{Eq. 2-3}$$

Or

$$\mathrm{H_2O} + \frac{1}{2}\mathrm{O_2} + 2\mathrm{e} \rightarrow \ 2\mathrm{OH^-} \qquad \text{Eq. 2-4}$$

The OH ions react with the Fe^{++} ions produced at the anode

$$\mathrm{Fe^{2+}} + 2\mathrm{OH^-} \rightarrow \mathrm{Fe(OH)_2} \qquad \text{Eq. 2-5}$$

In different environments, corrosion happens only if dissolved oxygen is present. Dissolved oxygen from the air is the basis of oxygen required in the corrosion process. Repeated accumulation multiplies solid corrosion which comes from interactions between anode and cathode products. Iron combines with water and oxygen to produce an insoluble reddish-brown corrosion product which dissolves form the solution (Roberge, 2008).

$$\mathrm{Fe(OH)_2} + \mathrm{O_2} + 2\mathrm{H_2O} \rightarrow 4\mathrm{Fe(OH)_3} \qquad \text{Eq. 2-6}$$

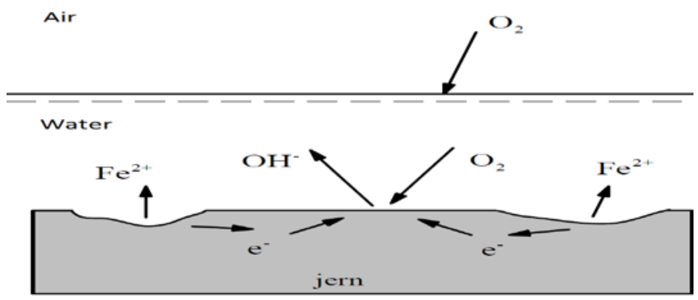

Figure 2-2 Reaction of iron in water

Figure 2-2 shows the anodic and cathodic reactions happening at several areas of the surface. In seawater, the salts ((NaCL, MgCl), dissolve and provide electrolyte with better conductivity. This makes the corrosion process run faster in saltwater.

2.4 RECOGNIZING THE FORMS OF CORROSION

A variation of corrosion problems considered in the industry is a result of the combination of materials, environment and service conditions. The corrosion may not instantly harm the material, but can effects the strength, shape, operation. To identify type and environment is very important, classifying potential hazard with method to mitigate the attacks is important for the design (Ahmad & Institution of Chemical, 2006).

Many types of corrosion can be found by visual examination to decide which mechanism has contributed to the degradation of the metal. In the widely used NACE document, three groups of corrosion have been classified (Roberge, 2008).This thesis will be devoted mostly to the localized corrosion.

Table 2-1 Corrosion group

Group	Description
Group 1	Identifiable by visual inspection
Group 2	Identifiable with special inspection tool
Group 3	Identifiable by microscopic examination

2.4.1 Uniform corrosion

Uniform corrosion, as the name implies, occurs on the majority of the surface of a metal at a steady and expected rate. It is the corrosion type that gives the biggest weight loss which is a common sight when the metal is abounded without any service. From visual inspection, it is usually not an issue to detect the uniform attack and its effect, hence it is deemed to be less troublesome than other corrosion type unless the corroding material is hidden from sights.

2.4.2 Pitting corrosion

Most common type of localized corrosion is pitting where a small volume of metal has been removed leading to the creation of cracks or pits. The driving force for pitting corrosion is the change of condition within a small area, which then becomes anodic whilst an unknown area becomes cathodic, leading to localized corrosion. Pitting corrosion may occur on a metal surface in a stagnant or slow moving liquid. It can be more dangerous than uniform, considering it is hard to detect because of corrosion products often cover the pits). Pitting corrosion can be formed as an open hole (uncovered) or covered with a thin layer of corrosion products. Pits can be either hemispherical or cup-shaped. In Figure 2-3 illustrate pitting corrosion in its different shapes(Roberge, 2008).Pitting corrosion is initiated by:

- Localized chemical or mechanical damage to the protective oxide film
- Localized damage to, or poor application of, a protective coating
- The presence of non-uniformities in the metal structure of the component, e.g. non-metallic inclusions.

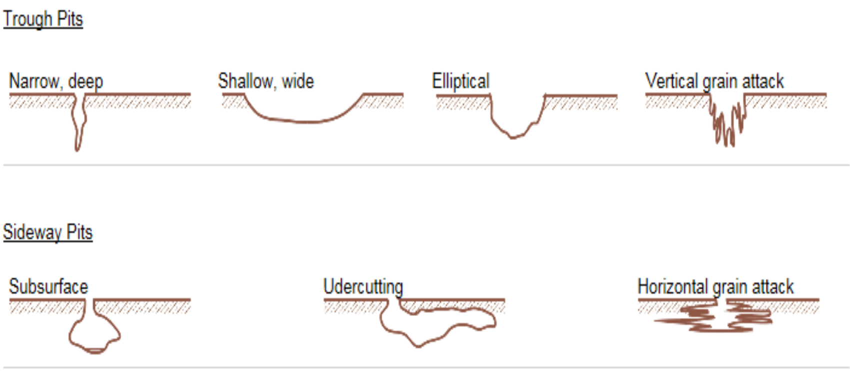

Figure 2-3 Different pitting corrosion shape (NACE, 2015c)

2.4.3 Crevice corrosion

Crevice corrosion is a type of localized corrosion which occurs in existing voids and gaps or between mating surfaces of metal components. It can also happen under surface deposits below loose fitting seals that fail to block entry of liquid between them. It is one of the most common forms and at the same time one of the most dangerous ones. (Roberge, 2008). It occurs in areas which normally have a good corrosion resistance and are not immediately visible. A high concentration of oxygen on the surface outside the crevice and low oxygen concentration inside creates differential aeration cells. The following reaction takes place:

Anode (in the crevice)

$$M \rightarrow M^{++} + 2e \ \ (M = \text{metal}) \qquad \text{Eq. 2-7}$$

Cathode:

$$M \rightarrow M^{++} + 2e \ \ (M = \text{metal}) \qquad \text{Eq. 2-8}$$

Dissolved oxygen in the liquid, present deep in the crack, is used up by reaction with the metal. As oxygen into the crevice is limited, a differential cell tends to be set up between the crevice microenvironment and the external surface. The corrosion now occurs in the crevice (anode) but the concentration of oxygen at the cathode (surface) remains unchanged.

The cathodic oxidation reaction cannot be maintained in the crevice area, giving it an anodic behavior in the concentration cell. This can lead to the creation of highly corrosive micro-environmental conditions in the crevice, conducive to further metal loss. This creates an acidic microenvironment, together with a chloride ion concentration.(Roberge, 2008).

To preserve electro neutrality, the chloride ions are attracted by the metal ions and metallic chlorides are formed:

$$\mathrm{Cr^{+++} + 3Cl^- \rightarrow CrCl_3} \qquad \text{Eq. 2-9}$$

$$\mathrm{M^{++} + 2Cl^- \rightarrow MCl_2} \qquad \text{Eq. 2-10}$$

With creation of metallic chlorides , the condition of anode dissolution continues and the crack become larger(Ahmad & Institution of Chemical, 2006).

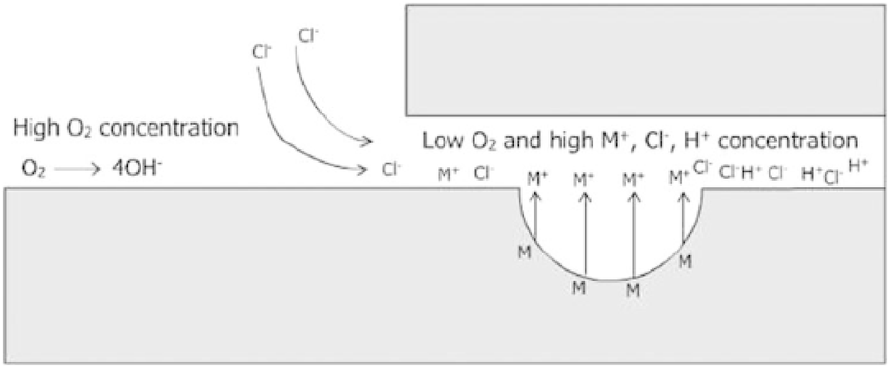

Figure 2-4 Crevice corrosion mechanism (Ahmad & Institution of Chemical, 2006)

2.4.4 Fretting corrosion

The ASM Handbook on Fatigue and Fracture defines fretting as: "*A special wear process that occurs at the contact area between two materials under load and subject to minute relative motion by vibration or some other force.* » Fretting is associated with corrosion damage at the contact surfaces. Cracks and grooves are typically found in machinery, bolted connections, and bearings. The failure occurs at the highly loaded contact surfaces which are not designed for dynamic motion against each other. The protective layer at the metal surface is worn away by rubbing action, which becomes available for corrosion activity. Condition for occurrence of fretting is (1) the interface must be subjected to load, (2) vibration or furcation motion of small amplitude that makes surfaces grinds each other (Roberge, 2008). The result of fretting corrosion is:

- Metal loss in the connection area
- Production of oxide debris
- Galling , Seizing, or cracking

2.4.5 Corrosion fatigue

Corrosion fatigue is fatigue in corrosive environment and results in a degradation of material under alternating or cycles loading. It starts with destruction of protection coating, which causes corrosion to accelerate. If the metal instantaneously defers to a corrosive environment, the failure can occur lower loads. Compared to classic fatigue, there is no fatigue limit load in corrosion-assisted fatigue. A lower failure stresses and smaller number of cycles to failure can happen in a corrosive atmosphere compared to the situation where corrosion does not present a hazard. (NACE, 2015a)

2.5 MITIGATION

The type of corrosion is generally triggered by one or more factors and conditions. Some of the types of corrosion are describe by local effect and the mitigation start by taking into account how to decrease these factors and local cells.

2.5.1 Pitting corrosion

Pitting corrosion occurs in materials that have a protective layer which breaks down. The metal reacts more easily with the environment .Since the pitting corrosion is an electro-chemical process, it can be mitigated by cathodic protection, or by using of inhibitors to change the electrode reaction of the local cell and remove their driving force. It can also be prevented by coating the surface with a layer to protect the metal, such as Zink-rich paint. Other method can be used, such as (Nimmo & Hinds, February 2003):

- Ensuring a high enough flow velocity of fluids in contact with the material or frequent washing
- Control of the chemistry of fluids and use of inhibitors
- Use of a protective coating
- Maintaining the material's own protective film.

2.5.2 Crevice corrosion

Crevice corrosion is prevented in the planning phase by filling not corroded dry crevices with a durable jointing compound that will exclude moisture and remain resilient. The potential for crevice corrosion can be reduced by(Nimmo & Hinds, February 2003):

- Avoiding sharp corners and designing out stagnant areas
- Use of sealants
- Use welds instead of bolts or rivets
- Select a resistant material

2.5.3 Fretting corrosion

Fretting corrosion can be avoided by removing any slipping motions between two surfaces. It is also possible to overcome fretting by increasing the friction load on the surface to prevent the movement. Other methods which can be used are(Nimmo & Hinds, February 2003):

- Avoiding vibrations
- Lubrication of metal surfaces with oil or grease
- Surface treatment to decrease wear and increase friction

2.5.4 Corrosion fatigue

The combined action of cyclic stresses and a corrosive atmosphere reduce the lifetime of components. This can be reduced or prevented by(Nimmo & Hinds, February 2003):

- Coating the material
- Good design that reduces stress concentration avoiding sudden changes of the cross section
- Reducing of cyclic stress

3 THEORIES OF FAILURE

When designing a material it is important to determine the limit that defines material failure. The material is often categorized in two groups, ductile and brittle. The ductile material is specified with yielding (plastic deformation) which may cause a permanent deflection. Whereas if the material is brittle it is specified with fracture(Boresi & Schmidt, 2003). Structural steel has a ductile behavior but if the material contains a large enough crack, it can become brittle.

3.1 ELASTICITY/YIELDING

Stress and strain curve is created from tensile test results, and show constitutive relation between stress and strain. The curve is plotted using calculated stress and corresponding strain obtained from the reference length and cross-section. There are serval regions in the stress-strain curve illustrated in the

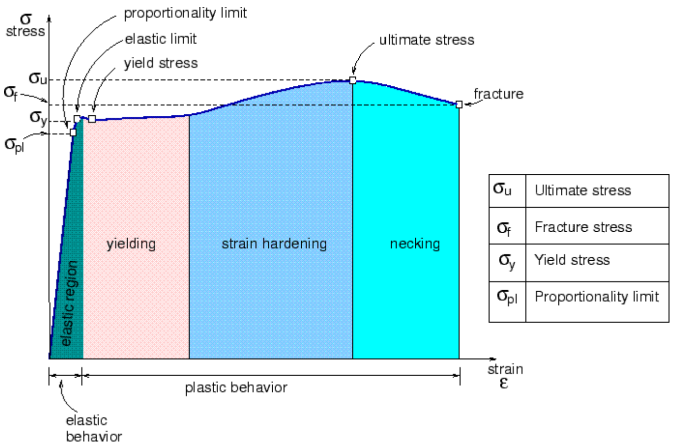

Figure 3-1 stress strain curve for steel

In the elastic region, stress is linearly proportional to strain, and it can be seen that the curve is almost a straight line. The relation in this line can be described mathematically by young modulus according to Hooke Law where stress is:

$$\sigma = E \cdot \varepsilon \qquad \text{Eq. 3-1}$$

The upper stress limit in this linear relation is called proportional limit, σ_{pl}. A material deformed beyond this point of stress is no longer proportionate to the strain. Most structures are designed to not exceed the elastic deformation. Increasing the stress above the elastic limit will caused yielding. In this region there will be large increase in strain with little increase in stress. Plasticity is also important as an energy-absorbing mechanism for structures in service(MacDonald, 2007).

3.2 FAILURE CRITERIONS

A failure criterion considers whether a state of stress will result in yielding or fracture in an isotropic material. In order to select a failure criterion, the designer has to find out if the fracture is brittle or ductile. Selection of failure criteria depends not only on the type of material, but also on other conditions, such as material properties. A temperature reduction can also transform the material from ductile to brittle (Hibbeler & Fan, 2008).Failure criteria are just rules of design to provide a good approximation to observed material behavior, and usually restricted to linear elasticity. No criterion is best under all circumstances. Different conditions as high material temperatures and hydrostatic pressure can transform the materials from brittle to ductile.

3.3 DUCTILE FAILURE

If the material is subjected to large strain before its rapture is called ductile material. It's often choses because the ability absorbed a large amount of energy and can embrace large deformation before failing. Ductile failure initiate with yielding witch mean slipping with material, but not fracture. Commonly used criteria in multi-dimensional state of stress are the Maximum Shear-Stress Theory and Von Mises criterion (Hibbeler & Fan, 2008).

3.3.1 Max shear stress yielding criterion

The maximum shear yielding criterion considers yielding of member exposed to two or three axial state of stress and when the maximum shear stress at a point reaches the value of the shear stress capacity in subjected only in axial tension. The failure under combine stresses can be defined as :

$$\sigma_{\max} - \sigma_{\min} = \sigma_{ys} \qquad \text{Eq. 3-2}$$

Where σ_{max} and σ_{min} are the maximum and minimum principal stress. It's important to note that if the case $\sigma_1 > \sigma_2 > \sigma_3$ the failure criterion would be: (Pilkey, 1994)

$$\sigma_1 - \sigma_2 = \sigma_{ys} \qquad \text{Eq. 3-3}$$

3.3.2 Von Mises Criterion

When a material is exposed to external loading, it tends to absorb the energy internally throughout its volume. The energy per unit volume of the material is called the strain energy density. The Von Mises theory depends on the strain energy which is distributed in the material and not the one which enlarges the volume. The criterion state that the failure happens when the energy reaches the same energy for failure in under axial loading. That is failure takes place when the principal stress is (Hibbeler & Fan, 2008):

$$(\sigma_1 - {\sigma_2}^2) + (\sigma_2 - {\sigma_3}^2) + (\sigma_1 - {\sigma_3}^2) = 2\sigma_{ys} \qquad \text{Eq. 3-4}$$

This criteria does not regard to the direction or the relative magnitude of $\sigma_1, \sigma_2, \sigma_3$ .Its commonly referred as to the equivalent stress. Yield boundary may be constructed using the Eq.3-4, which takes the shape of an ellipse. Inside the surface, materials undergo elastic deformation. Approaching the boundary means the material experiences plastic deformations. It is physically impossible for a material to go beyond its yielding.

3.4 BRITTLE MATERIAL

Materials that show no yielding before failure are known as brittle materials. Brittle materials absorb relatively little energy before fracture and there is small or no evidence of plastic deformation. (Hibbeler & Fan, 2008)

3.4.1 Maximum stress Theory:

In the maximum stress theory stress is chosen as the criterion failure. The failure can be determined by yielding or stress level such as ultimate stress. According to this theory failure happened induced in a material under complex load when the max principal stress reteaches the uniaxial strength. Smaller principle stress has no effect on the yielding. Failure criteria in which the equivalent stress is a vector are usually known as critical plane approaches. For material with the same properties in compression and tension the failure condition can be expressed as(Pilkey, 1994):

$$\sigma_1 = \sigma_{ys} \text{ or } [\sigma_3] = \sigma_{ys} \qquad \text{Eq. 3-5}$$

4 FINITE ELEMENT METHOD

The finite element method divides the structure into small elements held together by nodes. Given the applied loads, finite element equations solve the displacements at the nodes with different degrees of freedom. The displacement on the nodes determine the stress and strain in each element .The equation is expressed as :(Cook, 2002)

$$K^e \cdot u = f \qquad \text{Eq. 4-1}$$

K^e= Element stiffness matrix

u = Nodal displacement of the element

f = Nodal displacement vector of the element load vector

The stiffness matrix is produced by combining the stiffness matrices for each individual element. When all elements are joined together in a system, they obtain stiffness in the nodes which are the sum of all element ($K^T = \sum K^e$). The constitutional relation system matrix is expressed in the form:

$$K^T \bullet U = F \qquad \text{Eq. 4-2}$$

K^T= System stiffness matrix

U= System displacement vector

F = System load factor

The stiffness of the elements derives from the principal of virtual work. It state that the internal strain energy must be offset by a similar change in external work due to the applied load(Kosloski, 2014).

4.1 GENERAL STRESS ANALYSIS

The Finite element method is one of the most commonly used numerical method for solution of different engineering problem. The technique is suited for problem with irregular shapes and different boundary conditions. To find the solution for the stress analysis, FEM derive a function ů which is an approximation to the displacement u (Roylance, 2001) :

$$\mathring{u}(x, y) = u(x, y) \quad \text{Eq. 4-3}$$

FEM dissolves the solution into element witch has own approximating functions. The displacement $\mathring{u}(x, y)$ is expressed as a combination of unknown displacement at the node related to the element.

$$\mathring{u}(x, y) = N_j(x, y)u_j \quad \text{Eq. 4-4}$$

j = Ranges over the element's nodes

u_j= Node displacements

N_j = Interpolation functions.

The interpolations function or shape function are generally simple polynomials which is set to be 1 in j node and zero at the other element node. The interpolation functions can be addressed at any point within the element by using standard sub calculations, so the approximate displacement at any position within the element can be achieved the nodal displacements directly from Eq.4-4.Approximations for the strain and stress follow directly from the displacements:

$$\varepsilon' = L \cdot \mathring{u} = L \cdot N_j \cdot u_j = B \cdot u_j \quad \text{Eq. 4-5}$$

Where B_j (x, y) = L• N_j (x, y) is an array of derivatives of the interpolation functions:

$$B_j = \begin{matrix} Nj,x & 0 \\ 0 & Ni,x \\ Nj,y & Nj,x \end{matrix} \quad \text{Eq. 4-6}$$

Virtual work" argument can now be involved to determine the nodal displacement u_j appearing at node j to the forces applied externally at node. If a small virtual displacement is added on the node, the increase in strain energy δU within an element connected to that node is given by:

$$\delta U = \int \delta\varepsilon^T \sigma \; dV \quad \text{Eq. 4-7}$$

Where V is the volume of the element. By using Eq.4-6 from the interpolated displacement and combine it Eq.4-7 increase in the strain energy (with the mathematical concept $AB^T = A^T \bullet B^T$):

$$\delta U = \delta u_i^T \int B_i^T \cdot D \cdot B_j \, dV \cdot u_j \qquad \text{Eq. 4-8}$$

The increase in strain energy δU must equal the work done by the nodal forces, this gives

$$\delta W = \delta u_i^T \cdot f_i \qquad \text{Eq. 4-9}$$

Equating Eq. 4-8 and 4-9 and canceling the common $\delta u_i^T \bullet f_i$ factor gives:

$$\delta U = \left[\int B_i^T \cdot D \cdot B_j \, dV\right] \cdot u_j = f_i \qquad \text{Eq. 4-10}$$

This gives the same form as Eq.4-2 where $K^T = \int B_i^T \cdot D \cdot B_j \, dV$ is the element stiffness. This integral is solved via numerical integration, that is, the terms are evaluated at certain locations in the element, and the total integration is calculated from the evaluation at these locations. These locations are known as the integration points

4.1 SOLIDS ELEMENT

A mesh consists of elements jointed together in nodes, the mesh is used to find an approximately solution of the stresses and strain on the calculation domain. There are two types of element available for solids: brick, and tetrahedron, also called Tet. Tetrahedral elements are equivalent of 2d triangles and has basically pyramid shape. Hexahedral elements are equivalent of 2d quadrilateral element and are brick shape(MacDonald, 2007). A tetrahedron mesh can fill any geometry and shape and commonly it will be the first choice for many designer because it’s easy to use. The other element don’t have the same ability any mesh particular geometry, and require more programming skills to create good mesh. Some of the biggest advantages of using brick is the ability to decrease the number of elements but increase the computational time as well .Rectangular elements responds to the linear strain distribution across the edge of volume and give more accurate result for stress analysis. With tetrahedron Elements only capture a single strain-value, there for a larger number triangular element is needed to get the same results.(Adams & Askenazi, 1999)

5 FATIGUE

The term fatigue refers to long term degradations proses of a component or construction that fails rapidly under applied load witch is can be lower than the static strength of the component. The load responsible for failure is called fatigue load(Pook, 2007).

5.1 CONSTANT AMPLITUDE

A constant amplitude load is where all load cycles are identical. The notation is illustrated in the Figure 5-1 below. The load cycles are often a sinusoidal where $\sigma_a$the alternating stress is, σ_m is the means stress, σ_{min} is the minimum stress and σ_{max} is the maximum stress. Mathematically the load is written as $\sigma_m + \sigma_a$, compressive loading is taken as negative.(Pook, 2007)

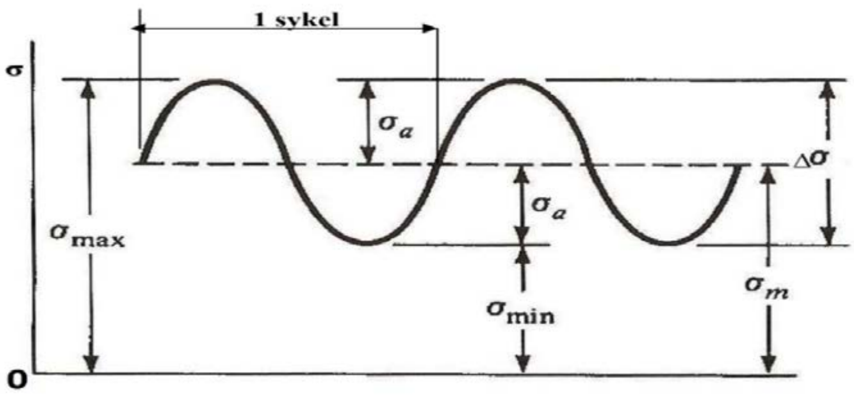

Figure 5-1 Constant amplitude loading (Pook, 2007)

Where:

The stress range:

$$\Delta\sigma = \sigma_{max} - \sigma_{min} \qquad \text{Eq. 5-1}$$

Amplitude stress:

$$\sigma_a = \frac{\sigma_{max} - \sigma_{min}}{2} \qquad \text{Eq. 5-2}$$

Means stress:

$$\sigma_m = \frac{\sigma_{max}+\sigma_{min}}{2} \quad \text{Eq. 5-3}$$

Minimum stress:

$$\sigma_{min} = \sigma_m - \sigma_a \quad \text{Eq. 5-4}$$

Maximum stress:

$$\sigma_{max} = \sigma_m + \sigma_a \quad \text{Eq. 5-5}$$

5.2 FATIGUE ANALYSIS BASED ON SN-DATA

S-N curves are obtained from tests on samples of the material under regular sinusoidal loading by a rotating bending machine. The method has been in use for more than 100 years and is still the most widely used for members where stresses are in the elastic range. The result are presented as an S-N curve. These are the plots of stress range versus number of cycles to fail. Failure is defined as breaking the specimen in two or evidence of crack of a specified size.(Pook, 2007) The S-N-curves used for design are given in DNV-RP-C203 .The S-N curves shall in general be based on a 97.6% probability for not failing, and are based on static values where the mean value is minus two times the standard deviation for relevant experimental data.

The basic design S-N-curve is given

$$\log \mathrm{N} = \log \tilde{\hat{a}} + m \cdot \log \Delta\sigma \quad \text{Eq. 5-6}$$

$$\log \mathrm{N} = \log \tilde{\hat{a}} - \log \Delta\sigma^m \quad \text{Eq. 5-7}$$

$$\log \mathrm{N} = \log \frac{\log \tilde{\hat{a}}}{\log \Delta\sigma^m} \quad \text{Eq. 5-8}$$

$$\mathrm{N} = \frac{\tilde{\hat{a}}}{\Delta\sigma^m} \quad \text{Eq. 5-9}$$

N –Number of cycles to failure for stress range $\Delta\sigma$

$\Delta\sigma$ –Stress range

m –Negative inverse slope of the design S-N-curve

ā –Intercept of the design S-N-curve with the log (N) axis

There are three types of environmental conditions that effecting S-N curves. Fatigue tests that form the curves are carried out (a) in air, (b) seawater free to corrode, (c) seawater with cathodic protection. S-N charts shall state the corresponding environmental condition under which the fatigue testing is conducted. From Figure 5-2 it can be seen that the specimens tested in air have a longer fatigue life than the specimens tested in seawater when exposed to the same fatigue loading. In addition to environmental conditions, there are two possible states of stress ranges to be considered. It is important to distinguish from concentrated stress and analytical stress σ_{nom}. The analytical stress is a global parameter that is not affected by the stress concentrations. The combination of the analytical stress and correct SN curve will give a good estimate of the fatigue life. However, this also means that S-N curve is needed for all possible connections between members which is not practicable.

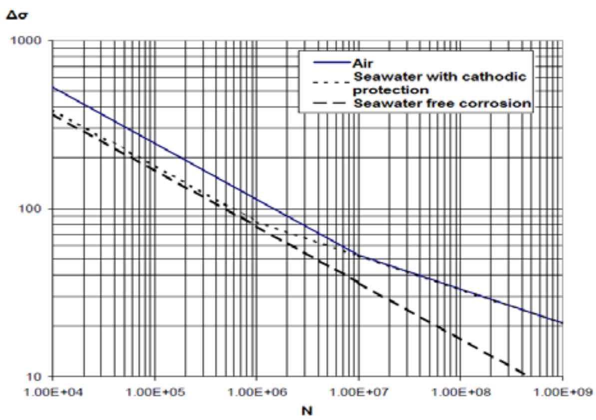

Figure 5-2 SN-curve for different environment

5.3 STRESS CONCENTRATION

A stress concentration is a term used to describe the localized stress state in a section area where stresses are larger compared to the analytical values, hence concentrated. An object is strongest when force is evenly distributed over its area. A change in the cross-section, gives a local increase in the intensity of a stress field. Examples of shapes that cause stress concentrations are cracks, sharp corners, holes. These can lead to failure when the stress concentrated exceeds the material's theoretical strength. The maximum stress occurs at the side of the hole is(Pilkey, 1994):

$$\sigma_{SCF} = 3 \cdot \sigma_{nom} \qquad \text{Eq. 5-10}$$

The peak stress is three times higher the analytical uniform stress. To account for the peak stress near a stress concentration, the factor is defined as the ratio of the calculated peak stress to the analytical that would exist in the member if the stress distribution remain uniform

$$SCF = \frac{\sigma_{SCF}}{\sigma_{nom}} \qquad \text{Eq. 5-11}$$

The maximum stress near a crack occurs in the area of lowest radius of curvature. In an elliptical crack of length 2a and width 2b, under an applied external stress σ_{nom} the stress at the ends of the axes are given by(Anderson, 2005):

$$\sigma_{SCF} = \sigma_{nom} \cdot (1 + 2\frac{a}{b}) \qquad \text{Eq. 5-12}$$

5.4 MEAN STRESS EFFECT

The empirical description of fatigue life is fully reversed fatigue load where the mean stress is zero. Most of the SN-curves today are based on cyclic loading between maximum and minimum stresses with a mean stress σ_m=0 with a constant amplitude However fully reversed stress cycles with a zero mean stress are not always applicable to many applications. The mean stress effect represented with Goodman relation is an equation used to quantify the influence of actual mean stress on the fatigue life of a material(Suresh, 1992) .The Goodman relation is :

$$\sigma_a = \sigma_{a\_\sigma_{m=0}} \cdot (1 - \frac{\sigma_m}{\sigma_u}) \qquad \text{Eq. 5-13}$$

The amplitude using to plot in SN-curve:

$$\sigma_{a\_\sigma_{m=0}} = \frac{\sigma_a}{(1 - \frac{\sigma_m}{\sigma_u})} \qquad \text{Eq. 5-14}$$

Giving stress range:

$$\Delta\sigma = 2 \cdot \sigma_{a\_\sigma_{m=0}} \qquad \text{Eq. 5-15}$$

5.5 CONTACT FATIGUE

Contact fatigue differs from classic structural fatigue which is based on bending or axial loading. Herzian contact analysis explain the stresses when curved surfaces of two objects are in contact under loading. This may result rolling motion between the surfaces as in a ball rolling. The contact and the motion of the rolling produces an alternating subsurface shear stress. Plastic strain builds up with accumulated cycles until a crack is created. The crack will grow until a pit is shaped. Once pitting has formed, fracture can result catastrophic failure (Glaeser & S.J. Shaffer, 1996).

5.5.1 Effect of corrosion on SN-curve

The consequence of corrosion on a member is illustrated in the Figure 5-3 bellow .Curve A shows the fatigue behavior of a material tested in air. Curves B and C characterize the fatigue behavior of the same material in two corrosive environments. In curve B, the fatigue failure at high stress levels is underdeveloped, and the fatigue limit is not existing. In curve C, the whole curve is shifted to the left; this indicates a more conservative leading to degradation of the fatigue-strength. The fatigue limit is not existing in the presence of a corrosive environment (Kitegava, 1972)

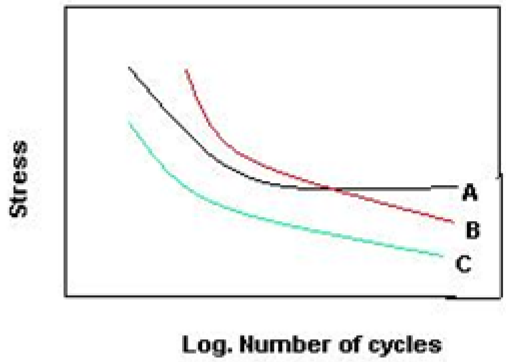

Figure 5-3 Corrosion effect on the SN-curve

6 FRACTURE MECHANICS

The study for behavior of cracked body under load condition is known as fracture mechanism.it does not offer any detail about the process involving in fatigue crack propagation. However it provide an analytical description for their nature and data to practical engineering problem.

6.1 STRESS ANALYSIS FOR CRACK

For certain cracked body subjected external load, it is approximately possible to derive expression for stresses. Assumption like isotropic body and linear elastic behavior drive the present's day fracture mechanism. Crack surfaces are assumed to be smooth, hence microscopic sample show otherwise with irregular surface. Fracture mechanism describes the reaction of the material at a crack tip. If an external load applied in a member, the crack face will move relative to each other. Theory describe 3 modes illustrated in the Figure 6-1.

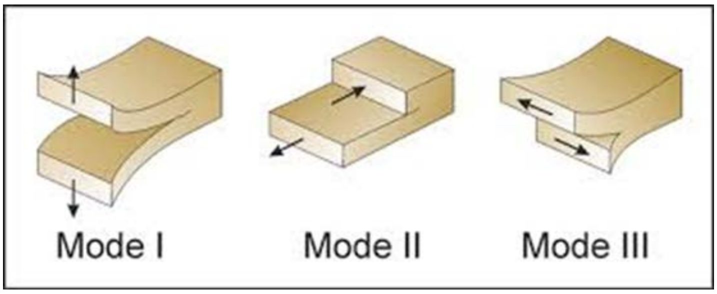

Figure 6-1 Different crack mode

Mode I is where crack planes separate apart out of plane direction. Mode II and mode III are in plane and anti-shear modes respectively (Hearn, 1997). The stress intensity factor K is usually given to determine the mode of loading and most common is mode I. It is often that materials are generally characterized by resistance in that mode. In this work the stress intensity factor mode I is considers only. The stress field near the crack in a linear elastic body can be written as (Anderson, 2005):

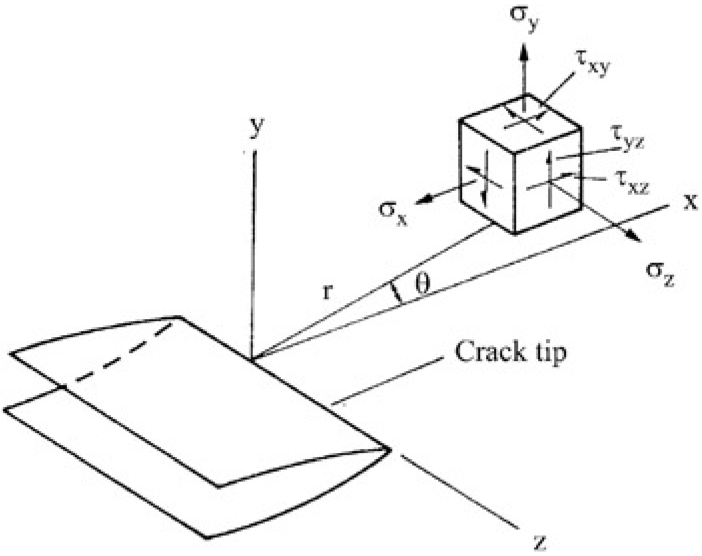

Figure 6-2 Stresses near the crack (Hearn, 1997)

$$\sigma_{yy} = \frac{K}{\sqrt{2\pi r}} \cdot \cos\frac{\theta}{2} \cdot \left[1 + \sin\frac{\theta}{2} \cdot \sin\frac{3\theta}{2}\right] \quad \text{Eq. 6-1}$$

$$\sigma_{xx} = \frac{K}{\sqrt{2\pi r}} \cdot \cos\frac{\theta}{2} \cdot \left[1 - \sin\frac{\theta}{2} \cdot \sin\frac{3\theta}{2}\right] \quad \text{Eq. 6-2}$$

$$\tau_{xy} = \frac{K}{\sqrt{2\pi r}} \cdot \cos\frac{\theta}{2} \cdot \left[\sin\frac{\theta}{2} \cdot \sin\frac{3\theta}{2}\right] \quad \text{Eq. 6-3}$$

Figure 6-2 shows an element near the crack tip in an elastic material with associated in plane stresses. From the equations above it can be seen that the stresses are proportional to K in every direction .If this constant is known, the entire stress distribution at the crack tip can be computed with the equations above. This factor determines whether the crack will propagate or not. The stress intensity factor K is given by for a center crack length 2 a under remote uniaxial tension with analytical stress σ_{nom} (Hearn, 1997):

$$\mathrm{K} = \sigma_{nom} \cdot \sqrt{\pi \cdot a} \quad \text{Eq. 6-4}$$

For an edge crack in a semi-infinite sheet:

$$\mathrm{K} = 1.12 \cdot \sigma_{nom} \cdot \sqrt{\pi \cdot a} \quad \text{Eq. 6-5}$$

The K factor for different load and geometry can be modified to :

$$\mathrm{K} = \sigma_{nom} \cdot Y \cdot \sqrt{\pi \cdot a} \quad \text{Eq. 6-6}$$

In Eq.6-6, Y is a geometric correction factor, and a is the characteristics crack length. Y depends on the ratio $\frac{a}{W}$ where W is the un-cracked specimens width. Values for Y factor for different crack geometries is explain in the Figure 6-3.

Compliance function $Y = A\left(\frac{a}{W}\right)^{1/2} - B\left(\frac{a}{W}\right)^{3/2} + C\left(\frac{a}{W}\right)^{5/2} - D\left(\frac{a}{W}\right)^{7/2} + E\left(\frac{a}{W}\right)^{9/2}$
with W = uncracked specimen width; a = length of edge crack; b = specimen thickness;
P = total load; L = distance between loading points

Specimen geometry	Specimen nomenclature	Equation for K	Compliance function constants				
			A	B	C	D	E
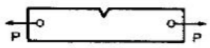	Single edge notched (S.E.N.)	$K = \frac{P}{bW^{1/2}} \cdot Y$	1.99	0.41	18.70	38.48	53.85
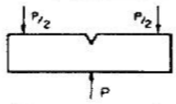	Three-point bend ($L = 4W$)	$K = \frac{3PL}{bW^{3/2}} \cdot Y$	1.93	3.07	14.53	25.11	25.80
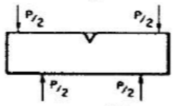	Four-point bend	$K = \frac{3PL}{bW^{3/2}} \cdot Y$	1.99	2.47	12.97	23.17	24.80
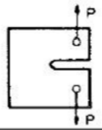	Compact tension (C.T.S.)	$K = \frac{P}{bW^{1/2}} \cdot Y$	29.60	185.50	655.70	1017.0	638.90

Figure 6-3 Geometry factor Y for different load case(Hearn, 1997)

The factor K is essential parameter because it describes the stress field around existing crack tip. For a crack with a plane angle θ = π., it can be observed that the photoelastic fringes showed in Figure 6-4 that they are corresponding to the max shear stress $\tau_{\max}$.

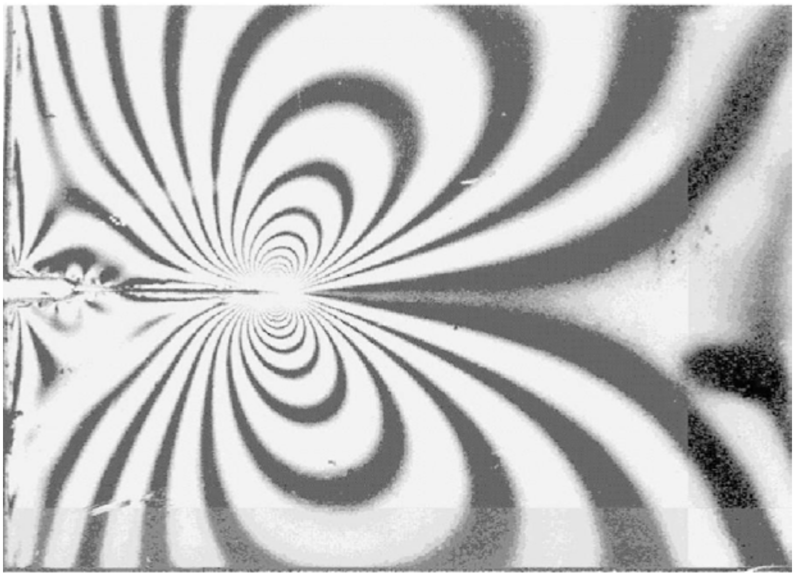

Figure 6-4 Photoelastic fringes for an edge crack(Hearn, 1997)

Mohr circle define the max shear stress as:

$$\tau_{xy} = \frac{1}{2} \cdot \sqrt{(\sigma_{xx} - \sigma_{yy})^2 + 4\tau_{xy}{}^2} \qquad \text{Eq. 6-7}$$

Substituting with Eq. 6-7 gives:

$$\tau_{xy} = \frac{K}{2 \cdot \sqrt{2\pi r}} \qquad \text{Eq. 6-8}$$

Consider the mode I singular field on crack plane θ = 0, then the stresses in the x and y direction are equal to:

$$\sigma_{yy} = \sigma_{xx} = \frac{K}{\sqrt{2\pi r}} \qquad \text{Eq. 6-9}$$

When θ = 0 the shear stress is equal to zero, which means the crack plane as a principal plane for pure mode I loading.

6.2 CRACK TIP PLASTICITY

Linear elastic stress analysis of cracks predicts infinite stresses at the crack tip. The elastic stress analysis becomes inaccurate in the plastic region as the inelastic region at the crack tip get larger. The most common method to estimate crack tip yielding zone is proposed by Irwin, where elastic stress analysis is used to define the plastic region(Anderson, 2005). If a state where assumed to be σ_{yy} the maximum principle stress and σ_{zz} is the minimum principle stress. By the Tresca criterion the material will yield if:

$$\sigma_{yy} - \sigma_{zz} = \sigma_{ys} \qquad \text{Eq. 6-10}$$

A length away from the crack, r_0 will give a value σ_{yy} =σ_{ys}. As seems in the figure below that the area from the crack tip to r_0 can be defines as $2 \cdot \sigma_{ys} \cdot r_0$. The shaded area in Figure 6-5 derived by integration of Eq 6-9 has a value of $\sigma_{ys} \cdot r_0$. This will give a plastic zone region in crack direction with length:

$$r_y = 2 \cdot r_0 = \frac{K}{\pi \cdot \sigma_{ys}{}^2} \qquad \text{Eq. 6-11}$$

This seemed contradictory because K is derived from an elastic notation. However, if the plastic region is small, the elastic stress field around this region can be described by Eq 7-1 to 7-3. A good citations is if the plastic region size is less than one fiftieth of undamaged member(Hearn, 1997).

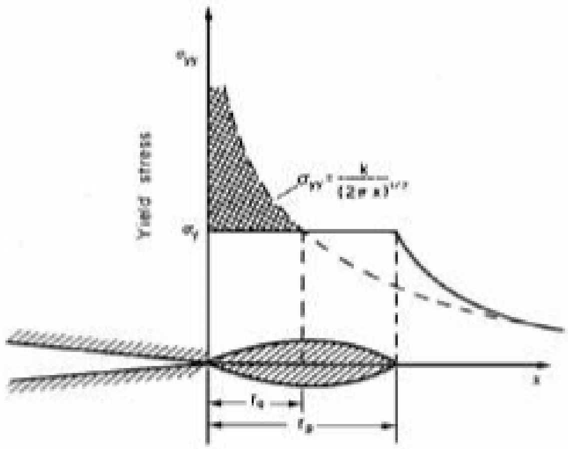

Figure 6-5 plastic zone region in crack (Hearn, 1997)

7 STATIC ANALYSIS

7.1 PIN

Simple beam theory has been implemented to calculate the behavior of the pin and determine the stress in the pin caused by bending from the chain force. Beams are members who are slender and support loading that is applied perpendicularly to their longitudinal axis. In general, beams are long straight having a constant cross section. It is important to be noted that our shackle does not meet these requirements. The pin is not slender and have complex support with friction and contact stress. The beam where calculations used to give verification of the FEA and determine approximately analytical stress for the fatigue calculation. The system chosen to represent the deformation was fixed supported at the end due to the long span of padeye. This will give small deflection of pin that will give results closer to the real deflection.

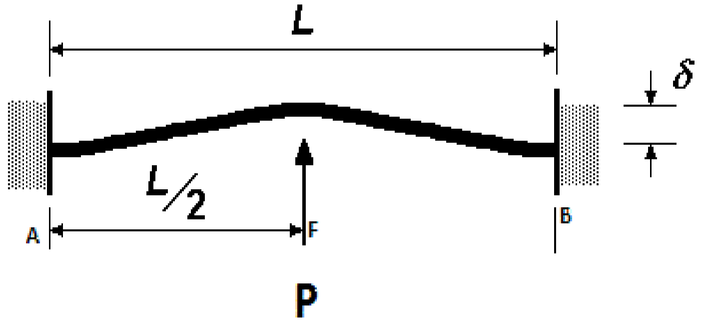

Figure 7-1 Static system for pin

The reaction force is

$$R_A = R_B = \frac{P}{2} \qquad \text{Eq. 7-1}$$

$$M_A = M_B = M_F = \frac{P \cdot L}{8} \qquad \text{Eq. 7-2}$$

$M_A = M_B = M_F$: Moment at point A, B and F

Deflection:

$$\delta = \frac{P \cdot L^3}{192 \cdot E \cdot I} \qquad \text{Eq. 7-3}$$

E: Module of elasticity

I: Moment of inertia

The bending stress will vary linearly in the cross-section as long it stay on the elastic zone.

$$\sigma_{nom} = \frac{M \cdot c}{I} \qquad \text{Eq. 7-4}$$

c: The perpendicular distance from the natural axis to a point farthest away from the natural axis

M: The resultant Moment

I: Moment of inertia

Stresses and moments M_A, M_B are balanced by contact and friction forces.

7.2 PADEYE

Simple axial load analysis will be will be performed using the reaction force from section (7.1).Concentration factor will be taken into consideration near the holes from (Hibbeler & Fan, 2008).

$$\sigma_{nom} = \frac{P}{A} = \sigma_{nom} = \frac{Ra}{(w - 2r) \cdot t} \qquad \text{Eq. 7-5}$$

F: Applied force

A: Cross-section Aria

7.3 HERZIAN CONTACT STRESS

Contact mechanism consider deformation of two elastic solids in contact. Herzian contact stress theory is used using the assumptions, which are listed as follows (Johnson, 1985):

- Surfaces are continuous
- Strains are small
- Solids are elastic
- Surfaces are frictionless

Designing component to resist contact stresses is very important in engineering problem such as bearings and pin-jointed links. Hertz contact stresses represents compressive stresses developed from surface pressures between two curved bodies pressed together. The size of the contact area depends on loading conditions, structural geometry and material properties. It gives the contact stress as a function of the normal contact force, the radii of curvature and the modulus of elasticity of both bodies (Hearn, 1997)

7.4 GENERAL CASE OF CONTACT OF TWO SOLIDS

In the theory of contact, contacting bodies are assumed to be elastic and made of an isotropic material. Hertz has demonstrated that the intensity of the pressure between the contact surfaces has an elliptical or semi- elliptical distribution.

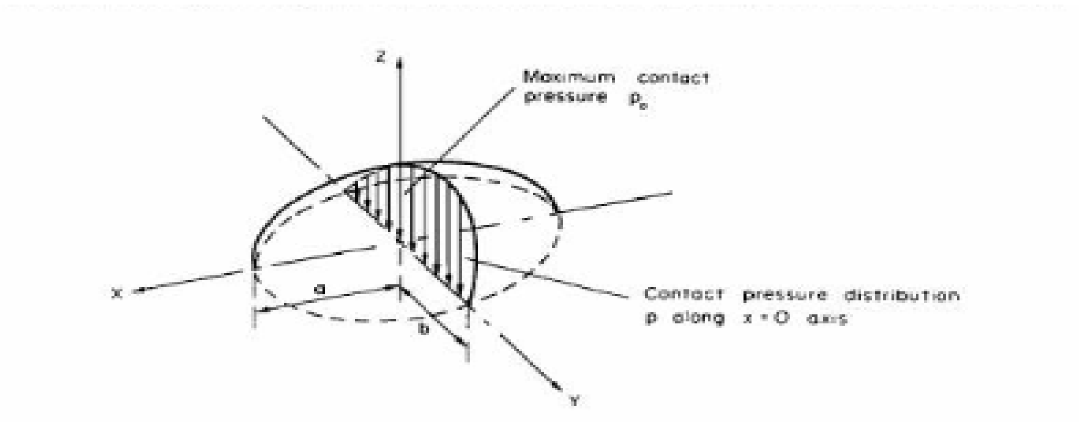

Figure 7-2 Herzian contact model (Hearn, 1997)

The highest pressure occurs at the center of contact initiated by p_o, the pressure at random point within the contact region was showed by(Hearn, 1997):

$$p = p_o \cdot \sqrt{1 - \frac{x^2}{a^2} - \frac{x^2}{b^2}} \qquad \text{Eq. 7-6}$$

Where ***a*** and **b** is the major and minor semi-axes. The total contact load is given by the volume of the semi- ellipsoid:

$$P = \frac{2}{3} \cdot \pi \cdot a \cdot b \cdot p_o \qquad \text{Eq. 7-7}$$

From the equation 8-8, deriving the equation for maximum compressive stress gives:

$$p_o = \sigma_c = \frac{3 \cdot P}{2 \cdot \pi \cdot a \cdot b}$$ Eq. 7-8

For different contact load P, it is important to determine the value of **a** and **b** before calculating the max contact stress. These values are found by:

$$a = m \cdot [\frac{3 \cdot P \cdot \Delta}{4 \cdot A}]^{-0,33}$$ Eq. 7-9

Where

$$\Delta = \frac{1 - {v_1}^2}{E_1} + \frac{1 - {v_2}^2}{E_2}$$ Eq. 7-10

And

$$b = n \cdot [\frac{3 \cdot P \cdot \Delta}{4 \cdot A}]^{0,33}$$ Eq. 7-11

m and n are functions of contact geometry of the contact surface and are shown for different values of $\alpha = \cos^{-1}\frac{A}{B}$:

α degrees	20	30	35	40	45	50	55	60	65	70	75	80	85	90
m	3.778	2.731	2.397	2.136	1.926	1.754	1.611	1.486	1.378	1.284	1.202	1.128	1.061	1.000
n	0.408	0.493	0.530	0.567	0.604	0.641	0.678	0.717	0.759	0.802	0.846	0.893	0.944	1.000

Figure 7-3 Contact geometry for different values of α(Hearn, 1997)

Where:

$$A = \frac{1}{2}[\frac{1}{R_1} + \frac{1}{R_1^`} + \frac{1}{R_2} + \frac{1}{R_2^`}]$$ Eq. 7-12

$$B = \frac{1}{2}[\left(\frac{1}{R_1} - \frac{1}{R_1^`}\right)^2 + \left(\frac{1}{R_2} - \frac{1}{R_2^`}\right)^2 + 2\left(\frac{1}{R_1} - \frac{1}{R_1^`}\right)^2 \cdot \left(\frac{1}{R_2} - \frac{1}{R_2^`}\right)^2]$$ Eq. 7-13

A and B is function of elastic contact E and v of the contacting bodies .With R and R` the maximum and minimum radii of curvature of the unloaded surfaces in two perpendicular planes The maximum shear stress will occur beneath surface with value of b = 0.78z (where z is the vertical coordinate) with an angle of 45 degree.

$$\tau_{max} = 0.3 \cdot p_o$$ Eq. 7-14

8 ANALYSIS SETUP IN ANSYS

The FE (Finite Element) analyses for the shackle design were performed using the general FE software ANSYS v15. ANSYS v15 workbench starts up with a project where the analyze type is decided. To obtain a solution several steps have to be performed. For the Ultimate limit stress, and fatigue check the static structural analysis sytem is chosen.

8.1 DEFINITION OF THE SYSTEM

The riser system is provided with 3 Mid Water Arches (MWA) each with a separate anchor block. Each MWA is tethered by 2 chains anchored to each end of the anchor block. The general arrangement and its orientation are shown in Figure 8-1. The anchor pad-eye is connected to the anchor block through two hinges provided with central pins, allowing rotation of the pad eye. The pins are locked in place by a steel bracket which is welded to the pin. The variation of the load is represented by the change in position of the hinges.

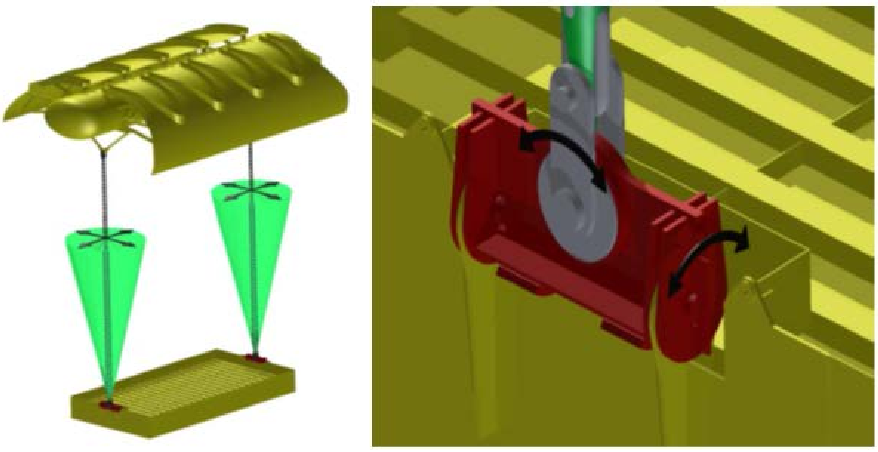

Figure 8-1 System description

8.2 ENGINEERING DATA

The International Association of Classification Society (IACS) denotes the steel grades with an R followed by a number to describe the strength. Steel grade R3S, R4 and R4S are considered as high-strength steel. Offshore DNV Standard DNV-OS-E302 provides mechanical properties for various steel grades. The different material required capacity are listed in Table 8-1.

Table 8-1 Material properties required for different grade

Steel grade	Yield Stress [MPa]	Tensile Strength [MPa]	Elongation [%]	Reduction of area
R3	410	690	17	50
R3S	490	770	15	50
R4	580	860	12	50
R4S	700	960	12	50
R5	760	1000	12	50

The shackle was modelled as an assembly of homogenous solids made in structural steel. The Young's Modulus was set to 207 000 MPa and the Poisson's ratio was set to 0.3. The Density was set to 7850 kg/m3, as provided in (Standard, 2008), s.39, Table A.4.. The Material used in the models is steel of steel grade R4. The minimum breaking load (MBL) is assigned to be 6000 KN.

8.3 MODEL DESCRIPTION

8.3.1 General

The geometry of the modeled shackle is according to engineering design given to match the dimensions provided by production drawing provided by Wood Group Kenny, see Appendix A. Assuming a central symmetry axis, only a half of the geometry is modelled. The upper half was considered because it was the most critical area with thinnest cross section. Because of FE analysis is time consuming and the geometry is complex the computational time can be long.

Geometry used in ANSYS workbench can be either modeled in Design Modeler or it can be imported from other CAD programs. The first draft was simplified by removing objects that are not important for the analysis like the pinhead and the nut on the pin. These was replaced with a planar joints. The joint allowed lateral and vertical sliding with rotation around z axis. There were some problems with this model, because the pin had large stresses concentrations where it attaches to the planar join. This behavior was deemed unrealistic so some changes had to be made which resulted in a model included with pinhead and nut.

8.3.2 Models description

8.3.2.1 Model 1

The first model represent the fabricated shackle provided by engineering design in Appendix A. This model is used to observe how the shackle react to the forces prior of any corrosion. This will provide basis to compare the result before and after corrosion.

8.3.2.2 Model 2 Shackle with uniform corrosion

Safety against mooring corrosion and wear is normally provided by increasing the chain/shackle diameter. Normal practice according to DNV-OS-E301, p.50 is to increase the chain diameter by 0.2 mm to 0.4 mm per service year. The recommended corrosion allowance is given in Table 8-2 for different position mooring lines.

Table 8-2 Corrosion allowance for chain from DNV-OS-E301

Corrosion allowance for chain			
Part of mooring line	Corrosion Allowance referred to the chain diameter		
	Regular inspection (mm/year)	Regular inspection (mm/year)	Requirements for the Norwegian continental shelf
Splash zone	0.4	0.2	0.8
Catenary	0.3	0.2	0.2
Bottom	0.4	0.3	0.2

For simplicity, corrosion is assumed to be 0.3 mm/year. The shackle have been in the field since for 7 years, and this give an approximately total uniform corrosion of 2 mm. The method used to simulate the corrosion was to change the dimension of the shackle according to the amount of material lost. This was done by decreasing the high, length, and width and pin diameter with 2 mm. The pin hole and the gap did increase with 2 mm.

8.3.2.3 Model 3 Uniform corrosion with pitting

After couple of simulation with Ansys mechanical, the results indicated that the most critical stresses was in the contact region. This model will demonstrate the effect of fretting in critical contact area with uniform corrosion (2mm). Due to penetration between pin and padeye, the coating will disappear and initiation of corrosion will happen. Fretting is associated to corrosion damage at the contact surfaces. The cause of failure occurs at the highly loaded contact surface which is not designed for dynamic contact motion. The protective layer at the metal surface is worn away by rubbing action, which becomes available for corrosion activity.Fretting corrosion result metal loss developing a crack. To show that effect, a crack is added with elliptical shape. Because of uncertain degree of corrosion it is assumed that the crack have a depth equal to 8 mm. The dimension of the crack is illustrated bellow.

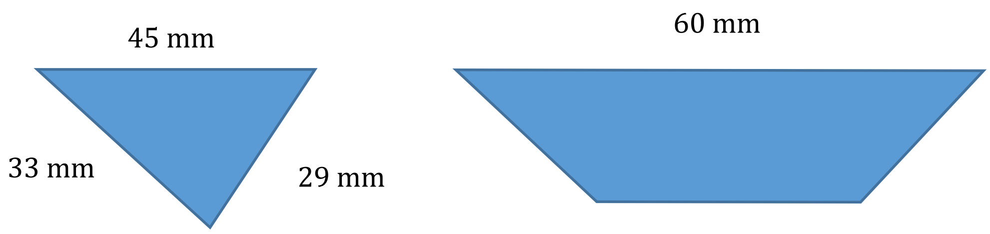

8.4 SURFACE CONTACT MODELLING IN ANSYS

Ansys defines contact as two different planes touching each other such that they form a tangent surface. Mechanical understanding of surfaces in contact are characterized by: (ANSYS, 2010):

- They do not interpenetrate.
- They can transfer compressive forces and tangential friction forces.
- They often do not conduct normal forces. They are therefore avail to separate

Contact in Ansys is non-linear and the contact status controls the stiffness of the system. As mention before, contact members cannot interpenetrate. The relation between the two contacts elements is such that they are not allowed to pass each other. This is known as enforced contact compatibility. Ansys has several different contact functions available to assure compatibility at the contact interface:

$$Pure\ Penelty\ : F_{Normal} = K_{normal} \cdot X_{penetration} \quad \text{Eq. 8-1}$$

$$\mathrm{Augmented\ Larange}\ : \mathrm{F}_{\mathrm{Normal}} = \mathrm{K}_{\mathrm{normal}} \cdot \mathrm{X}_{\mathrm{penetration}} + \lambda \quad \text{Eq. 8-2}$$

$$Normal\ Lagrange\ : F_{Normal} = DOF \quad \text{Eq. 8-3}$$

$\mathrm{F}_{\mathrm{Normal}}$ = Finite contact force

$\mathrm{K}_{\mathrm{normal}}$ = Contact stiffness

$\mathrm{X}_{\mathrm{penetration}}$= Penetration

From the equation for Pure Penalty and Augmented Lagrange it can be seen than an infinite large stiffness will result in zero penetration. This will change as it not possible in the analysis, but as long as the penetration is small or negligible the result will be approximately correct. Both methods use the integration point detection and results more detection points. The difference between Pure Penalty and Augmented Lagrange is the extra term λ that make the method less sensitive to the magnitude of the stiffness$\mathrm{K}_{\mathrm{normal}}$.The Normal Lange function adds an additional degree of freedom, the contact pressure. This practice has no need to model contact stiffness and has nearly zero penetration but requires the Direct Solver, which can be computationally more expensive.

8.5 PIN AND THE PAD-EYE

The contact area between the two parts in Figure 8-2 was located within a range of predefined contact surfaces. The Interaction properties defines how surfaces respond each other. The contact between the pin and pad-eye was defined as frictional with ramped set to zero offset. This make the contact intense and consecrated and not uniformly distributed along the surfaces. The interaction properties between the two bodies were defined as tangential contact and normal contact. The coefficient of friction of steel-to-steel contact depends on lubrication and surface finish and has values from 0.15 to 0.8. In this case the friction coefficient was set to 0.2 and the contact was defined as hard. The red surface area is the contact surface while the blue area is the target surface. The red and blue surfaces represent areas in which contact may occur.

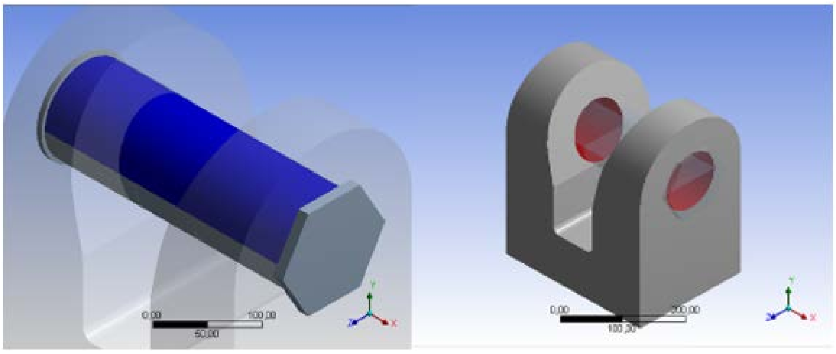

Figure 8-2 Contact between pin and padeye

8.5.1 Pin-head and the pad-eye

The contact between the pinhead and padeye was establish as frictional with ramped with adjust to touch. This mean that Ansys creates a surface where the contact is uniformly distributed. This will avoid high concentrated contact stresses between these two surfaces. The coefficients factor was set 0.2. The red and blue surfaces represent areas in which contact may occur. The actual contact area is located within the range of these predefined contact surfaces.

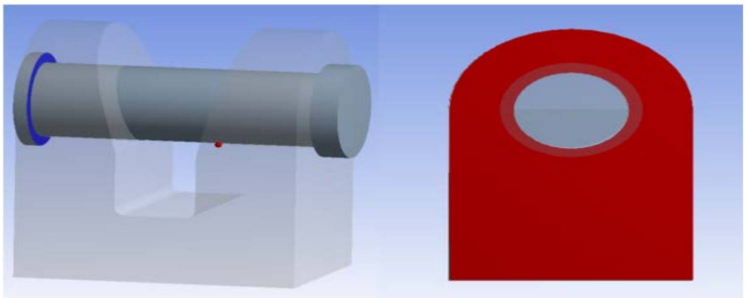

Figure 8-3 Contact between pinhead and padeye

8.5.2 Mesh

Figure 8-4 illustrates FE mesh of the model made by tetrahedral elements. The model must have a serval elements in the pin and the area around the hole in the pad eye to make sure that the stress and strain get captured. The University License has a restricted number of mesh nodes. Ansys has a function named inflation wish make the contact results more accurate. This requires a denser mesh than the mesh restriction allows for. Therefor the sizing function with an element size of 10 mm was set around hole and the surface facing the pin. These area is considered important to catch accurate contact results on padeye. Unfortunately it was not possible to establish the same sizing on pin because of restricted element number on the university license. This final mesh has 29788 nodes and 16925 elements within the model.

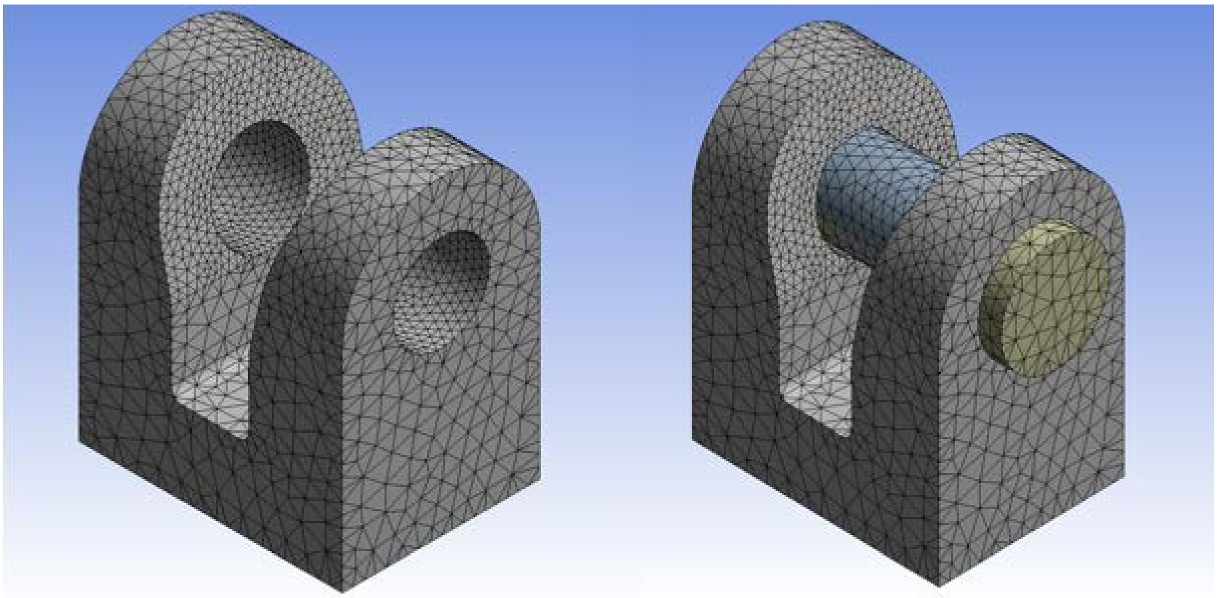

Figure 8-4 FE mesh of the shackle

8.5.3 Load and boundary condition

The load is defined as bearing force distributed at the surface acting in the perpendicular to the pin. The bearing load (point B) in Figure 8-5 has an elliptical distribution with the highest pressure at the center of the surface describing the contact-surface between the chains and pin. Point A at the bottom of the shackle is constrained with fixed support .This boundary condition constrains the region all direction with no degree of freedom. This specifies that there is no deformation in all direction. The cordinate system is defined as the figure below.

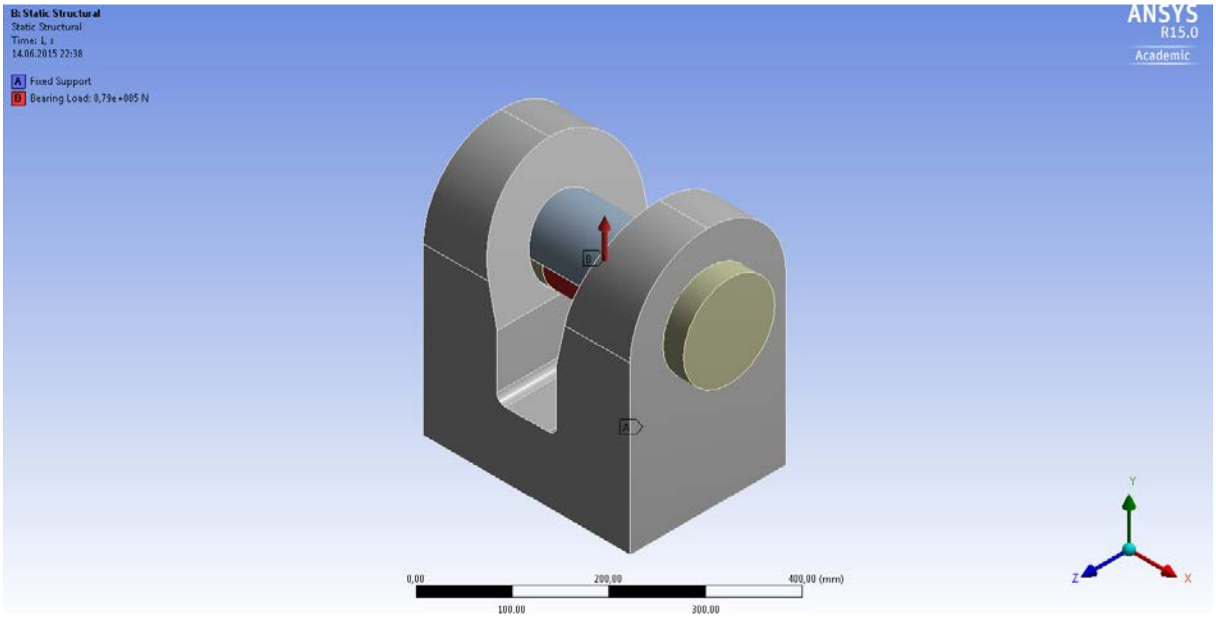

Figure 8-5 Load and boundary condition

The load sequence applied in the models is applied in 3 condition, normal operation, extreme operation and abnormal operation. The load applied in assumed to be constant sinus dual load with the max and min load as described in the table below. The load cases are extracted from Project Design Report.

Table 8-3 Different load cases

Load-case	Normal operation		Extreme operation		Abnormal Operation	
	Max	Min	Max	Min	Max	Min
	666 KN	75.8KN	665.1 KN	115.3 KN	676.4 KN	88 KN

9 Design Basis

9.1 Action Factors

9.1.1 Ultimate limit state

According to Norsok Standard N-001, the ultimate limit states shall be checked for two action combinations, I and II, with action factor according to Table 9-1. The actions are to be combined in the most unfavorable way, provided the combination is physically feasible and permitted according to the action specifications.

Table 9-1 Action factor from Norsok N-001

Action Combinations	Permanent Actions	Variable actions	Environmental actions
I	1.3	1.3	0.7
II	1.0	1.0	1.3

9.1.2 Fatigue limit state

According to NORSOK N-001 the purpose of fatigue analysis is to confirm that the structure will satisfy the service life. This means that the structure shall not be damage or fail during the design life of the structure. A cycling loading is considered for the fatigue analyses and action factor of 1.0 is used for loads. In addition according to NORSOK N-001 the number of load cycles shall be multiplied with the factor in Table 9-2.

Table 9-2 Design fatigue factor

Classification of structural components based on damage consequence	Not accessible for inspection and repair or in the splash	Accessible for inspection, change or repair And where inspection or change is assumed.	
Substantial consequences	10	Below splash zone	Above splash zone or internal
		3	1
Without substantial consequences	3	2	1

For simplicity the shackle is classified as “No access or in the splash zone” and the “No access”. This means that a DFF factor of 10 is to be used in the calculations.

9.2 ACCEPTANCE CRITERIA

To fulfill the requirements of design code or standard, the results for capacity should be checked against the acceptance criteria. The relevant acceptance criteria for different components are described in the following sections

9.2.1 Yielding

The allowable stress based-approach is used for design against yielding. According to Norsok-001 the design safety factor for the shackle system is taken as 1.15. For the shackle the yield stress is given as 580 MPa. The design yield is then:

$$\sigma_{yd} = \frac{\sigma_{ys}}{1.15} = 508\ \mathrm{MPa} \qquad \text{Eq. 9-1}$$

Combining with failure take place when the Von Mises stress is higher than the yield design value:

$$\sqrt{\frac{(\sigma_1 - {\sigma_2}^2) + (\sigma_2 - {\sigma_3}^2) + (\sigma_1 - {\sigma_3}^2)}{2}} > \sigma_{yd} \qquad \text{Eq. 9-2}$$

10 RESULT

The results from the analyses are presented as von Mises stresses for the yielding results. Maximum principal stresses is used for the padeye for the fatigue calculation while shear stress is used for the pin as DNV specified. . Von Mises stresses central when using failure criteria to predict failure in ductile materials. However, von Mises yield criterion do not decide between tensile stresses and compressive stresses. When it comes to fatigue, the sign of the stress is essential. As a rule of thumb, a tensile mean stress reduces fatigue life while a compressive mean stress increases fatigue life due to a mean stress equal to zero. The sign of the stress is also a key factor due to crack initiation. Unlike Mises stresses, the principal stresses are denoted as positive or negative.

10.1 VERIFICATION OF THE FE MODEL AND ANALYSIS PROCEDURE

The aim of this chapter model 1 was chosen to demonstrate the relation between the static analysis and numerical analysis establish by FEA. This will be give basis to compare the analytical with the numerical results. The Verification of the FE model calculation is established by action factor in section 9.1.1. The load applied on the shackle is assumed to be environmental load. The combination II will give the most critical load condition giving:

$$\mathrm{P} = 1.3 \cdot max \text{ load case} = 1.3 \cdot 676 \text{ KN} = 879 \text{ KN} \qquad \text{Eq. 10-1}$$

10.1.1 Pin

Using the beam theory to determine the displacement and the bending stress on pin at the center of the pin:

$$\mathrm{R_a} = \frac{P}{2} = \frac{879000N}{2} = 439500\ N \qquad \text{Eq. 10-2}$$

$$M_F = \frac{F \cdot L}{4} = \frac{879000N \cdot 303mm}{8} = 33292125\ Nmm \qquad \text{Eq. 10-3}$$

$$\sigma_{nom} = \frac{M \cdot c}{I} = \frac{33292125\ Nmm \cdot 53mm}{6194027\ mm^4} = 285\ MPa \qquad \text{Eq. 10-4}$$

$$\delta = \frac{P \cdot L^3}{192 \cdot E \cdot I} = \frac{676000 \cdot 303^3}{192 \cdot 210000 \cdot 5739618} = 0{,}01\ mm \qquad \text{Eq. 10-5}$$

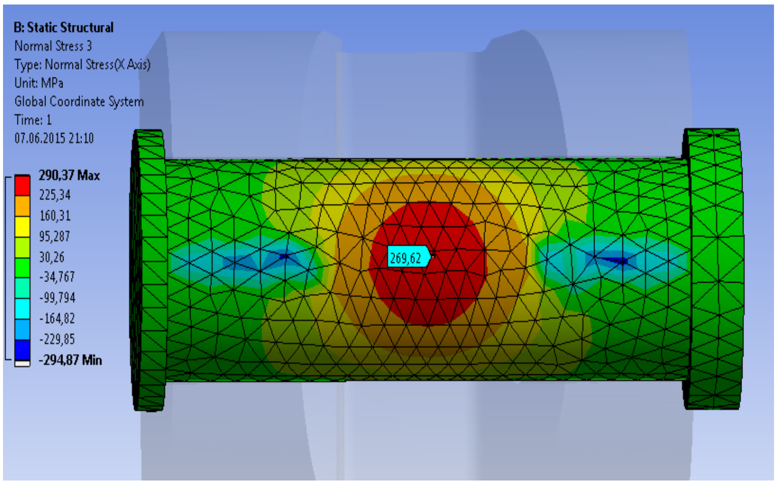

Figure 10-1 Normal stress in x-direction

It can be seen from the Ansys FE analysis that the accurate $\sigma_x = 270$ at the center of the pin. The analytical calculation gives a good approximation of the stress on the pin. The numerical deformation gives a value $\delta = 0{,}036$. The results are almost equal which makes it that the static analysis gives a good approximation on the behavior of the pin.

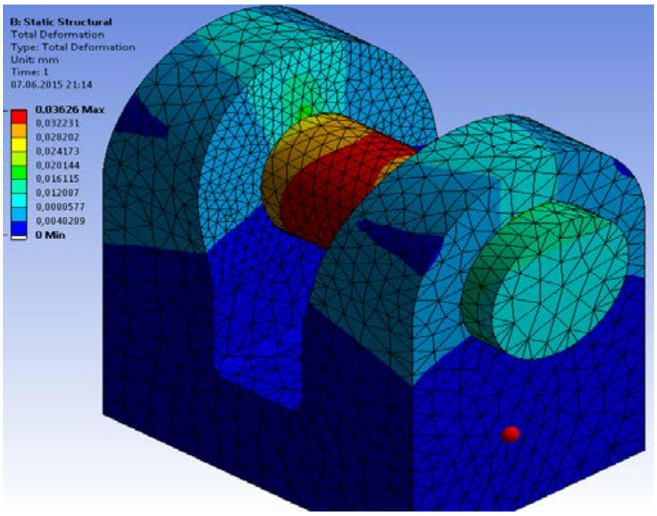

Figure 10-2 Total deformation on the shackle

10.1.2 Padeye

The analytical stress in the padeye is:

$$\sigma_{nom} = \frac{Ra}{(w-2r)\cdot t} = \frac{338000\ N}{(180-106)\cdot 96} = 61.7\ Mpa \qquad \text{Eq. 10-6}$$

The stress concentration around the hole:

$$\sigma_{SCF} = 3\cdot\sigma_{nom} = 185\ \text{MPa} \qquad \text{Eq. 10-7}$$

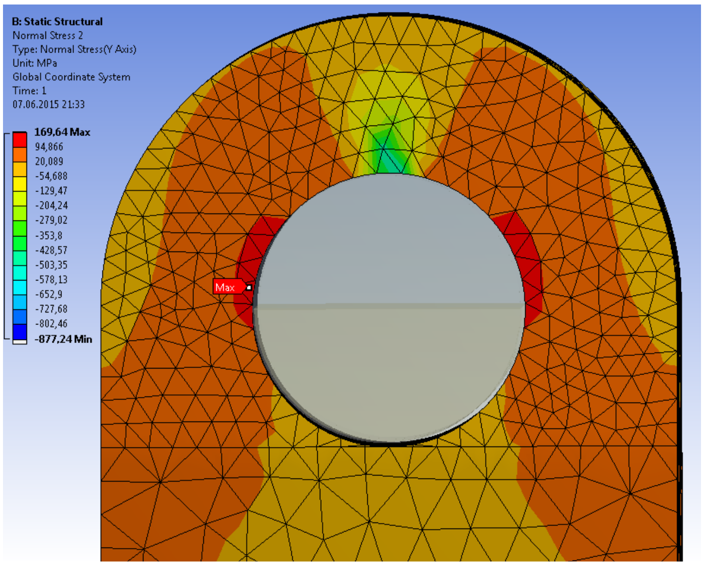

Figure 10-3 Stresses near the hole on padeye

The analytical calculation shows higher stress than numerical result (Figure 10-3). This is because Ansys use the total width in the calculation of the normal stresses. In the analytical calculation it is assumed that the impact of the load have a width of 180 mmm.A static determination of the contact stress between the pin and shackle

$$\Delta = \frac{1-{v_1}^2}{E_1} + \frac{1-{v_2}^2}{E_2} = \frac{1-0{,}3^2}{210000} + \frac{1-0{,}3^2}{210000} = 8{,}66\cdot 10^{-6} \qquad \text{Eq. 10-8}$$

The half of the contact width is:

$$b = \sqrt{\frac{2\cdot P\cdot\Delta}{L\cdot\pi\cdot\left(\frac{1}{R_1}+\frac{1}{R_2}\right)}} = \sqrt{\frac{2\cdot 439500\cdot 8{,}66\cdot 10^{-6}}{84\cdot\pi\cdot\left(\frac{1}{53}+\frac{1}{-54}\right)}} = 9mm \qquad \text{Eq. 10-9}$$

The maximum contact pressure is:

$$p_o = \sigma_c = \frac{2 \cdot P}{\pi \cdot L \cdot b} = \frac{2 \cdot 439500N}{\pi \cdot 84mm \cdot 9\ mm} = 370\ MPA \qquad \text{Eq. 10-10}$$

The numerical solution is illustrated in the fig bellow:

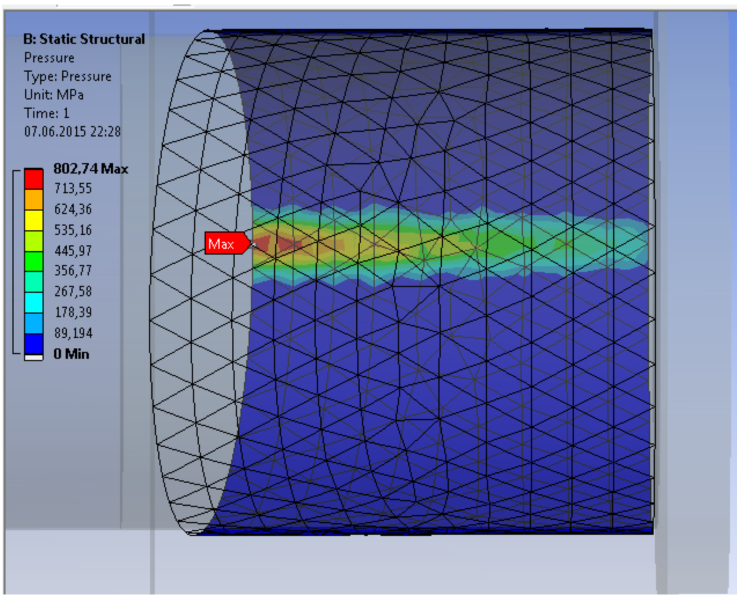

Figure 10-4 Contact pressure on the padeye

The result is far from the numerical solutions, the Herzian contact stress assumes constant pressure throughout the length. The contact stress is twice as big as the max pressure derived from Herzian contact equation. FE calculation has the strongest impact at the start of the contact range with almost twice as value of the Herzian contact stress calculation. This is due the fact that the contact in Ansys in not linear.

10.1.3 Contact area

The contact stress is defined as σ_{yy} . Comparing with the contact stress Figure 10-4, the table above it can be seen that the normal forces are not equal for both sides of the padeye. This triggers a bending moment around Y axis giving compression which gives higher σ_{yy} than Figure 10-4. The pin have lower normal stresses, but still much higher stress than the analytical calculation .It seems that there is little relation between the analytical and the numerical in the contact region. They are based on different in two different assumption giving various results. The only viable explanation is poor representation of the contact area in the FE – element model due to coarse mesh and use of elements not appropriate to describe contact. Unfortunately this is a limitation of the academic Ansys license. For this reason, it was not possible to do a sensitivity study of change in stresses as a function of mesh density. To overcome this problem, one should use a special purpose contact elements, defines by Ansys as INFLATION, which is believed to give more accurate contact results, but required a fine mesh. Further, an assumption was made that the model in itself is correct giving stresses higher compared to the analytical calculation.

Table 10-1 Normal stress for the contact area and pin

Normal stress in Y direction : Padeye	Normal stress in Y direction : Pin
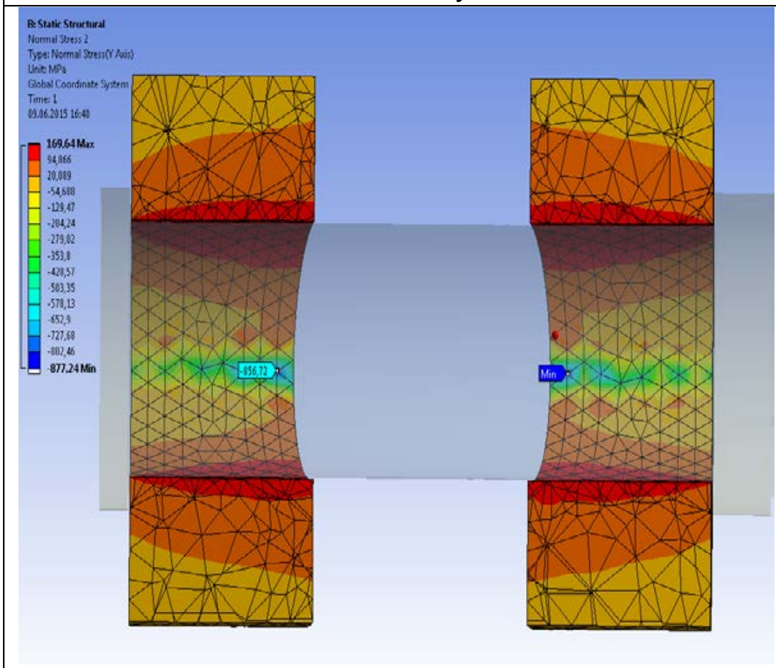	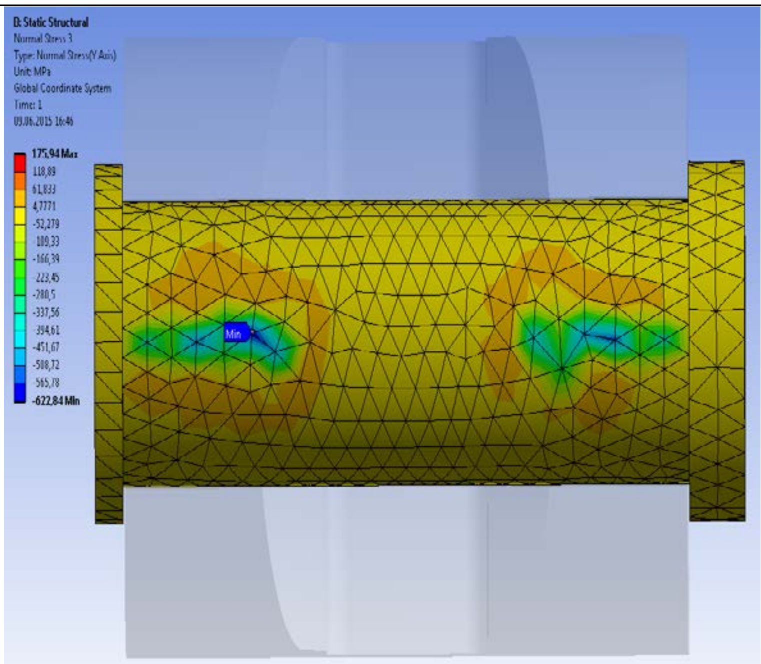

10.2 ULS CALCULATION

The ULS calculation is based on the action factor in section 9.1.1. The load applied on the shackle is assumed to be environmental load. The combination II will give the most critical load condition giving:

$$F = 1.3 \cdot max \text{ load case} = 1.3 \cdot 676 \text{ KN} = 878.8 \text{ KN} \qquad \text{Eq. 10-11}$$

The utilization ratio against yield capacity (i.e. degree of utilization of yield) of shackle design concept (i.e. shackle geometry) was obtained by dividing the maximum von Mises equivalent stress which given from the FE analysis by the allowable stress value 508.MPa

10.2.1 Model 1

The figure below show the von Mises stress for the padeye and pin. The most critical area on the padeye is on the tip of the contact area giving 542 MPa. Same location on the pin giving 319 MPa. It also describes the max Von Mises in the bending zone giving 203.6 MPa.

Table 10-2 Von Mises stress on model 1

Equivalent stress : Padeye	Equivalent stress : Pin
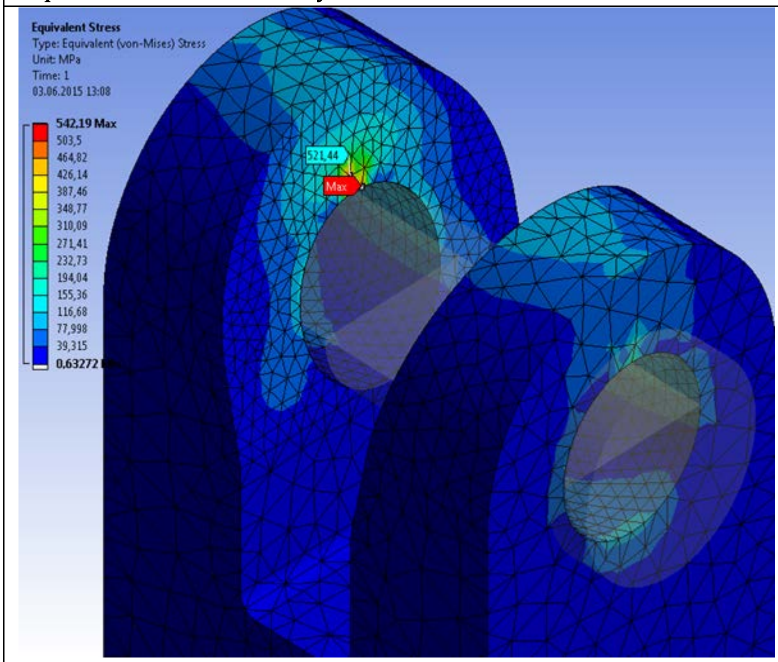	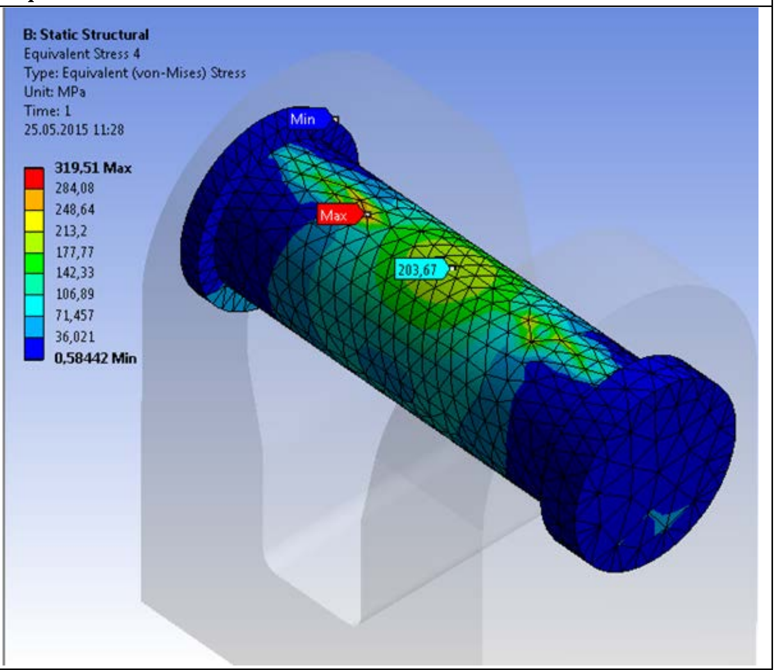
$Utulity\ factor : \frac{542}{508} = 1.06$	$Utulity\ factor : \frac{320}{508} = 0{,}63$

10.2.2 Model 2

This model show the von Mises stress with uniform corrosion on the shackle. The stresses increase almost with 200 MPa in both members. This cause both members fail according to yielding criterion.

Table 10-3 Von Mises stress on model 2

Equivalent stress : Padeye	Equivalent stress : Pin
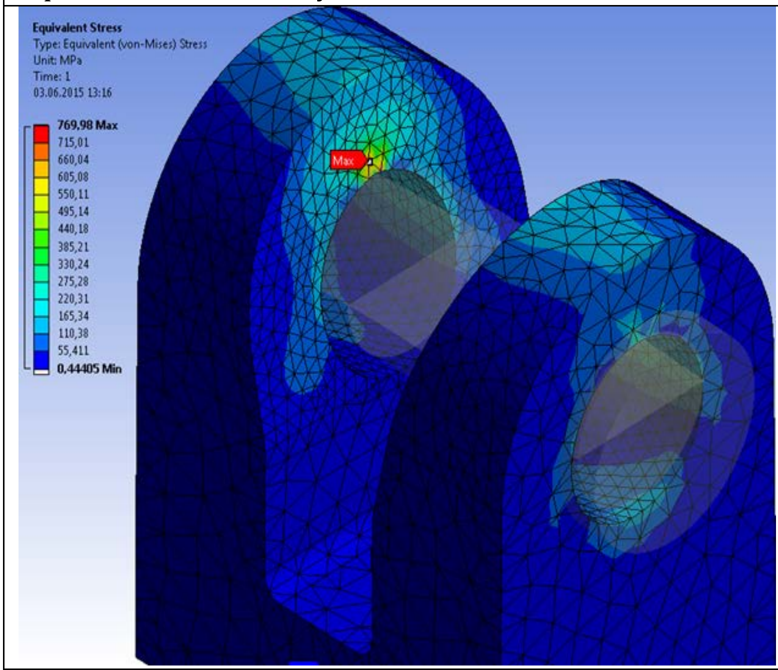	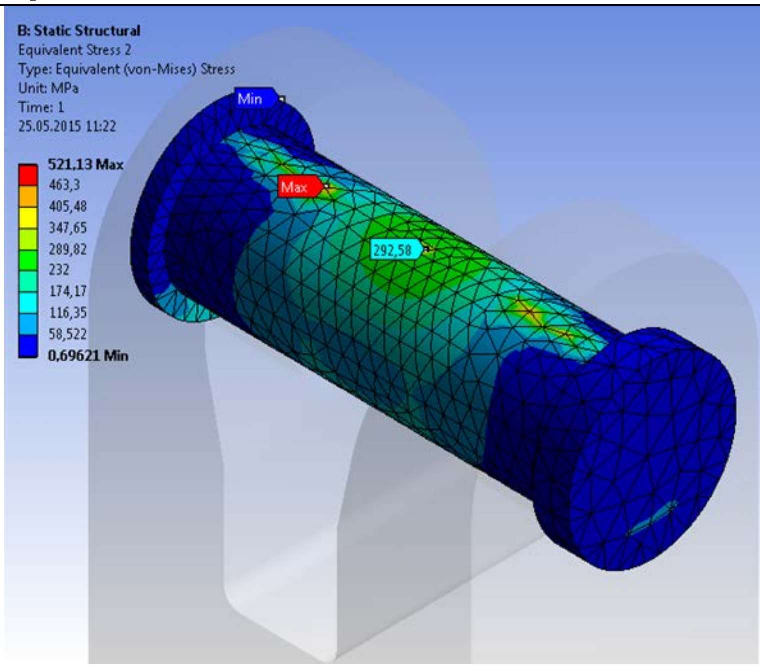
$Utility\ factor : \dfrac{770}{508} = 1.52$	$Utulity\ factor : \dfrac{521}{508} = 1.03$

10.2.3 Model 3

This model show the Von Mises result with uniform corrosion and applied crack as a consequence of fretting between the padeye and pin. The stresses rises near the cracks due to stress concentration giving 872 MPa.

Table 10-4 Von Mises stress for model 3

<table>
<tr><td>Equivalent stress : Padeye</td><td>Equivalent stress : Pin</td></tr>
<tr><td>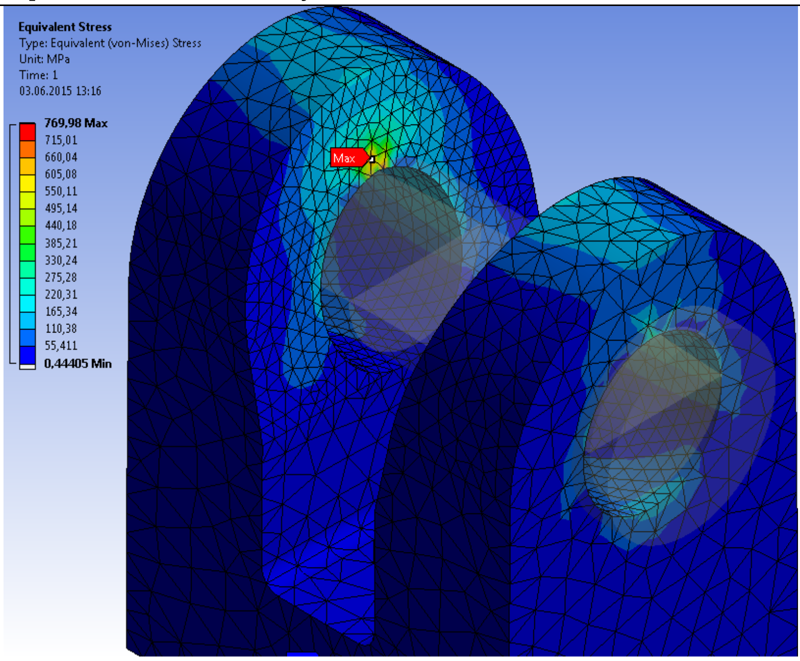
</td><td>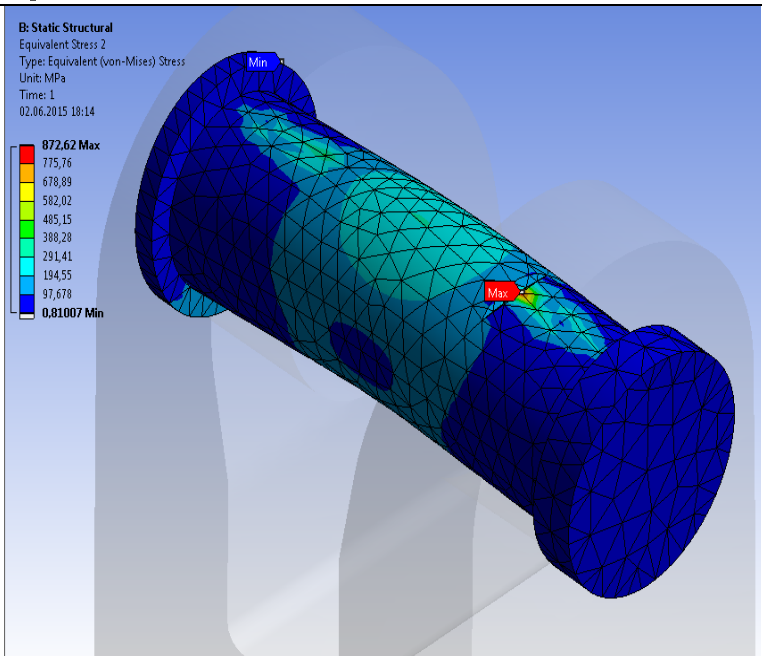
</td></tr>
<tr><td>$Utulity\ factor: \frac{770}{508} = 1.52$</td><td>$Utulity\ factor: \frac{873}{508} = 1.71$</td></tr>
</table>

10.3 FATIGUE CALCULATION

The fatigue calculation of the shackle is based on critical selected point in pin and pad eye. Stresses near the pinhead and the nut are neglected because of lack of knowledge of the connection and interaction in this area. In the reality the pin is allowed to slide sideways, leading to reduction of the stresses compared to high stresses when in case of locked position of the pin assumed in the models. A analytical and numerical fatigue analysis will be provided. The analytical stress are calculated from chapter 10.1 and this will provide foundation for comparing the results from the static analysis and numerical result. The calculations will be based on separating the system in two members, pin and pad-eye. The procedure for calculation fatigue is :

1. Choose CLASSIFICATION OF STRUCTURAL DETAILS from Appendix A from DNV-RP-C203. (F1)

2. Calculate the analytical stress for critical point from Appendix A

3. Retrieve stresses in the padeye and pin from FEM analysis

4. Using design curves from DNV-RP-C203 with selected calculated stress to determine the number of cycles to failure.

10.3.1 Pin

DNV does not offer a construction detail for bolts in bending, hence just for bolt in pure tension or shear is assumed. Therefore, the fatigue design of pin will be based on max shear stress. Structural detail used for the pin chosen from Appendix a, table A-2. From DNV-RP-C203. For bolts subject to shear loading the following methodology may be used for fatigue assessment .Then number of cycles to failure can be derived from:

$$\log \mathrm{N} = 16.301 + 5 \cdot \log \Delta\sigma \qquad \text{Eq. 10-12}$$

The analytical shear stress will be obtained from the Herzian contact stress. For the numerical analysis the shear stress will be extracted from the FE- analysis using sampling tool (probe) in ANSYS.

10.3.2 Padeye

The S-N Curve D is recommended to use for welded geometries and C is recommended to use for cast design geometries in order to allow for weld repairs after possible casting defects and possible fatigue cracks after some service life. Curve C will be used for the pad-eye. The SN-Curve without any cathodic protection, i.e. free to corrode is used. DNV does not specify which stress to use from FE analysis, but recommended practices relate to use of max principal stress in tension. The maximum principal stress is considered to be a significant parameter for analysis of fatigue crack growth. It is normally, assumed that compressive stresses do not contribute to crack propagation

10.3.3 Model 1

10.3.3.1 Analytical fatigue analysis on the Pin.

Von-misses stress result shows that the critical stresses is in the contact area. A large surface of the pin is under contact, so a fatigue check for this area will be more realistic. Using shear stress derived from Herzian contact stress gives under normal operation:

Max load:

$$\tau_{max} = 0.3 \cdot p_o \qquad \text{Eq. 10-13}$$

$$\tau_{max} = 0.3 \cdot 319 \text{ MPa} = 95.8 \text{ MPa} \qquad \text{Eq. 10-14}$$

Min load:

$$\tau_{max} = 0.3 \cdot p_o \qquad \text{Eq. 10-15}$$

$$\tau_{max} = 0.3 \cdot 107 \text{ MPa} = 37.5 \text{ MPa} \qquad \text{Eq. 10-16}$$

The mean stress is not zero because the shackle is always in tension. Hence use of Goodman relation to convert the result to mean stress equal to zero:

Amplitude stress:

$$\tau_a = \frac{\tau_{max} - \tau_{min}}{2} = \frac{95.8\ MPa - 37.5\ MPa}{2} = 29.2\ MPa \qquad \text{Eq. 10-17}$$

Means stress:

$$\tau_m = \frac{\tau_{nom\_max} + \tau_{nom\_min}}{2} = \frac{98.8\ MPa + 37.5\ MPa}{2} = 66.7\ MPa \qquad \text{Eq. 10-18}$$

The Goodman relation :

$$\tau_{\mathrm{a}\_\tau_{\mathrm{m}=0}} = \frac{\tau_{\mathrm{a}}}{(1 - \frac{\tau_{\mathrm{m}}}{\sigma_{\mathrm{u}}})} = \frac{29.2}{(1 - \frac{66.7}{860})} = 31.6 \text{ MPa} \qquad \text{Eq. 10-19}$$

Giving stress range:

$$\Delta\tau_{nom} = 2 \cdot \tau_{\tau_{\mathrm{m}=0}} = 2 \cdot 31.6\ MPa = 63.2\ MPa \qquad \text{Eq. 10-20}$$

Number of cycles to failure for stress range:

$$N = \frac{\tilde{\hat{a}}}{\Delta\sigma^m} = \frac{\tilde{\hat{a}}}{\Delta\sigma^m} = \frac{10^{16.301}}{34.6^{\ 5}} 19837599\ \mathrm{MPa} \qquad \text{Eq. 10-21}$$

Using the same approach as above giving number to cycles to failure:

Table 10-5 Fatigue calculation based on contact shear stress for model 1

Load case	τ_{max}	τ_{min}	τ_a	τ_m	$\tau_{a\_\sigma_{m=0}}$	$\Delta\tau_{nom}$	N	$\frac{1}{DDF}\cdot N$
Normal Operation	95,8	37,5	29,2	66,7	31,6	63,2	19837599	**1983760**
Abnormal Operation	95,8	39,8	28,0	67,8	30,4	60,8	24084731	**2408473**
Extreme Operation	96,5	34,8	30,9	65,7	33,4	66,8	15036315	**1503632**

10.3.3.2 Numerical fatigue analysis of the pin:

The criteria for this analysis are the max shear stress are x-y plane. The table below shows the max shear stress in a pin for different load-case. The output of the shear stress is based on counterforce direction. This is giving the max shear stress value and will be in the same direction as crack formation.The table shows the max and min -stress in most critical point. (The blue point in the figure).

Table 10-6 Stress ratio between max shear stress and yielding stress

	Stress ratio between max shear and yielding capacity from FEA on the pin						
Load : 666 KN	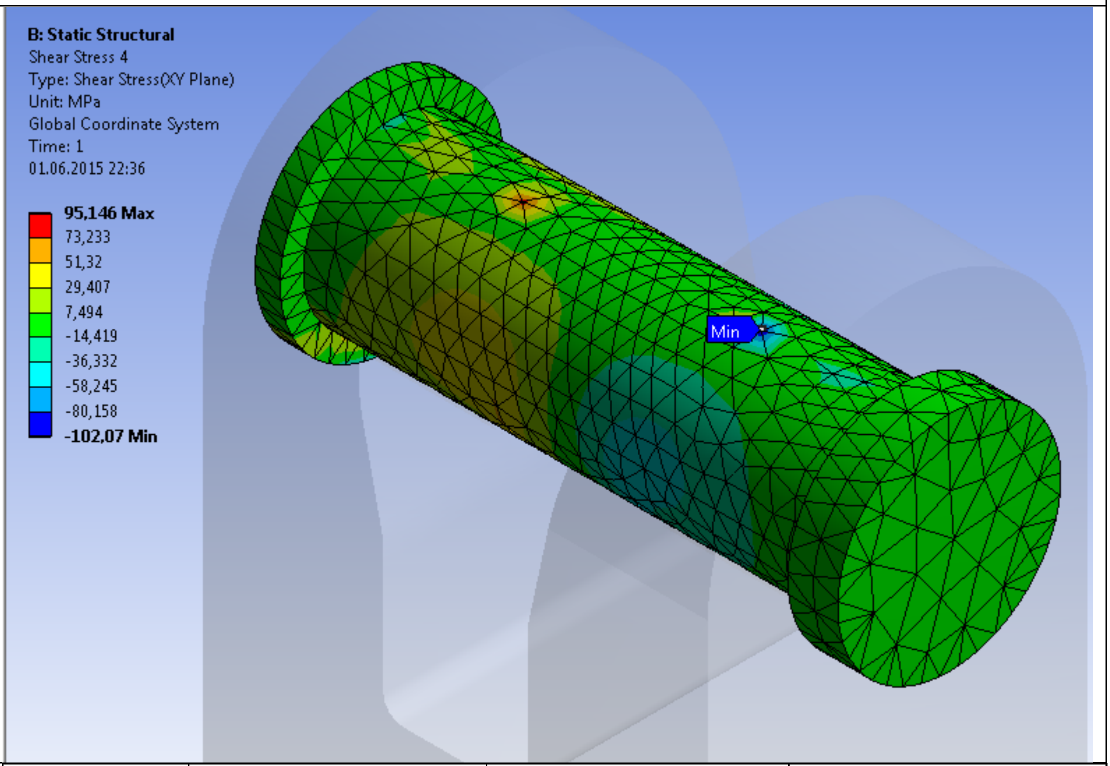						
	Load case	Normal Operation		Extreme Operation		Abnormal Operation	
		Max load 666 KN	Min load 75 KN	Max load 665 KN	Min load 115 KN	Max load 676 KN	Min load 88 KN
		$\sigma_{Max\ P}$	$\sigma_{Max\ P}$	$\sigma_{Max\ P}$	$\sigma_{Max\ P}$	$\sigma_{Max\ P}$	$\sigma_{Max\ P}$
		102 MPa	11 MPa	102 MPa	19MPa	109 MPa	14 MPa

The mean stress is not zero because the shackle is always in tension. Hence use of Goodman relation to convert the result to mean stress equal to zero:

Amplitude stress:

$$\sigma_a = \frac{\sigma_{max\_shear} - \sigma_{min\_shear}}{2} = \frac{102 \text{ MPa} - 11 \text{ MPa}}{2} = 45.5 \; MPa \qquad \text{Eq. 10-22}$$

Means stress:

$$\sigma_m = \frac{\sigma_{max\_shear} + \sigma_{min\_shear}}{2} = \frac{102 \; MPa + 11 \text{ MPa}}{2} = 56.5 \text{ MPa} \qquad \text{Eq. 10-23}$$

The Goodman relation :

$$\sigma_{a\_\sigma_{m=0}} = \frac{\sigma_a}{(1 - \frac{\sigma_m}{\sigma_u})} = \frac{45.5}{(1 - \frac{56.5}{860})} = 48.7 \text{ MPa} \qquad \text{Eq. 10-24}$$

Giving stress range:

$$\Delta\sigma = 2 \cdot \sigma_{a_{\sigma_{m=0}}} = 2 \cdot 48.7 \; MPa = 97.4 \text{ MPa} \qquad \text{Eq. 10-25}$$

Number of cycles to failure $\Delta\sigma$:

$$N = \frac{\tilde{\hat{a}}}{\Delta\sigma^m} = \frac{\tilde{\hat{a}}}{\Delta\sigma^m} = \frac{10^{16.301}}{97.4^{\,5}} = 228155 \qquad \text{Eq. 10-26}$$

The table below show the result for all load case:

Table 10-7 Fatigue calculation based on FEA stress for model 1

Load case	σ_a	σ_m	$\sigma_{a\_\sigma_{m=0}}$	$\Delta\sigma$	N	$\frac{1}{DDF} \cdot N$
Normal Operation	45,5	56,5	48,7	97,4	2281551	**228155**
Abnormal Operation	41,5	60,5	44,6	89,3	3525410	**352541**
Extreme Operation	47,5	61,5	51,2	102,3	1783464	**178346**

10.3.3.3 *Analytical analysis of the padeye*

Because the contact stresses are compressive, it is assumed that highest tension stresses are near the holes. This area has a potential for crack formation.Accurate result in that region is hard to detect by simple hand calculation due curves beam and bending moment around the Y-axis. Therefore the analytical stress range will be determined by reaction force deduced from the static analysis. The estimated width w of the impact of the vertical stress is approximately 180 mm. giving the normal analytical stress in the padeye:

Max load:

$$\sigma_{nom} = \frac{Wa}{(w-2r)\cdot t} = \frac{333000\ N}{(180-106)\cdot 96} = 46{,}9\ Mpa \qquad \text{Eq. 10-27}$$

The stress concentration around the hole.

$$\sigma_{SCF} = 3\cdot\sigma_{nom} = 141\ MPa \qquad \text{Eq. 10-28}$$

Min load:

$$\sigma_{nom} = \frac{Wa}{(w-2r)\cdot t} = \frac{37500\ N}{(180-106)\cdot 96} = 5.3\ Mpa \qquad \text{Eq. 10-29}$$

The stress concentration around the hole.

$$\sigma_{SCF} = 3\cdot\sigma_{nom} = 16\ MPa \qquad \text{Eq. 10-30}$$

The mean stress is not zero because the shackle is always in tension. Hence use of Goodman relation to convert the result to mean stress equal to zero:

Amplitude stress:

$$\sigma_a = \frac{\sigma_{max}-\sigma_{min}}{2} = \frac{141\ KN - 16\ KN}{2} = 62.5\ MPa \qquad \text{Eq. 10-31}$$

Means stress:

$$\sigma_m = \frac{\sigma_{max}+\sigma_{min}}{2} = \frac{141\ \mathrm{KN} + 16\ \mathrm{KN}}{2} = 78.5\ \mathrm{MPa} \qquad \text{Eq. 10-32}$$

The Goodman relation :

$$\sigma_{a\_\sigma_{m=0}} = \frac{\sigma_a}{(1-\frac{\sigma_m}{\sigma_u})} = \frac{48}{(1-\frac{78.5}{860})} = 68.8\ MPa \qquad \text{Eq. 10-33}$$

Giving stress range:

$$\Delta\sigma = 2 \cdot \sigma_{a_{\sigma_{m=0}}} = 2 \cdot 68.8\ \mathrm{MPa} = 137.6\ \mathrm{MPa} \qquad \text{Eq. 10-34}$$

Number of cycles to failure for stress range $\Delta\sigma$:

$$\mathrm{N} = \frac{\tilde{\hat{a}}}{\Delta\sigma^{m}} = \frac{\tilde{\hat{a}}}{\Delta\sigma^{m}} = \frac{10^{12.115}}{137.6^{3}} = 500682 \qquad \text{Eq. 10-35}$$

The table below show the result using same approach

Table 10-8 Calculation based on concentrated stress near the hole on padeye for model 1

Load case	σ_a	σ_m	$\sigma_{a\_\sigma_{m=0}}$	$\Delta\sigma$	N	$\frac{1}{DDF}\cdot N$
Normal Operation	62,5	78,5	68,8	137,6	**500682**	**50068**
Abnormal Operation	58,5	82,5	64,7	129,4	**601241**	**60124**
Extreme Operation	62,2	80,9	68,6	137,2	**504608**	**50460**

10.3.3.4 Numerical fatigue analysis of padeye

The table below show maximum principal stress on padeye for model 1.

Table 10-9 Max principal stress on padeye for model 1

	Max principle stress from Ansys FEA on the pad-eye
Load : 666 KN	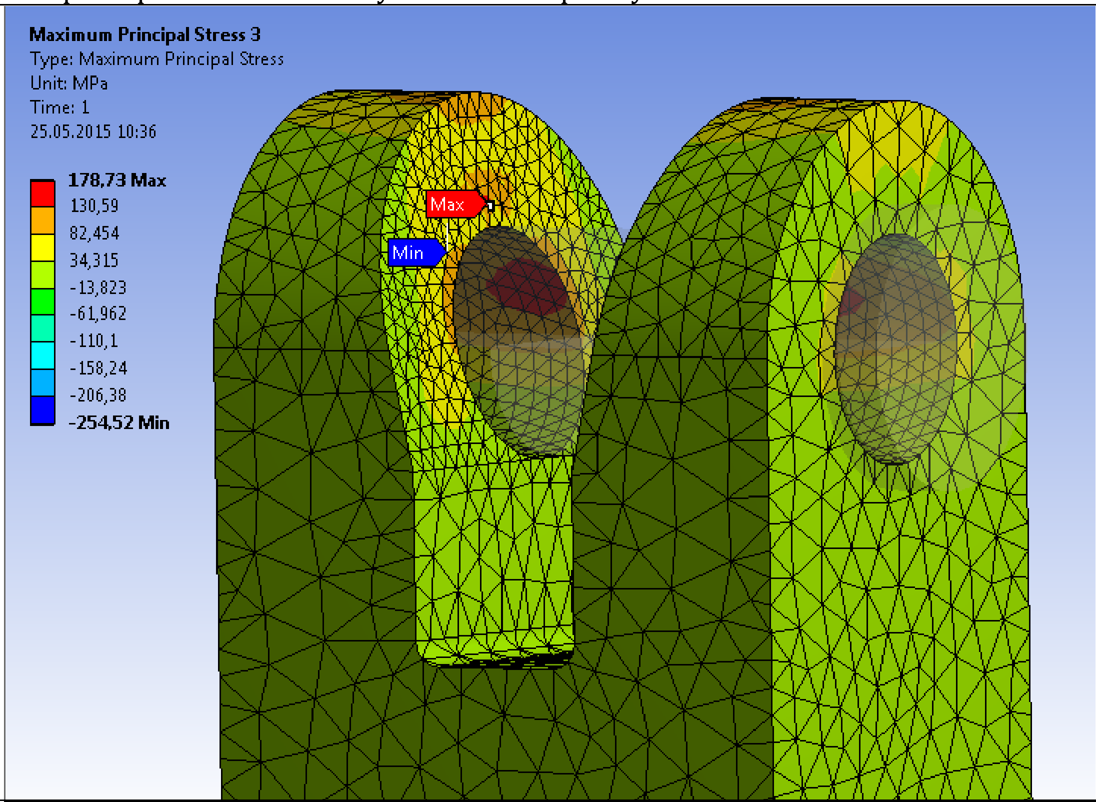

Load case	Normal Operation		Extreme Operation		Abnormal Operation	
	Max load	Min load	Max load	Min load	Max load	Min load
	666 KN	75 KN	665 KN	115 KN	676 KN	88 KN
	$\sigma_{Max\,P}$	$\sigma_{Max\,P}$	$\sigma_{Max\,P}$	$\sigma_{Max\,P}$	$\sigma_{Max\,P}$	$\sigma_{Max\,P}$
	179 MPa	26 MPa	179 MPa	39 MPa	181 MPa	30 MPa

Fatigue calculation for the normal operation based on equations in chapter 6:

Amplitude stress:

$$\sigma_a = \frac{\sigma_{max} - \sigma_{min}}{2} = \frac{179\ \text{KN} - 26\ \text{KN}}{2} = 76.5\ \text{MPa} \qquad \text{Eq. 10-36}$$

Means stress:

$$\sigma_m = \frac{\sigma_{max} + \sigma_{min}}{2} = \frac{179\ \text{MPa} + 26\ \text{MPa}}{2} = 102{,}5\ \text{MPa} \qquad \text{Eq. 10-37}$$

The Goodman relation :

$$\sigma_{a\_\sigma_{m=0}} = \frac{\sigma_a}{(1-\frac{\sigma_m}{\sigma_u})} = \frac{76.5}{(1-\frac{102.5}{860})} = 86.9\ \text{MPa} \qquad \text{Eq. 10-38}$$

Giving stress range:

$$\Delta\sigma = 2 \cdot \sigma_{a_{\sigma_{m=0}}} = 2 \cdot 86.9\ \text{MPa} = 173.7\text{MPa} \qquad \text{Eq. 10-39}$$

Number of cycles to failure for $\Delta\sigma$:

$$\text{N} = \frac{\tilde{\hat{a}}}{\Delta\sigma^{m}} = \frac{\tilde{\hat{a}}}{\Delta\sigma^{m}} = \frac{10^{12.115}}{155^{\ 3}} = 248644 \qquad \text{Eq. 10-40}$$

The table below show the result using same approach

Table 10-10 Fatigue analysis based on max principal stress for model 1

Load case	σ_a	σ_m	$\sigma_{a\_\sigma_{m=0}}$	$\Delta\sigma$	N	$\frac{1}{DDF}\cdot N$
Normal Operation	76,5	102,5	86,9	173,7	**248644**	**24864**
Abnormal Operation	70,0	109,0	80,2	160,3	**316257**	**31626**
Extreme Operation	75,5	105,5	86,1	172,1	**255595**	**25560**

10.3.4 Model 2

10.3.4.1 Analytical analysis on pin

Same approach is used for this model to calculate number of circles to failure with 2mm uniform corrosion.

Table 10-11 Fatigue analysis based on contact shear stress for model 2

Load case	τ_{max}	τ_{min}	τ_a	τ_m	$\tau_{a\_\sigma_{m=(}}$	$\Delta\tau$	N	$\frac{1}{DDF}\cdot N$
Normal Operation	168,0	56,4	55,8	112,2	64,2	128,3	574267	**57427**
Abnormal Operation	168,0	69,8	49,1	118,9	57,0	114,0	1040721	**104072**
Extreme Operation	169,2	61,1	54,1	115,2	62,4	124,8	660273	**66027**

10.3.4.2 Numerical fatigue analysis on pin

The table below shows the shear stress on x-y plane for model 2.

Table 10-12 Fatigue analysis based on contact shear stress for model 2

	Stress ratio between max shear and yielding capacity from FEA on the pin						
Load : 666 KN	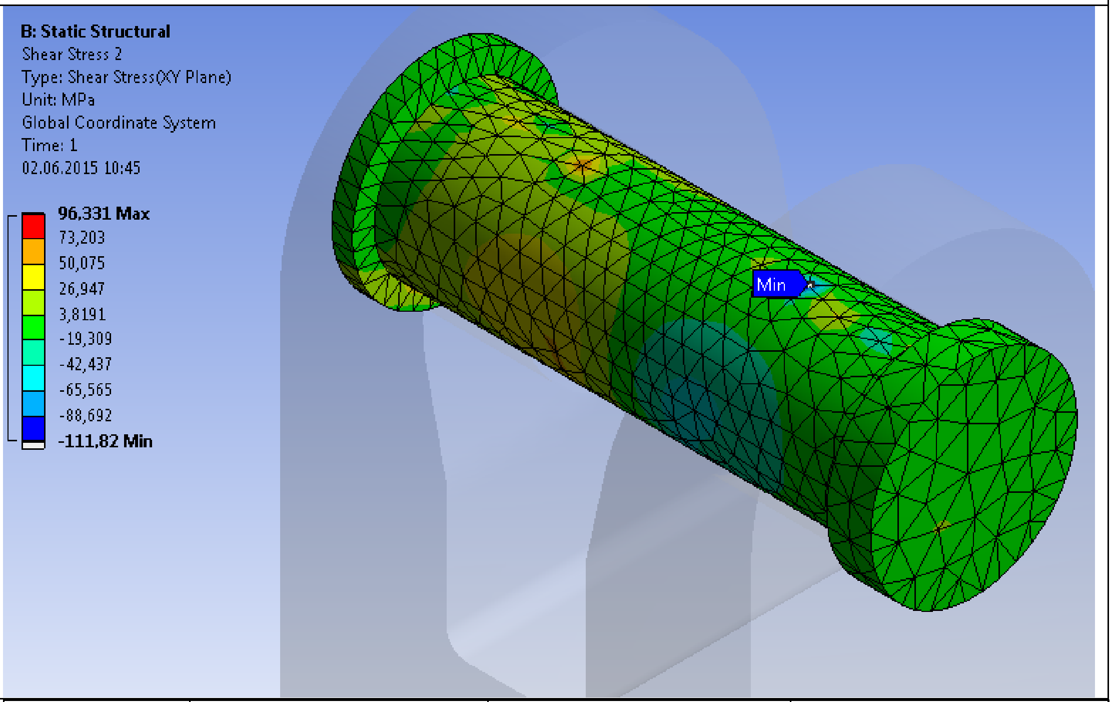						
	Load case	Normal Operation		Extreme Operation		Abnormal Operation	
		Max load 666 KN	Min load 75 KN	Max load 665 KN	Min load 115 KN	Max load 676 KN	Min load 88 KN
		$\sigma_{Max\,P}$ 112 MPa	$\sigma_{Max\,P}$ 20 MPa	$\sigma_{Max\,P}$ 112 MPa	$\sigma_{Max\,P}$ 29 MPa	$\sigma_{Max\,P}$ 113 MPa	$\sigma_{Max\,P}$ 23 MPa

Result for all load cases:

Table 10-13 Fatigue analysis based on FE max shear stress for model 2

Load case	τ_a	τ_m	$\tau_{a\_\tau_{m=0}}$	$\Delta\tau$	N	$\frac{1}{DDF}\cdot N$
Normal Operation	46,0	66,0	49,8	99,6	2035500	203550
Abnormal Operation	41,5	70,5	45,2	90,4	3310381	331038
Extreme Operation	45,0	68,0	48,9	97,7	2243474	227347

10.3.4.3 *Analytical fatigue analysis on padeye*

Result on table 2 are derived in same way as model, using the stress concentration near holes as criteria for fatigue. The result is summarized below:

Table 10-14 Fatigue analysis based concentrated stress near the hole on padeye for model 2

Load case	σ_{max}	σ_{min}	σ_a	σ_m	$\sigma_{a\_\sigma_{m=0}}$	$\Delta\sigma$	N	$\frac{1}{DDF} \cdot N$
Normal Operation	141	16,0	69,6	87,4	77,5	154,9	252610	25261
Abnormal Operation	141	24,0	64,9	92,2	72,6	145,3	306559	30656
Extreme Operation	143	18,7	69,7	90,6	77,9	155,8	248412	24841

10.3.4.4 *Numerical fatigue analysis on padeye*

The table below shows the max principal stress on padeye for model 2

Table 10-15 Max principal stress on padeye for model 2

<table>
<tr><td></td><td colspan="7">Max principle stress from Ansys FEA on the pad-eye</td></tr>
<tr><td>Load : 666 KN</td><td colspan="7">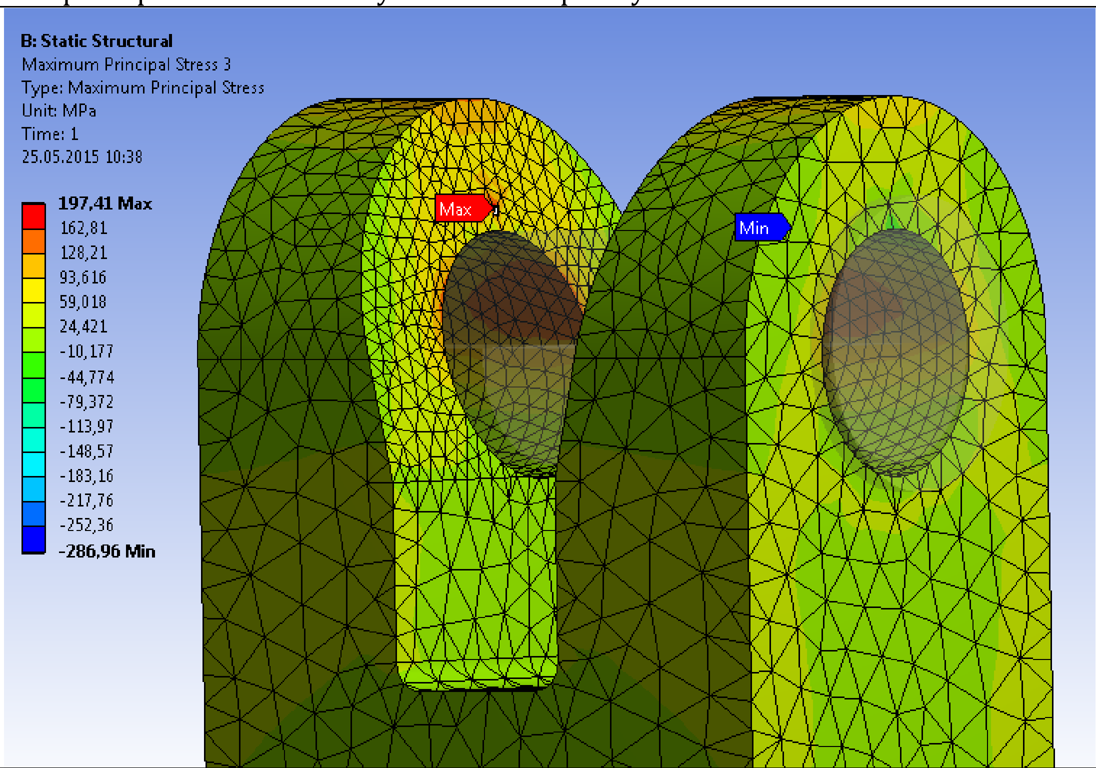
</td></tr>
<tr><td></td><td>Load case</td><td colspan="2">Normal Operation</td><td colspan="2">Extreme Operation</td><td colspan="2">Abnormal Operation</td></tr>
<tr><td></td><td></td><td>Max load</td><td>Min load</td><td>Max load</td><td>Min load</td><td>Max load</td><td>Min load</td></tr>
<tr><td></td><td></td><td>666 KN</td><td>75 KN</td><td>665 KN</td><td>115 KN</td><td>676 KN</td><td>88 KN</td></tr>
<tr><td></td><td></td><td>$\sigma_{Max\ P}$</td><td>$\sigma_{Max\ P}$</td><td>$\sigma_{Max\ P}$</td><td>$\sigma_{Max\ P}$</td><td>$\sigma_{Max\ P}$</td><td>$\sigma_{Max\ P}$</td></tr>
<tr><td></td><td></td><td>197 MPa</td><td>28 MPa</td><td>197 MPa</td><td>41 MPa</td><td>200 MPa</td><td>32MPa</td></tr>
</table>

Result for different load cases:

Table 10-16 Fatigue analysis based on max principal stress for model

Load case	σ_a	σ_m	$\sigma_{a\_\sigma_{m=0}}$	$\Delta\sigma$	N	$\frac{1}{DDF}\cdot N$
Normal Operation	86	112	99	198	**168509**	**16851**
Abnormal Operation	79	118	92	183	**212200**	**21220**
Extreme Operation	85	115	98	196	**172436**	**17244**

10.3.5 Model 3

10.3.5.1 Numerical analysis on Pin

No analytical analysis has been carried out in the crack area. The contact stress and friction force in the contact area make it hard to determine the analytical stress to calculate the intensity factor K. This will not allow to calculate the shear stress near the near the crack to determine the number of cycles to failure. The fatigue calculations on this model will be based the numerical results. The crack on the pin did not show any significant change on the padeye, and therefore choose not to perform analysis on padeye because model 2 gives a good approximation.The table below shows the shear stress on pin in x-y plane.

Table 10-17 stress ratio between max shear stress and yielding stress for model 3

	Max principle stress from Ansys FEA At the Center of the Pin						
Load : 666 KN	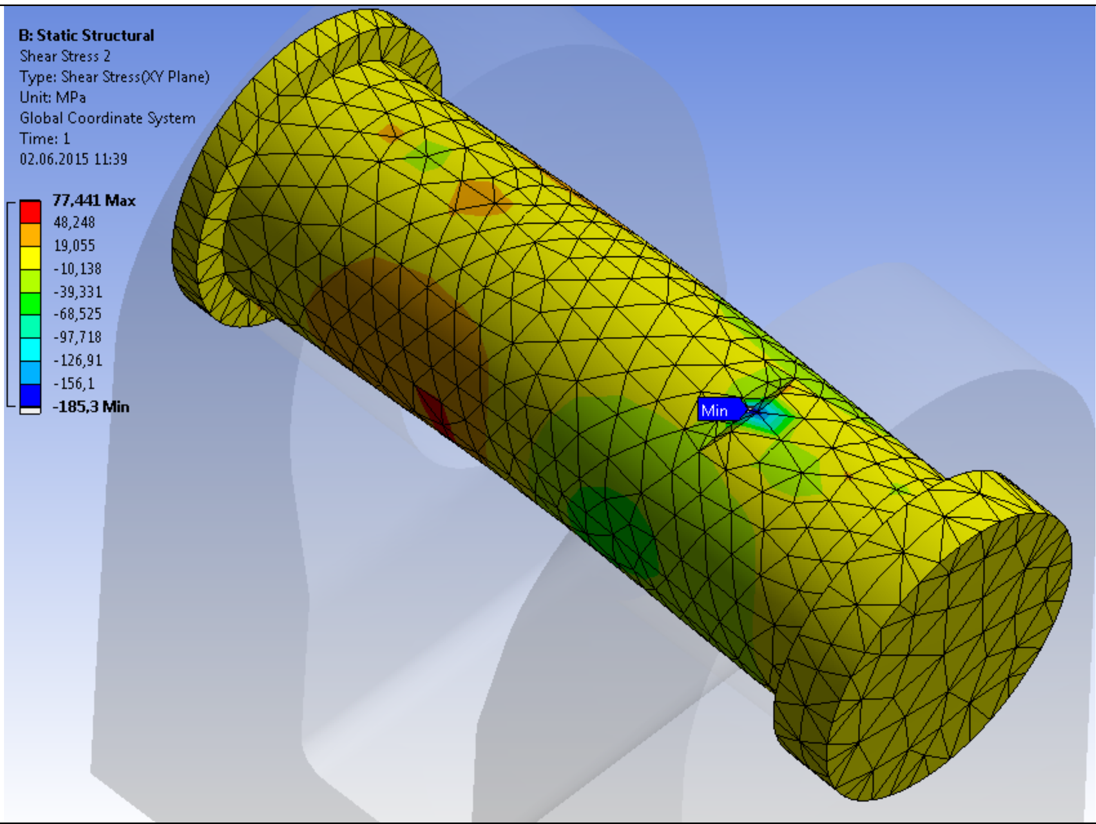						
	Load case	Normal Operation		Extreme Operation		Abnormal Operation	
		Max load	Min load	Max load	Min load	Max load	Min load
		666 KN	75 KN	665 KN	115 KN	676 KN	88 KN
		$\sigma_{Max\ P}$	$\sigma_{Max\ P}$	$\sigma_{Max\ P}$	$\sigma_{Max\ P}$	$\sigma_{Max\ P}$	$\sigma_{Max\ P}$
		185 MPa	26 MPa	185 MPa	38 MPa	188 MPa	30 MPa

Result for different load cases:

Table 10-18 Fatigue analysis based on FE max shear stress for model 3

Load case	τ_a	τ_m	$\tau_{a\_\tau_{m=0}}$	$\Delta\tau$	N	$\frac{1}{DDF}\cdot N$
Normal Operation	79,5	105,5	90,6	181,2	102287	**10229**
Abnormal Operation	73,5	111,5	84,4	168,9	145506	**14551**
Extreme Operation	79,0	109,0	90,5	180,9	103139	**10314**

11 DISCUSSION OF THE RESULTS

11.1 ULS CHECK

The capacities found by using von Mises yield criterion are much lower than the proof load and minimum breaking load specified by Appendix A. For instance, the plastic capacities of the shackle is found by the result to be less than 666 KN. By comparison, the proof load is the minimum breaking load specified as 6000 KN for the shackle. This shows that load capacities cannot be found with formulas based on classic failure theory. Using yield strength as failure criterion will give a conservative result, predicting failure before reaching the utilized max capacity. The minimum breaking load are determined both with experimentally and with empirical formulas.

The ULS result illustrate small plastic yielding restricted to a small area, this produces permanent deformation so that the strain is in the plastic range. Yielding in these areas will produce local residual stresses after loading is decreased.Under cycles loading the plastic area will expand which may cause prematurely failure due to crack formation and growth.In the first model the results show that the majority of the stress levels in the shackle are in the range of 300-450 MPa which is below the maximum allowable stress of 501 MPa. However there are small areas in the contact region with high local stresses reaching Von Mises stresses as high as 542 MPa. Plasticity doesn't occur at the surface, According to (Hearn, 1997) specimens show that commences sub-surface yielding occur when the contact stresses approach 1.2 σ_{ys} .Using so-called "uncontained plastic flow" yielding starts when the stresses reach 2.8 σ_{ys} .Only in this point the material will "escape". The overall criteria for initiating the yielding is 609 MPa .According to Hearn the model results shown no sign of yielding and are in the safe elastic zone. This demonstrate that the yielding criteria from Norsok-001 will be too conservative in the contact area.

In the second model the uniform corrosion decreases the contact area, resulting in higher stresses in the contact region. The Von Mises stress on the padeye increase with 200 MPa. The same increase for the pin leading to Von Mises stress to 521 MPa. This is beyond the allowable stress of 501 MPa. Compering the result with Hearn criteria's, the pin are below the limit of initiating yielding, the plastic deformation will only be occur on the padeye. The hotspot stresses are concentrated on a small area, whether the system fails it unlikely when the MBL is 6000 KN. It is important to note that there are the hazards for crack formation because combination of residual stresses and cycles loading.

In the third model, the padeye is analyzed using same condition as on model 2. The fretting corrosion don't have a sufficient effect on the padeye. The pin shows a significantly increased stress near the crack. The results do not display any sign of yielding under the crack. The crack is too small to trigger aplastic zone. The Von Mises stress is high near the crack due to the concentrated contact. There is a hazard for yielding around the crack. This can the crack growth leading to failure.

Fig 12-1 illustrate the Von Mises stress accumulation for different models. From the graph it seems that there are some relation between Von Mises stress and corrosion rate. A 2 mm uniform corrosion results an increase in Von Mises stress of around 200 MPa. The most critical is the crack formation, the von missis double it value going far beyond the initiating yielding capacity. The crack can expend due to cycles loading which can lead failure.

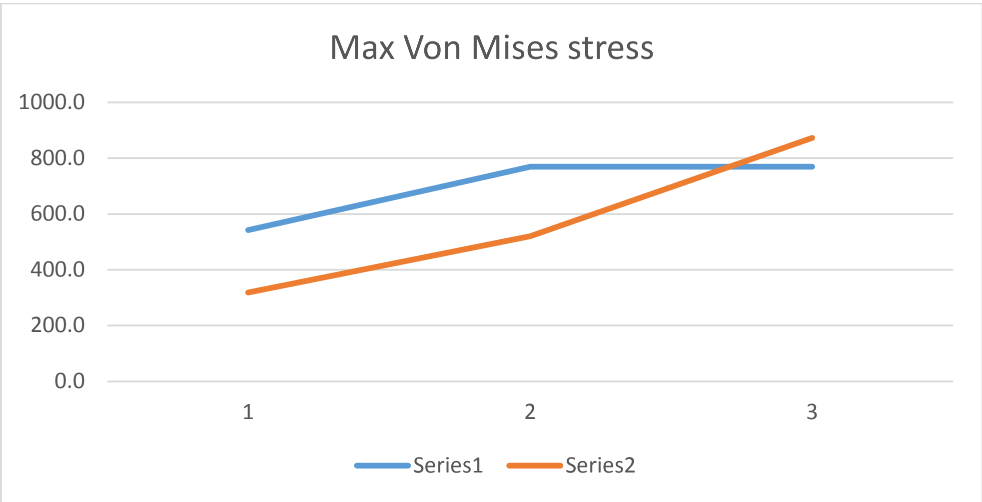

Figure 11-1 Von Mises stress accumulations for different model

11.2 FATIGUE ANALYSIS

The discussion of the fatigue result is for normal operation load case. No accidental load are taken into account.

11.2.1 Analytical Analysis

For the analytical analysis critical areas on the shackles were chosen for the fatigue analysis. For the padeye, it was the concentrated stress on tension near the holes with in the area with a potential for crack formation. For the pin, the shear stress was defined from the Herzian contact stress. From Figure 11-2 it can be seen that the padeye is more vulnerable for fatigue compared to the pin. The pin can receive almost 4 times load cycles before failure.

Model 2 shows the effect of uniform corrosion on the system. The fatigue capacity of the padeye is greatly reduced from 50068 to 25261 numbers of cycles to failure. According to Table 10-8 and Table 10-14, the stress range increases from 138 MPa to 155 MPa which is a consequence of the expansion of the hole and decrease of the width. The pin loses 75 percent of its capacity going from 198476 to 57427 cycles to failure. The uniform corrosion declines the contact area which increases the stress range from $\Delta\sigma = 63$ MPa to $\Delta\sigma = 128$ MPa. By changing the pin diameter to 52 mm and the hole to 55 mm change the max contact pressure increases from 319 MPa to 559 MPa contact stress .Since the shear stress in the contact region is a function of the pressure, it would have a corresponding change.

This calculation indicate the dramatic effect on stress field when loosing small fraction of the material. The fatigue failure on the padeye represents failure alongside the holes, a damage in this area has a major consequence of the integrity of the component. The fatigue calculation of the pin is based on the maximum shear stress theory. It is important to note that the contact pressure has an elliptical distribution with the highest value at the center. This means that number of cycles to failure is described by a thin shear area along the contact range

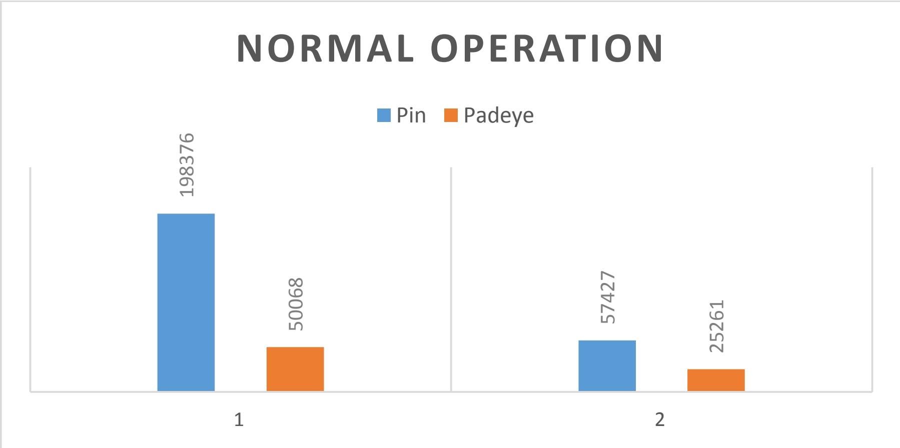

Figure 11-2 Number of cycles to failure for normal operation in model 1 and 2

11.2.2 Numerical Analysis

The result demonstrate that padeye is the most vulnerable to fatigue and withstands about 10 time less number of cycles to failure comparing to that of pin. This could be explained by the fact that the components of the system are analyzed in different ways. The stress used for fatigue life calculation for the padeye is multi-axial max principal stress which takes into account stresses in all three direction. Stresses used for the pin analysis is the highest shear stress in the x-y plane. The lower fatigue life obtained for the padeye could be the consequence of the limitations of the FE analysis (see Verification of the FE model and analysis procedure). The padeye is more vulnerable due to larger concentrated stresses, giving a lower number cycles to failure. The pin is exposed to lower stress which makes it more superior to fatigue damage. The uniform corrosion has almost no effect on pin, whereas crack has a catastrophic effect causing the pin to fail after only 10228 cycles. This means it loses it capacity by 10 times. This results is only based on the shear stress near the crack and is not taking into account the expansion of the crack. That means the failure can happen long before that. There are stresses in other directions witch can be higher making the model component fail sooner. Another threat is the removal of the protective coating due to penetration which make the crack susceptible for corrosion

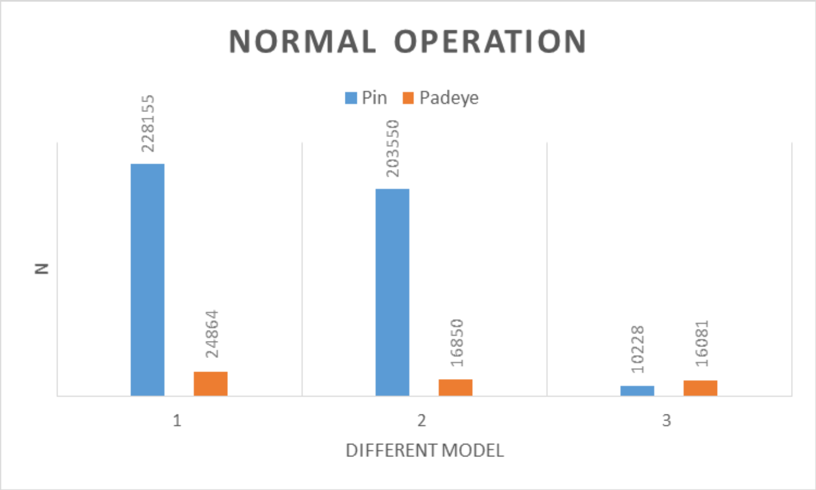

Figure 11-3 Number of cycles to failure for normal operation

11.2.3 Comparison of numerical and analytical results:

Numerical results for the padeye shows that the padeye consume the half of its capacity comparing with analytical calculation. The principal stress increases with almost 20 MPa by applying the uniform corrosion which is nearly the same as the stress obtained by the analytical results. The difference is not captured near the holes. This is because of contact pressure is more localized on the padeye due to the presence of contact stresses taken in FE analysis. Contact stresses are not linear and keeps increasing as approaching the starting positon of contact area. The analytical and numerical results follow the same pattern when implementing the uniform corrosion. It is also important to note that the analytical and the numerical results demonstrate failure at different position. The numerical results shows failure at a contact region o while analytical indicate failure alongside the holes. The area of failure for the analytical result is larger making it more critical. This also shown in Table 10-6 where the max shear stress is not in the same point as the maximum normal stress

(Verification of the FE model and analysis procedure) indicates that the contact stresses on the pin are quite smaller. This will cause a much smaller stress variation and will be results in longer fatigue life.The pin does not experiencethe similar increase in stresses when applying the uniform corrosion, only 10 MPa. This proves that the numerical shear stress don't have the same sensitivity to uniform corrosion. However Appendix B shows a large increase in the contact pressure when applying the uniform corrosion. This means the shear stress in the numerical does not have the same dependency on contact pressure making it hard to directly compare these to results.

It is important to note that the fatigue calculation in both members is obtained from numerical results are based on hotspot stresses. Ansys displays that outcome over a small area and it difficult to conclude if the system fail

11.2.4 Load

Before determining the cycles to failure, it is assumed that the shackle experiences a constant amplitude loading causing a low number of cycles to failure.. The load condition is based on the maximum and minimum measure load. The extreme values cause that component fail in fatigue at low number if cycles.Alternative approach is to use the method of rain flow counting where smaller load variation controls the specter and only a few these extreme values used in this work. This would display a more realistic behavior of the system.

11.3 SN-CURVE

DNV does not offer an SN-curve based on contact stress. The number of cycles to failure is based on SN-diagram witch express failure for different stress range. Failure is defined by the analytical stress range and which is multiplied with an appropriate stress concentration factor. The SN-curves used for the shackle is cast node with free to corrode and bolt in shear. The padeye calculation is more realistic due to taking into account corrosive environment in the SN-curve. For the bolt there is no detailed category for bolt in bending. Closest was bolt in shear, where the criteria was the average shear based on the shank area. In both the numerical and analytical results, the shear stress was used was obtained from the contact region contact region. These are consecrated stresses in small area that can lead to failure before the average shear reaches it limits. Another uncertainty that the SN-curve used for the pin was not defined in corrosive environment.

12 CONCLUSION

The ULS result shows that the shackle can absorb a great amount of energy before failing. The component experiences small yielding under normal condition in the field. Unfortunately it is not the load capacity that imposes the restriction. The load variation subjects the system to great pressure. The number of cycles to failure is based on SN-diagram which express failure for different stress range. In this thesis the stress range has been defined by the contact stress which are localized on small surfaces. Under contact fatigue plastic strain builds up until a crack is created. The crack will grow until a pit is shaped. Once pitting has formed, fracture can result in catastrophic failure. These SN curves do not represent these local failures on the structure. Failures can happen any time before estimated values.

Yielding occur in small areas when the shackle is subjected to corrosion making it vulnerable to crack formation. This means that fatigue calculation should be the dominating parameter to define failure. The results show that uniform and local corrosion have an effect on the integrity on the system. Both numerical and analytical results show that the padeye lose half of it capacity. The pin shows decline with different levels, the numerical results predict 20 present decline while the analytical calculation that the pin loses lose half of its capacity.

The crack formation is the most critical one, showing that the number of cycles to failure is greatly reduced and the pin loses 90 percent of its capacity. This means that if the shackle in field is design to withstand 20 year in service life. The shackle can fail in 2 year in presence if cracks according to the results obtained in this work

13 FURTHER WORK

This study focus on pure tensile load as the only external loading. The shackle in real life are exposed to bending and torsion as well. Further work recommended is better is building model with more accurate contact mechanism is represented. The mesh should have more density catching critical stresses. It also recommended to see effect of local corrosion in the padeye, in high tension region.

It also recommended to try the analysis based on different load scenario. The method that could be used is rain flow method where smaller load variation control the specter and some few who represent the extreme values used in this thesis. This study focus on pure tensile load as the only external loading. The tether system in real life are in some extent exposed to bending and torsion as well. Analyses of shackle subjected to tension in combination with out-of-plane bending when it comes to fatigue, further studies on standards, recommended practices and other regulations are highly recommended.

14 REFERENCE

Adams, V., & Askenazi, A. (1999). *Building better products with finite element analysis*. Santa Fe, N.M: OnWord Press.

Ahmad, Z., & Institution of Chemical, E. (2006). Principles of corrosion engineering and corrosion control (1st ed. ed.). Boston, MA: Elsevier/BH.

Anderson, T. L. (2005). *Fracture mechanics : fundamentals and applications* (3rd ed. ed.). Boca Raton, Fla: Taylor & Francis.

ANSYS. (2010). ANSYS Mechanical Structural Nonlinearities. Retrieved 12.06, 2015, from http://inside.mines.edu/~apetrell/ENME442/Labs/1301_ENME442_lab6_lecture.pdf

Boresi, A. P., & Schmidt, R. J. (2003). *Advanced mechanics of materials* (6th ed. ed.). New York: Wiley.

Cook, R. D. (2002). *Concepts and applications of finite element analysis* (4th ed. ed.). New York: Wiley.

Glaeser, W. A., & S.J. Shaffer. (1996). Contact FatigueASM Handbook (Vol. 19). Battelle Laboratories. Retrieved from http://www.asminternational.org/documents/10192/1849770/06197G_Sample.pdf.

Hearn, E. J. (1997). *Mechanics of Materials: The Mechanics of Elastic and Plastic Deformation of Solids and Structural Materials* (3rd ed ed. Vol. Volume 2). Burlington: Burlington : Elsevier Science.

Hibbeler, R. C., & Fan, S. C. (2008). *Mechanics of materials : SI conversion by S.C. Fan* (7th SI ed. ed.). Singapore: Prentice Hall.

Kitegava, H. (1972). *Corrosion Fatigue, Chemistry, Mechanics and Microstructure,* . Houston: O. Devereux et al. eds. NACE.

Kosloski, J. (2014). Where Does Stress Come From. Retrieved 22.05, 2015, from https://caeai.com/blog/where-does-stress-come

MacDonald, B. J. (2007). *Practical stress analysis with finite elements*. Dublin: Glasnevin publishing.

NACE, I. (2015a). Corrosion Fatigue. Retrieved 05.06, 2015, from https://www.nace.org/Corrosion-Central/Corrosion-101/Corrosion-Fatigue/

NACE, I. (2015c). Pitting Corrosion. Retrieved 10.06, 2015, from https://www.nace.org/Pitting-Corrosion/

Nimmo, B., & Hinds, G. (February 2003). Beginners Guide to Corrosion. 10. Retrieved from: http://www.npl.co.uk/upload/pdf/beginners_guide_to_corrosion.pdf

Pilkey, W. D. (1994). *Formulas for stress, strain, and structural matrices*. New York: Wiley.

Pook, L. P. (2007). *Metal fatigue : what it is, why it matters* (Vol. Vol. 145). Dordrecht: Springer.

Roberge, P. R. (2008). *Corrosion engineering : principles and practice*. New York: McGraw-Hill.

Roylance, D. (2001). Finite Element Analysis. Retrieved from: http://ocw.mit.edu/courses/materials-science-and-engineering/3-11-mechanics-of-materials-fall-1999/modules/fea.pdf

Standard, N. (2008). Prosjektering av stålkonstruksjoner *Del 1-1 Allmenne regler og regler for bygninger*. Stavanger: Standar Online AS.

Suresh, S. (1992). *Fatigue of materials* (1st paperback ed. (with corrections and exercises). ed. Vol. 8). Cambridge: Cambridge University Press.

Szary, T. (2006). *The Finite Element Method Analysis for Assessing the Remaining Strength of Corroded Oil Field Casing and Tubing.* (Doctorate), Universität Bergakademie Freiberg, Universität Bergakademie Freiberg.

APPENDIX A

A1 DESIGN DRAWING

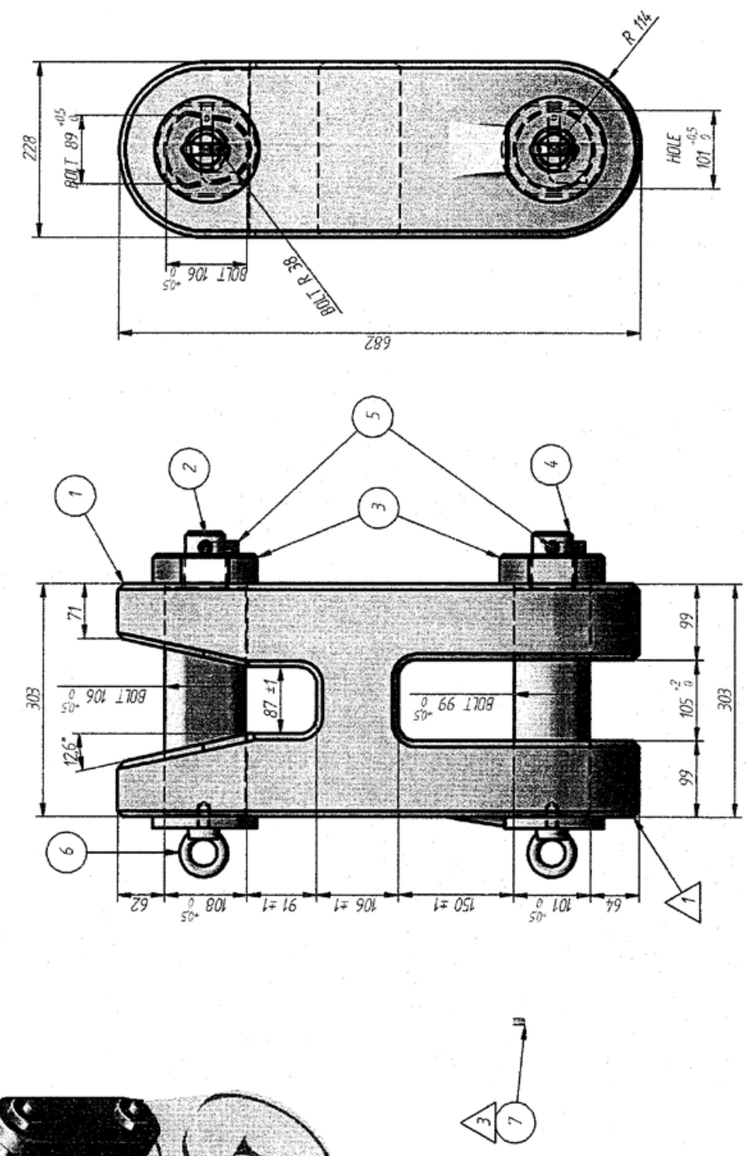

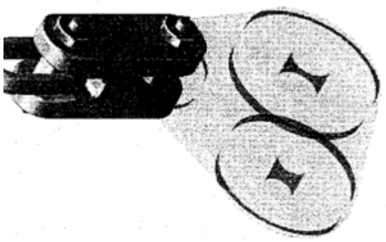

APPENDIX B

B1 VERIFICATION MODEL 2

Load case chosen for this analysis is extreme condition with load 676 KN.

Pin:

$$A = B = \frac{F}{2} = \frac{879000N}{2} = 439500\ N$$
$$M_F = \frac{F \cdot L}{8} = \frac{439500\ N \cdot 301\ mm}{8} = 16536188\ Nmm$$
$$\sigma_{nom} = \frac{M \cdot c}{I} = \frac{16536188\ Nmm \cdot 52\ mm}{5739618\ mm^4} = 299\ MPa$$

$$I = \frac{\pi r^4}{64}$$

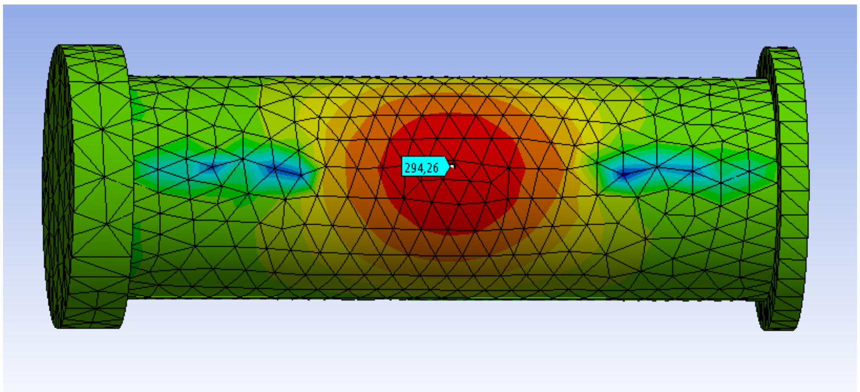

Stress on the x- direction on Model 2

We can see from the Ansys FEA that the accurate $\sigma_x = 294\ MPa$ at the center of the pin. The analytical calculation gives a good approximation of the stress on the pin.

Deformation:

The deformation for the numerical calculation:

$$\delta = \frac{F \cdot L^3}{192 \cdot E \cdot I} = \frac{879000 \cdot 301^3}{192 \cdot 210000 \cdot 5739618} = 0{,}103mm$$

The static defamation gives a good approximation of the numerical deformation with a value $\delta = 0{,}041$.

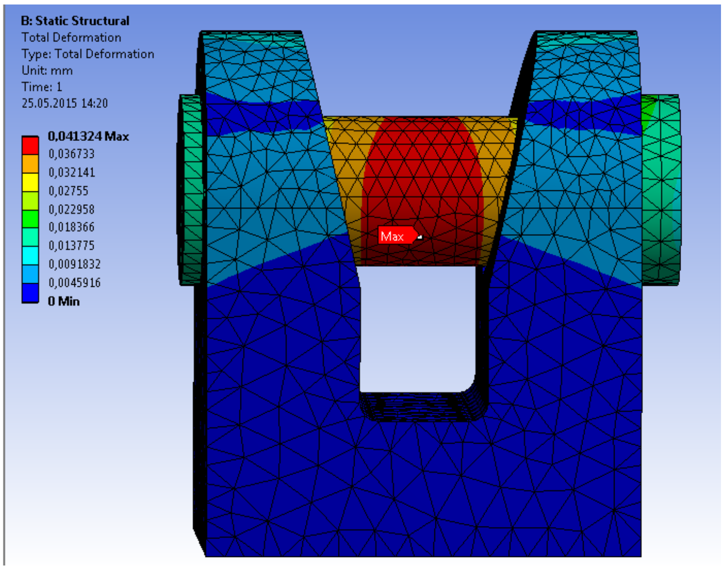

Deformation on shackle

Padeye:

The analytical stress in the padeye is:

$$\sigma_{nom} = \frac{Wa}{(w-2r)\cdot t} = \frac{338000\ N}{(226-110)\cdot 96} = 30\ Mpa$$

The stress concentration around the hole.

$$\sigma_{SCF} = 3 \cdot \sigma_{nom} = 90MPa$$

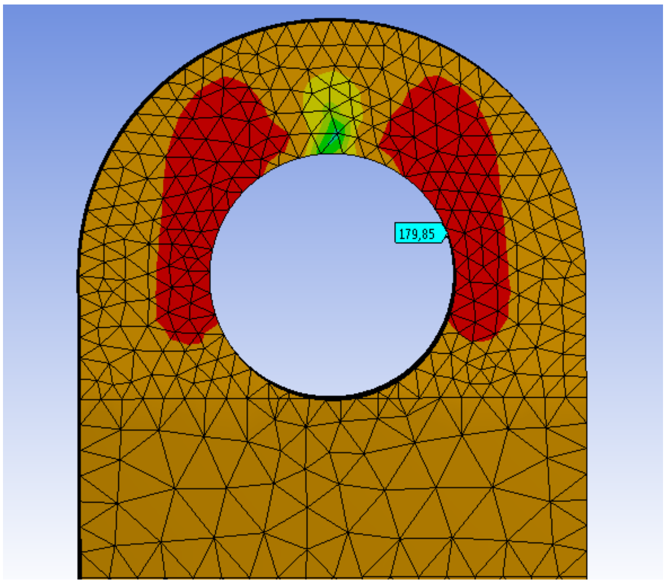

Stresses near the hole

From the numerical result, we can observe that the numerical stress is higher. This is because we have not takin account the stress concentration due to change of the cross-section (thinner section).

Contact stress:

A static determination of the contact stress between the pin and shackle

$$\Delta = \frac{1-v_1{}^2}{E_1} + \frac{1-v_2{}^2}{E_2} = \frac{1-0{,}3^2}{210000} + \frac{1-0{,}3^2}{210000} = 8{,}66 \cdot 10^{-6}$$

The half of the contact width is:

$$b = \sqrt{\frac{2 \cdot P \cdot \Delta}{L \cdot \pi \cdot \left(\frac{1}{R_1} + \frac{1}{R_2}\right)}} = \sqrt{\frac{2 \cdot 676000 \cdot 8{,}66 \cdot 10^{-6}}{82mm \cdot \pi \cdot \left(\frac{1}{52} + \frac{1}{-55}\right)}} = 8{,}1mm$$

$$p_o = \sigma_c = \frac{2 \cdot P}{\pi \cdot L \cdot b} = \frac{2 \cdot 676000N}{\pi \cdot 82mm \cdot 8{,}1mm} = 648\ MPa$$

We can see from the solution that the equation of contact stress is more accurate when the width is smaller .The high stresses extends in greater area, a consequence of smaller contact area.

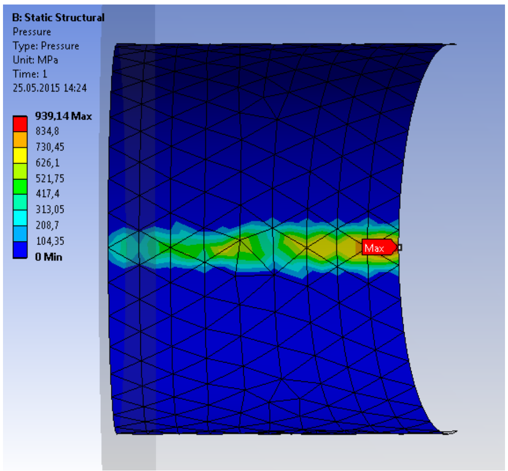

Contact pressure on padeye

$$\sigma_{nom} = \frac{M \cdot c}{I} = \frac{25434500Nmm \cdot 52mm}{5742529mm^4} = 230MPa$$

APPENDIX C

C1 MODEL 1

Project

First Saved	Friday, February 20, 2015
Last Saved	Tuesday, June 09, 2015
Product Version	15.0 Release
Save Project Before Solution	No
Save Project After Solution	No

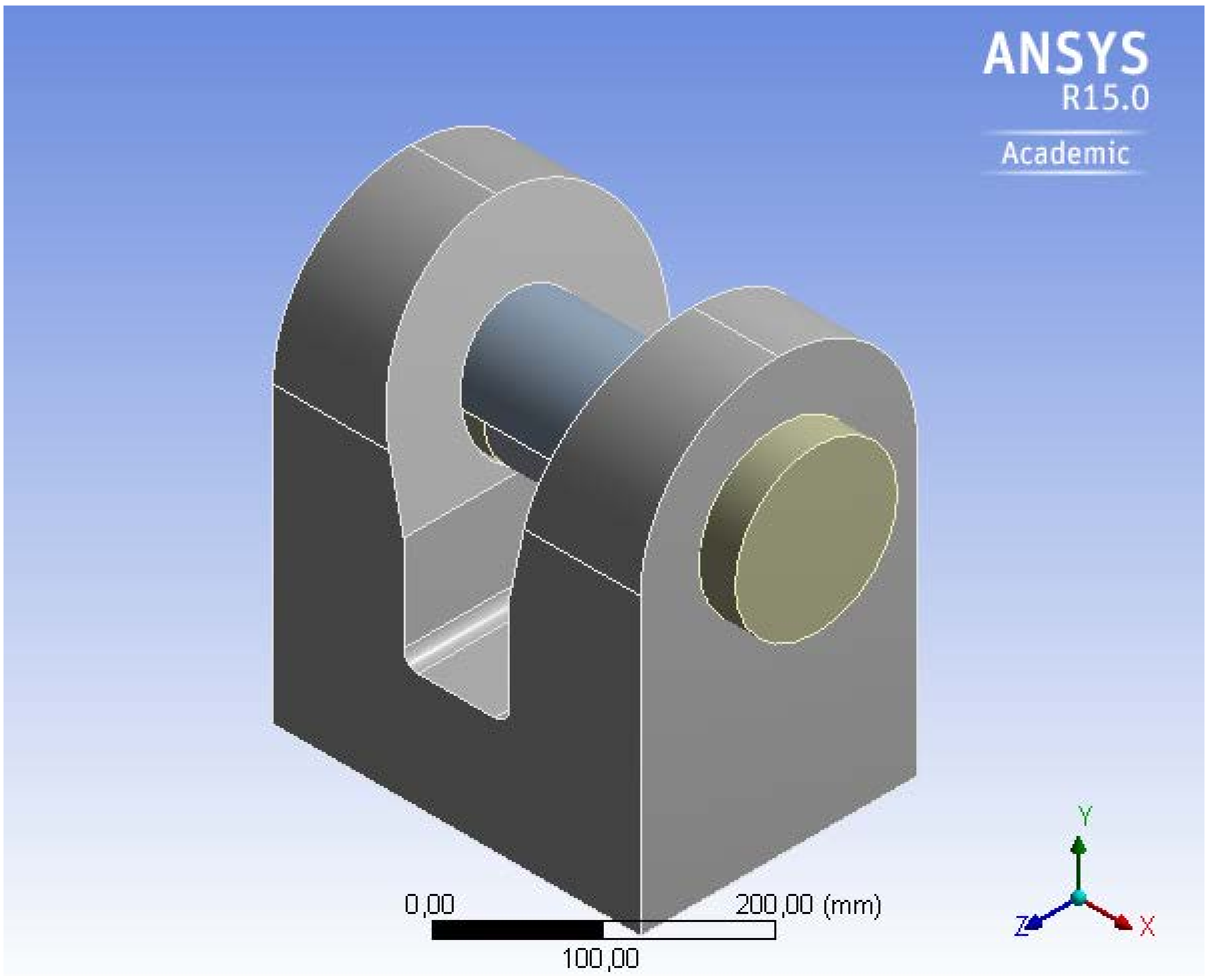

Contents

- **Units**
- **Model (B4)**
  - Geometry
    - Padeye
    - Pin

- Parts
- Coordinate Systems
- Connections
  - Contacts
    - Contact Regions
- Mesh
  - Mesh Controls
- **Static Structural (B5)**
  - Analysis Settings
  - Loads
  - Solution (B6)
    - Solution Information
    - Results
    - Stress Tool 2
      - Results
    - Stress Tool
      - Results
    - Contact Tool
      - Results
    - Force Reaction 3

- **Material Data**
  - R4 Grade Llink

Units

TABLE 1

Unit System	Metric (mm, kg, N, s, mV, mA) Degrees rad/s Celsius
Angle	Degrees
Rotational Velocity	rad/s
Temperature	Celsius

Model (B4)

Geometry

TABLE 2
Model (B4) > Geometry

Object Name	*Geometry*
State	Fully Defined
Definition	
Source	F:\Ansys\Workbench\Shackle\Model 1_files\dp0\Geom\DM\Geom.agdb
Type	DesignModeler
Length Unit	Millimeters
Element Control	Program Controlled
Display Style	Body Color
Bounding Box	
Length X	350, mm
Length Y	357, mm
Length Z	228, mm
Properties	
Volume	1,8774e+007 mm³
Mass	147,38 kg

Scale Factor Value	1,
Statistics	
Bodies	7
Active Bodies	7
Nodes	29788
Elements	16925
Mesh Metric	None
Basic Geometry Options	
Parameters	Yes
Parameter Key	DS
Attributes	No
Named Selections	No
Material Properties	No
Advanced Geometry Options	
Use Associativity	Yes
Coordinate Systems	No
Reader Mode Saves Updated File	No
Use Instances	Yes
Smart CAD Update	No
Compare Parts On Update	No
Attach File Via Temp File	Yes
Temporary Directory	C:\Users\213010\AppData\Roaming\Ansys\v150
Analysis Type	3-D
Decompose Disjoint Geometry	No
Enclosure and Symmetry Processing	Yes

TABLE 3
Model (B4) > Geometry > Parts

Object Name	*Padeye*
State	Meshed
Graphics Properties	
Visible	Yes
Transparency	1
Definition	
Suppressed	No
Stiffness Behavior	Flexible
Coordinate System	Default Coordinate System
Reference Temperature	By Environment
Material	
Assignment	R4 Grade Llink
Nonlinear Effects	No
Thermal Strain Effects	No
Bounding Box	
Length X	303, mm
Length Y	357, mm
Length Z	228, mm
Properties	
Volume	1,5448e+007 mm³
Mass	121,27 kg
Centroid X	151,5 mm
Centroid Y	135,59 mm
Centroid Z	114, mm
Moment of Inertia Ip1	1,6508e+006 kg·mm²
Moment of Inertia Ip2	1,7188e+006 kg·mm²
Moment of Inertia Ip3	2,2753e+006 kg·mm²
Statistics	
Nodes	22957

Elements	13107
Mesh Metric	None

TABLE 4
Model (B4) > Geometry > Body Groups

Object Name	*Pin*
State	Meshed
Graphics Properties	
Visible	Yes
Definition	
Suppressed	No
Assignment	R4 Grade Llink
Coordinate System	Default Coordinate System
Bounding Box	
Length X	350, mm
Length Y	134, mm
Length Z	134, mm
Properties	
Volume	3,3262e+006 mm³
Mass	26,11 kg
Centroid X	162,63 mm
Centroid Y	242, mm
Centroid Z	114, mm
Moment of Inertia Ip1	40498 kg·mm²
Moment of Inertia Ip2	3,1628e+005 kg·mm²
Moment of Inertia Ip3	3,1634e+005 kg·mm²
Statistics	
Nodes	6831
Elements	3818
Mesh Metric	None

TABLE 5
Model (B4) > Geometry > Pin > Parts

Object Name	*Solid*	*Solid*	*Solid*	*Solid*	*Solid*	*Solid*
State	Meshed					
Graphics Properties						
Visible	Yes					
Transparency	1					
Definition						
Suppressed	No					
Stiffness Behavior	Flexible					
Coordinate System	Default Coordinate System					
Reference Temperature	By Environment					
Material						
Assignment	R4 Grade Llink					
Nonlinear Effects	No				Yes	
Thermal Strain Effects	No				Yes	
Bounding Box						
Length X	305, mm	114,5 mm	76, mm	114,5 mm	15, mm	30, mm
Length Y	53, mm				134, mm	
Length Z	106, mm				134, mm	
Properties						
Volume	1,3458e+006 mm³	5,0522e+005 mm³	3,3534e+005 mm³	5,0522e+005 mm³	2,1154e+005 mm³	4,2308e+005 mm³
Mass	10,564 kg	3,9659 kg	2,6324 kg	3,9659 kg	1,6606 kg	3,3212 kg
Centroid X	151,5 mm	246,75 mm	151,5 mm	56,25 mm	-8,5 mm	319, mm

Centroid Y	264,44 mm	219,56 mm			242, mm	
Centroid Z	114, mm					
Moment of Inertia Ip1	9396,4 kg·mm²	3527,5 kg·mm²	2341,4 kg·mm²	3527,5 kg·mm²	3689,5 kg·mm²	7379, kg·mm²
Moment of Inertia Ip2	88824 kg·mm²	7067,8 kg·mm²	3090,6 kg·mm²	7067,8 kg·mm²	1875,7 kg·mm²	3937,3 kg·mm²
Moment of Inertia Ip3	83533 kg·mm²	5081,5 kg·mm²	1772,1 kg·mm²	5081,5 kg·mm²	1875,7 kg·mm²	3937,3 kg·mm²
Statistics						
Nodes	2781	1054	636	1061	880	1168
Elements	1459	528	313	531	405	582
Mesh Metric	None					

Coordinate Systems

TABLE 6
Model (B4) > Coordinate Systems > Coordinate System

Object Name	*Global Coordinate System*
State	Fully Defined
Definition	
Type	Cartesian
Coordinate System ID	0,
Origin	
Origin X	0, mm
Origin Y	0, mm
Origin Z	0, mm
Directional Vectors	
X Axis Data	[1, 0, 0,]
Y Axis Data	[0, 1, 0,]
Z Axis Data	[0, 0, 1,]

Connections

TABLE 7
Model (B4) > Connections

Object Name	*Connections*
State	Fully Defined
Auto Detection	
Generate Automatic Connection On Refresh	Yes
Transparency	
Enabled	Yes

TABLE 8
Model (B4) > Connections > Contacts

Object Name	*Contacts*
State	Fully Defined
Definition	
Connection Type	Contact
Scope	
Scoping Method	Geometry Selection
Geometry	All Bodies
Auto Detection	
Tolerance Type	Slider
Tolerance Slider	0,
Tolerance Value	1,3737 mm
Use Range	No
Face/Face	Yes
Face/Edge	No
Edge/Edge	No

Priority	Include All
Group By	Bodies
Search Across	Bodies

TABLE 9
Model (B4) > Connections > Contacts > Contact Regions

Object Name	*Frictional - Padeye To Solid*	*Frictional - Padeye To Solid*	*Frictional - Padeye To Solid*	*Frictional - Padeye To Solid*	*Frictional - Padeye To Solid*
State	Fully Defined				
Scope					
Scoping Method	Geometry Selection				
Contact	2 Faces	1 Face			
Target	1 Face				
Contact Bodies	Padeye				
Target Bodies	Solid				
Definition					
Type	Frictional				
Friction Coefficient	0,2				
Scope Mode	Automatic				
Behavior	Program Controlled				
Trim Contact	Program Controlled				
Trim Tolerance	1,3737 mm				
Suppressed	No				
Advanced					
Formulation	Augmented Lagrange				
Detection Method	Program Controlled				
Penetration Tolerance	Program Controlled				
Elastic Slip Tolerance	Program Controlled				
Normal Stiffness	Program Controlled				
Update Stiffness	Each Iteration				
Stabilization Damping Factor	0,2				
Pinball Region	Program Controlled				
Time Step Controls	Automatic Bisection				
Geometric Modification					
Interface Treatment	Add Offset, Ramped Effects			Adjust to Touch	
Offset	0, mm				
Contact Geometry Correction	None				

Mesh

TABLE 10
Model (B4) > Mesh

Object Name	*Mesh*
State	Solved
Defaults	
Physics Preference	Mechanical
Relevance	0
Sizing	
Use Advanced Size Function	Off
Relevance Center	Medium
Element Size	Default
Initial Size Seed	Active Assembly
Smoothing	Medium

Transition	Fast
Span Angle Center	Coarse
Minimum Edge Length	18,850 mm
Inflation	
Use Automatic Inflation	None
Inflation Option	Smooth Transition
Transition Ratio	0,272
Maximum Layers	5
Growth Rate	1,2
Inflation Algorithm	Pre
View Advanced Options	No
Patch Conforming Options	
Triangle Surface Mesher	Program Controlled
Patch Independent Options	
Topology Checking	Yes
Advanced	
Number of CPUs for Parallel Part Meshing	Program Controlled
Shape Checking	Standard Mechanical
Element Midside Nodes	Program Controlled
Straight Sided Elements	No
Number of Retries	Default (4)
Extra Retries For Assembly	Yes
Rigid Body Behavior	Dimensionally Reduced
Mesh Morphing	Disabled
Defeaturing	
Pinch Tolerance	Please Define
Generate Pinch on Refresh	No
Automatic Mesh Based Defeaturing	On
Defeaturing Tolerance	Default
Statistics	
Nodes	29788
Elements	16925
Mesh Metric	None

TABLE 11
Model (B4) > Mesh > Mesh Controls

Object Name	*Face Sizing*	*Patch Conforming Method*	*Face Sizing 2*	*Face Sizing 3*
State	Fully Defined			
Scope				
Scoping Method	Geometry Selection			
Geometry	2 Faces	6 Bodies	2 Faces	4 Faces
Definition				
Suppressed	No			
Type	Element Size		Element Size	
Element Size	10, mm		10, mm	15, mm
Behavior	Hard		Soft	
Method		Tetrahedrons		
Algorithm		Patch Conforming		
Element Midside Nodes		Use Global Setting		

Static Structural (B5)

TABLE 12
Model (B4) > Analysis

Object Name	*Static Structural (B5)*
State	Solved

Definition	
Physics Type	Structural
Analysis Type	Static Structural
Solver Target	Mechanical APDL
Options	
Environment Temperature	22, °C
Generate Input Only	No

TABLE 13
Model (B4) > Static Structural (B5) > Analysis Settings

Object Name	*Analysis Settings*
State	Fully Defined
Step Controls	
Number Of Steps	1,
Current Step Number	1,
Step End Time	1, s
Auto Time Stepping	Program Controlled
Solver Controls	
Solver Type	Program Controlled
Weak Springs	Program Controlled
Large Deflection	Off
Inertia Relief	Off
Restart Controls	
Generate Restart Points	Program Controlled
Retain Files After Full Solve	No
Nonlinear Controls	
Newton-Raphson Option	Program Controlled
Force Convergence	Program Controlled
Moment Convergence	Program Controlled
Displacement Convergence	Program Controlled
Rotation Convergence	Program Controlled
Line Search	Program Controlled
Stabilization	Reduce
--Method	Damping
--Damping Factor	0,2
--Activation For First Substep	Yes
--Stabilization Force Limit	0,2
Output Controls	
Stress	Yes
Strain	Yes
Nodal Forces	No
Contact Miscellaneous	No
General Miscellaneous	No
Store Results At	All Time Points
Analysis Data Management	
Solver Files Directory	F:\Ansys\Workbench\Shackle\Model 1_files\dp0\SYS-1\MECH\
Future Analysis	None
Scratch Solver Files Directory	
Save MAPDL db	No
Delete Unneeded Files	Yes
Nonlinear Solution	Yes
Solver Units	Active System
Solver Unit System	nmm

TABLE 14
Model (B4) > Static Structural (B5) > Loads

Object Name	*Fixed Support*	*Bearing Load*

State	Fully Defined	
Scope		
Scoping Method	Geometry Selection	
Geometry	1 Face	
Definition		
Type	Fixed Support	Bearing Load
Suppressed	No	
Define By		Components
Coordinate System		Global Coordinate System
X Component		Tabular Data
Y Component		Tabular Data
Z Component		Tabular Data

FIGURE 1
Model (B4) > Static Structural (B5) > Bearing Load

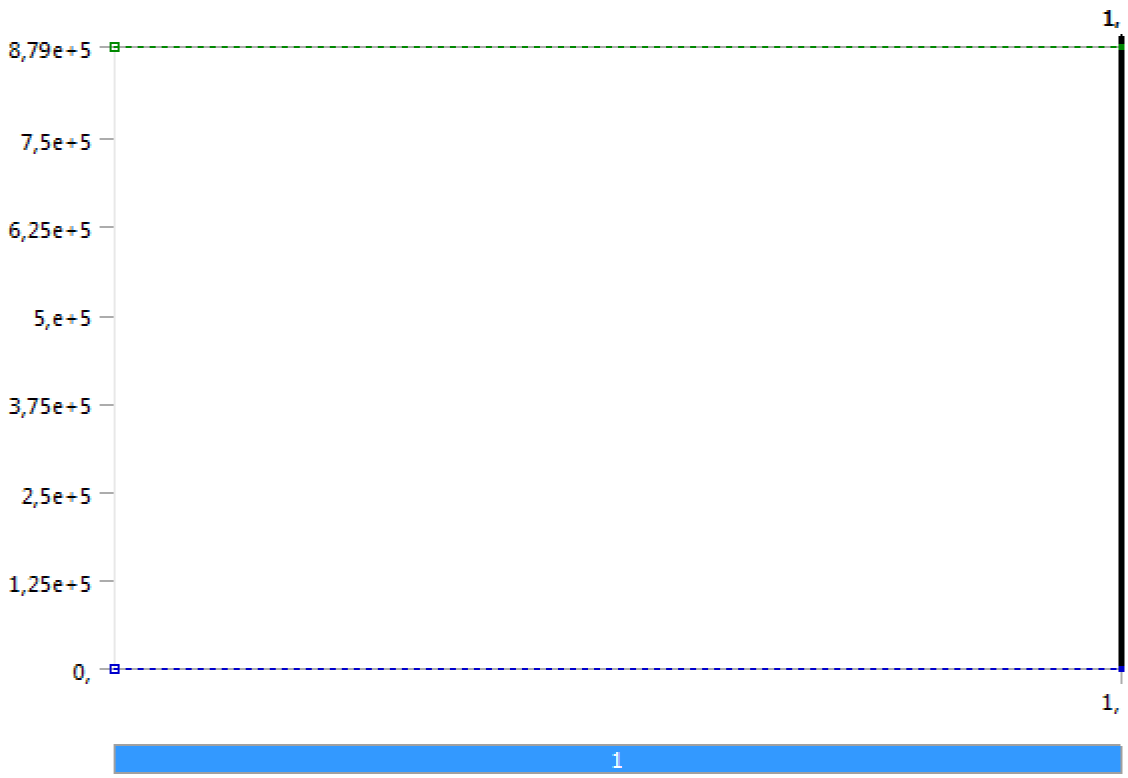

TABLE 15
Model (B4) > Static Structural (B5) > Bearing Load

Steps	Time [s]	X [N]	Y [N]	Z [N]
1	0,	= 0,	= 8,79e+005	= 0,
	1,	0,	8,79e+005	0,
N/A	2,		75000	
	3,		6,65e+005	
	4,		1,15e+005	
	5,		6,76e+005	
	6,		88000	

Solution (B6)

TABLE 16
Model (B4) > Static Structural (B5) > Solution

Object Name	*Solution (B6)*
State	Solved

Adaptive Mesh Refinement	
Max Refinement Loops	1,
Refinement Depth	2,
Information	
Status	Done

TABLE 17
Model (B4) > Static Structural (B5) > Solution (B6) > Solution Information

Object Name	*Solution Information*
State	Solved
Solution Information	
Solution Output	Force Convergence
Newton-Raphson Residuals	0
Update Interval	2,5 s
Display Points	All
FE Connection Visibility	
Activate Visibility	Yes
Display	All FE Connectors
Draw Connections Attached To	All Nodes
Line Color	Connection Type
Visible on Results	No
Line Thickness	Single
Display Type	Lines

FIGURE 2
Model (B4) > Static Structural (B5) > Solution (B6) > Solution Information

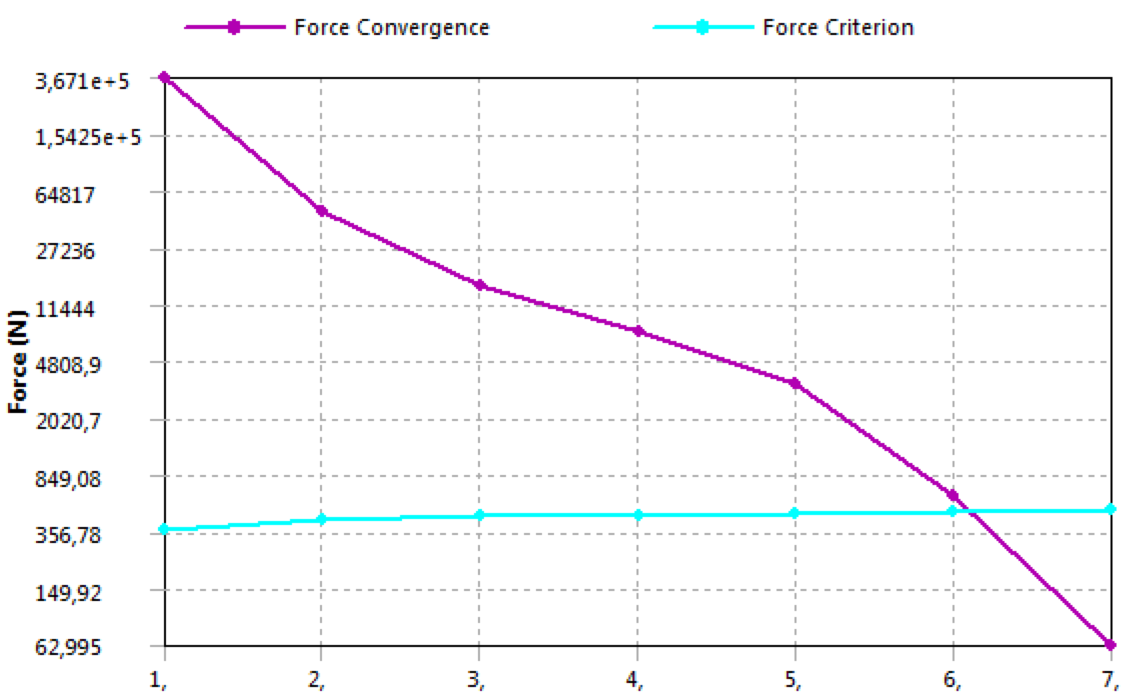

FIGURE 3
Model (B4) > Static Structural (B5) > Solution (B6) > Solution Information

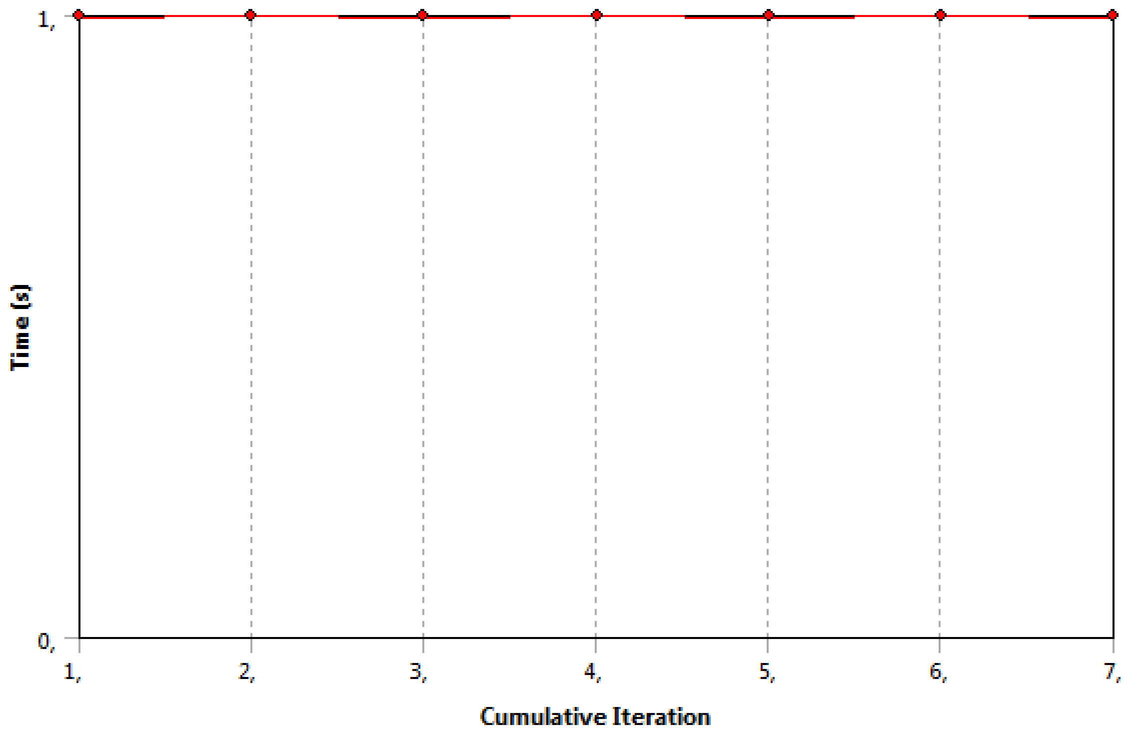

TABLE 18
Model (B4) > Static Structural (B5) > Solution (B6) > Results

Object Name	*Total Deformation*	*Directional Deformation*	*Normal Stress*	*Shear Stress*	*Equivalent Stress 3*	*Equivalent Stress*	*Maximum Principal Stress 3*	*Maximum Principal Stress*	*Shear Stress 2*	*Shear Stress 3*	*Equivalent Stress 4*
State	Solved										
Scope											
Scoping Method	Geometry Selection										
Geometry	All Bodies				5 Bodies	1 Body		6 Bodies	4 Bodies	1 Body	6 Bodies
Definition											
Type	Total Deformation	Directional Deformation	Normal Stress	Shear Stress	Equivalent (von-Mises) Stress		Maximum Principal Stress		Shear Stress		Equivalent (von-Mises) Stress
By	Time										
Display Time	Last										0,18009 s
Calculate Time History	Yes										
Identifier											
Suppressed	No										
Orientation		X Axis	Y Axis	XZ Plane					XY Plane		
Coordinate System		Global Coordinate System		Solution Coordinate System					Global Coordinate System		
Results											
Minimum	0, mm	-8,9217e-003 mm	-877,24 MPa	-105,14 MPa	0,76241 MPa	0,72261 MPa	-312,06 MPa	-263,55 MPa	-130,78 MPa	-72,986 MPa	0,76241 MPa
Maximum	3,626e-002	9,6819e-	175,94	105,37	406,8	691,12	220,5	368,49	125,65	69,551	406,8

	mm	003 mm	MPa	MPa	MPa	MPa	MPa	MPa	MPa	MPa	MPa
Minimum Occurs On	Padeye	Solid	Padeye		Solid			Solid			Solid
Maximum Occurs On	Solid			Padeye	Solid			Solid			Solid
Minimum Value Over Time											
Minimum	0, mm	-8,9217e-003 mm	-877,24 MPa	-105,14 MPa	0,76241 MPa	0,72261 MPa	-312,06 MPa	-263,55 MPa	-130,78 MPa	-72,986 MPa	0,76241 MPa
Maximum	0, mm	-8,9217e-003 mm	-877,24 MPa	-105,14 MPa	0,76241 MPa	0,72261 MPa	-312,06 MPa	-263,55 MPa	-130,78 MPa	-72,986 MPa	0,76241 MPa
Maximum Value Over Time											
Minimum	3,626e-002 mm	9,6819e-003 mm	175,94 MPa	105,37 MPa	406,8 MPa	691,12 MPa	220,5 MPa	368,49 MPa	125,65 MPa	69,551 MPa	406,8 MPa
Maximum	3,626e-002 mm	9,6819e-003 mm	175,94 MPa	105,37 MPa	406,8 MPa	691,12 MPa	220,5 MPa	368,49 MPa	125,65 MPa	69,551 MPa	406,8 MPa
Information											
Time	1, s										
Load Step	1										
Substep	1										
Iteration Number	7										
Integration Point Results											
Display Option			Averaged								
Average Across Bodies			No								

TABLE 19
Model (B4) > Static Structural (B5) > Solution (B6) > Results

Object Name	*Normal Stress 2*	*Shear Stress 4*	*Normal Stress 3*
State	Solved		
Scope			
Scoping Method	Geometry Selection		
Geometry	1 Body	6 Bodies	
Definition			
Type	Normal Stress	Shear Stress	Normal Stress
Orientation	X Axis	XY Plane	Y Axis
By	Time		
Display Time	Last		
Coordinate System	Global Coordinate System		
Calculate Time History	Yes		
Identifier			
Suppressed	No		
Integration Point Results			
Display Option	Averaged		
Average Across Bodies	No		
Results			
Minimum	-315,4 MPa	-130,78 MPa	-622,84 MPa
Maximum	85,232 MPa	125,65 MPa	175,94 MPa
Minimum Occurs On		Solid	
Maximum Occurs On		Solid	
Minimum Value Over Time			
Minimum	-315,4 MPa	-130,78 MPa	-622,84 MPa
Maximum	-315,4 MPa	-130,78 MPa	-622,84 MPa
Maximum Value Over Time			

Minimum	85,232 MPa	125,65 MPa	175,94 MPa
Maximum	85,232 MPa	125,65 MPa	175,94 MPa
Information			
Time	1, s		
Load Step	1		
Substep	1		
Iteration Number	7		

TABLE 20
Model (B4) > Static Structural (B5) > Solution (B6) > Stress Safety Tools

Object Name	*Stress Tool 2*
State	Solved
Definition	
Theory	Max Shear Stress
Factor	0,5
Stress Limit Type	Tensile Yield Per Material

TABLE 21
Model (B4) > Static Structural (B5) > Solution (B6) > Stress Tool 2 > Results

Object Name	*Safety Factor*	*Stress Ratio*	*Stress Ratio 2*
State	Solved		
Scope			
Scoping Method	Geometry Selection		
Geometry	All Bodies	6 Bodies	1 Body
Definition			
Type	Safety Factor	Stress Ratio	
By	Time		
Display Time	Last		
Calculate Time History	Yes		
Identifier			
Suppressed	No		
Integration Point Results			
Display Option	Averaged		
Average Across Bodies	No		
Results			
Minimum	0,74951	1,4476e-003	1,3494e-003
Minimum Occurs On	Padeye	Solid	
Maximum		0,77081	1,3342
Maximum Occurs On		Solid	
Minimum Value Over Time			
Minimum	0,74951	1,4476e-003	1,3494e-003
Maximum	0,74951	1,4476e-003	1,3494e-003
Maximum Value Over Time			
Minimum	15,	0,77081	1,3342
Maximum	15,	0,77081	1,3342
Information			
Time	1, s		
Load Step	1		
Substep	1		
Iteration Number	7		

TABLE 22
Model (B4) > Static Structural (B5) > Solution (B6) > Stress Safety Tools

Object Name	*Stress Tool*
State	Solved
Definition	
Theory	Max Equivalent Stress
Stress Limit Type	Tensile Yield Per Material

TABLE 23
Model (B4) > Static Structural (B5) > Solution (B6) > Stress Tool > Results

Object Name	*Safety Factor*	*Stress Ratio*
State	Solved	
Scope		
Scoping Method	Geometry Selection	
Geometry	All Bodies	
Definition		
Type	Safety Factor	Stress Ratio
By	Time	
Display Time	Last	
Calculate Time History	Yes	
Identifier		
Suppressed	No	
Integration Point Results		
Display Option	Averaged	
Average Across Bodies	No	
Results		
Minimum	0,83922	1,2459e-003
Minimum Occurs On	Padeye	
Maximum		1,1916
Maximum Occurs On		Padeye
Minimum Value Over Time		
Minimum	0,83922	1,2459e-003
Maximum	0,83922	1,2459e-003
Maximum Value Over Time		
Minimum	15,	1,1916
Maximum	15,	1,1916
Information		
Time	1, s	
Load Step	1	
Substep	1	
Iteration Number	7	

TABLE 24
Model (B4) > Static Structural (B5) > Solution (B6) > Contact Tools

Object Name	*Contact Tool*
State	Solved
Scope	
Scoping Method	Geometry Selection
Geometry	2 Faces

Model (B4) > Static Structural (B5) > Solution (B6) > Contact Tool

Name	Contact Side
Frictional - Padeye To Solid	Both
Frictional - Padeye To Solid	Both
Frictional - Padeye To Solid	Both

TABLE 25
Model (B4) > Static Structural (B5) > Solution (B6) > Contact Tool > Results

Object Name	*Status*	*Sliding Distance*	*Pressure*
State	Solved		
Definition			
Type	Status	Sliding Distance	Pressure
By	Time		
Display Time	Last		
Calculate Time History	Yes		

Identifier			
Suppressed	No		
Integration Point Results			
Display Option	Averaged		
Information			
Time	1, s		
Load Step	1		
Substep	1		
Iteration Number	7		
Results			
Minimum		0, mm	0, MPa
Maximum		1,3027e-002 mm	802,74 MPa
Minimum Value Over Time			
Minimum		0, mm	0, MPa
Maximum		0, mm	0, MPa
Maximum Value Over Time			
Minimum		1,3027e-002 mm	802,74 MPa
Maximum		1,3027e-002 mm	802,74 MPa

TABLE 26
Model (B4) > Static Structural (B5) > Solution (B6) > Probes

Object Name	*Force Reaction 3*
State	Solved
Definition	
Type	Force Reaction
Location Method	Boundary Condition
Boundary Condition	Fixed Support
Orientation	Global Coordinate System
Suppressed	No
Options	
Result Selection	All
Display Time	End Time
Results	
X Axis	-8,94e-003 N
Y Axis	-8,79e+005 N
Z Axis	5,3948e-003 N
Total	8,79e+005 N
Maximum Value Over Time	
X Axis	-8,94e-003 N
Y Axis	-8,79e+005 N
Z Axis	5,3948e-003 N
Total	8,79e+005 N
Minimum Value Over Time	
X Axis	-8,94e-003 N
Y Axis	-8,79e+005 N
Z Axis	5,3948e-003 N
Total	8,79e+005 N
Information	
Time	1, s
Load Step	1
Substep	1
Iteration Number	7

FIGURE 4
Model (B4) > Static Structural (B5) > Solution (B6) > Force Reaction 3

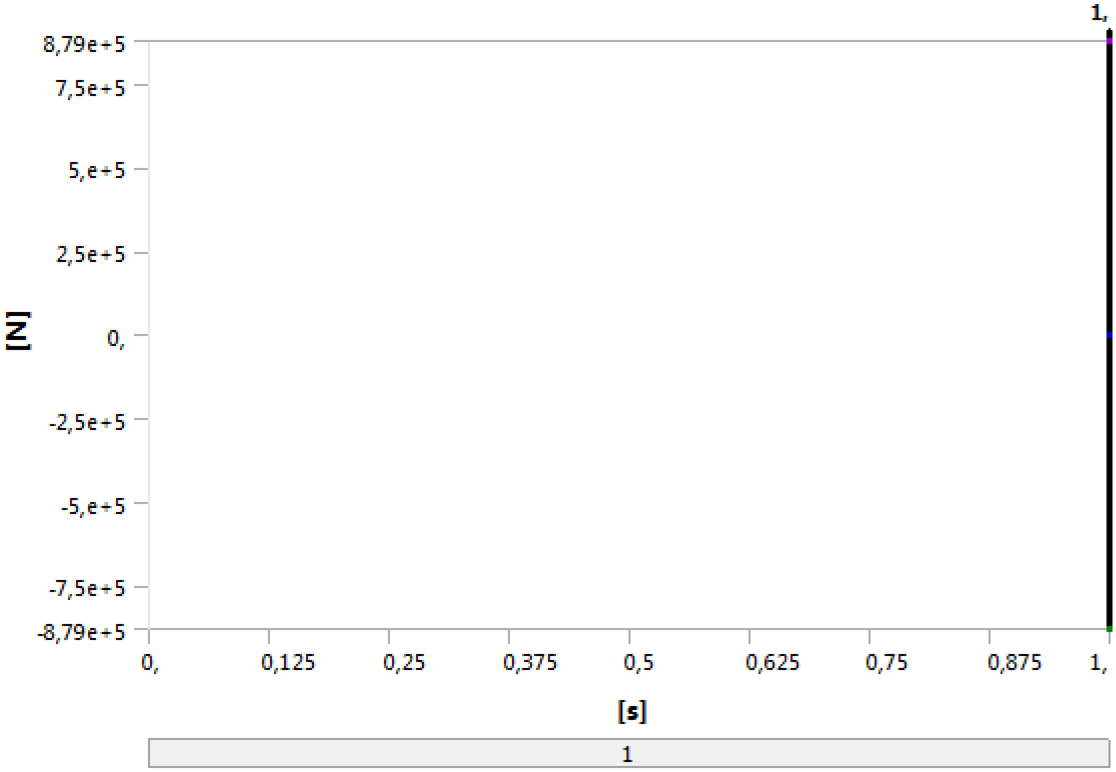

TABLE 27
Model (B4) > Static Structural (B5) > Solution (B6) > Force Reaction 3

Time [s]	Force Reaction 3 (X) [N]	Force Reaction 3 (Y) [N]	Force Reaction 3 (Z) [N]	Force Reaction 3 (Total) [N]
1,	-8,94e-003	-8,79e+005	5,3948e-003	8,79e+005

Material Data

R4 Grade Llink

TABLE 28
R4 Grade Llink > Constants

Density	7,85e-006 kg mm^-3
Coefficient of Thermal Expansion	1,2e-005 C^-1

TABLE 29
R4 Grade Llink > Tensile Yield Strength

Tensile Yield Strength MPa
580,

TABLE 30
R4 Grade Llink > Compressive Yield Strength

Compressive Yield Strength MPa
580,

TABLE 31
R4 Grade Llink > Tensile Ultimate Strength

Tensile Ultimate Strength MPa
860,

TABLE 32
R4 Grade Llink > Compressive Ultimate Strength

Compressive Ultimate Strength MPa

860,

TABLE 33
R4 Grade Llink > Isotropic Elasticity

Temperature C	Young's Modulus MPa	Poisson's Ratio	Bulk Modulus MPa	Shear Modulus MPa
	2,017e+006	0,3	1,6808e+006	7,7577e+005

TABLE 34
R4 Grade Llink > Isotropic Secant Coefficient of Thermal Expansion

Reference Temperature C
20,

C2 Model 2

Project

First Saved	Friday, February 20, 2015
Last Saved	Tuesday, June 02, 2015
Product Version	15.0 Release
Save Project Before Solution	No
Save Project After Solution	No

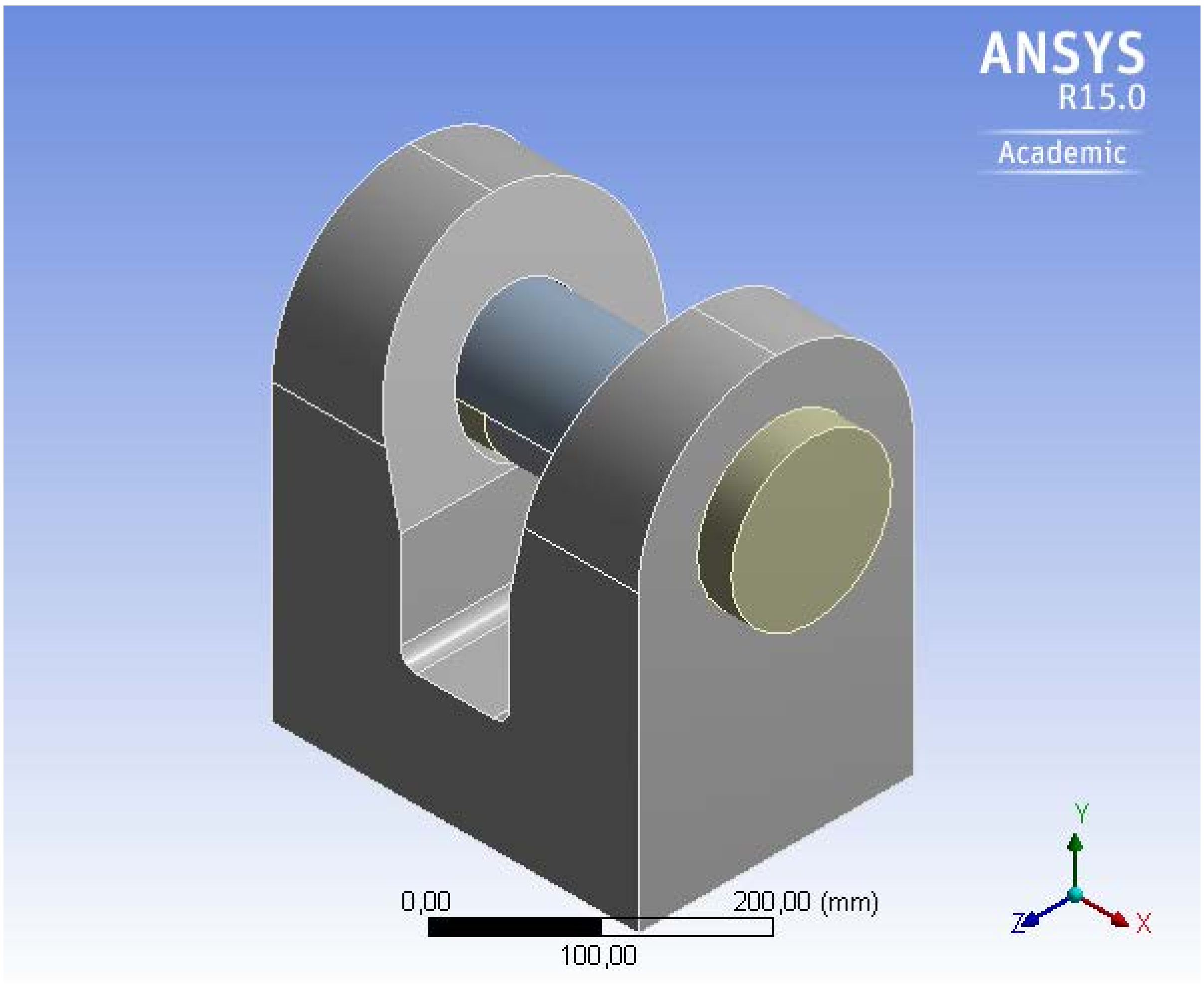

Contents

- **Units**
- **Model (B4)**
  - Geometry
    - Padeye
    - Pin

            - [Parts]
    - [Coordinate Systems]
    - [Connections]
        - [Contacts]
            - [Contact Regions]
    - [Mesh]
        - [Mesh Controls]
    - **[Static Structural (B5)]**
        - [Analysis Settings]
        - [Loads]
        - [Solution (B6)]
            - [Solution Information]
            - [Results]
            - [Stress Tool]
                - [Results]
            - [Stress Tool 2]
                - [Results]
            - [Contact Tool]
                - [Results]
            - [Force Reaction 3]

- **[Material Data]**
    - [R4 Grade Llink]

Units

TABLE 1

Unit System	Metric (mm, kg, N, s, mV, mA) Degrees rad/s Celsius
Angle	Degrees
Rotational Velocity	rad/s
Temperature	Celsius

Model (B4)

Geometry

TABLE 2
Model (B4) > Geometry

Object Name	*Geometry*
State	Fully Defined
Definition	
Source	F:\Ansys\Workbench\Shackle\Model 2_files\dp0\Geom\DM\Geom.agdb
Type	DesignModeler
Length Unit	Millimeters
Element Control	Program Controlled
Display Style	Body Color
Bounding Box	
Length X	344, mm
Length Y	355, mm
Length Z	226, mm
Properties	
Volume	1,804e+007 mm³
Mass	141,61 kg

Scale Factor Value	1,
Statistics	
Bodies	7
Active Bodies	7
Nodes	29885
Elements	16976
Mesh Metric	None
Basic Geometry Options	
Parameters	Yes
Parameter Key	DS
Attributes	No
Named Selections	No
Material Properties	No
Advanced Geometry Options	
Use Associativity	Yes
Coordinate Systems	No
Reader Mode Saves Updated File	No
Use Instances	Yes
Smart CAD Update	No
Compare Parts On Update	No
Attach File Via Temp File	Yes
Temporary Directory	C:\Users\213010\AppData\Roaming\Ansys\v150
Analysis Type	3-D
Decompose Disjoint Geometry	No
Enclosure and Symmetry Processing	Yes

TABLE 3
Model (B4) > Geometry > Parts

Object Name	*Padeye*
State	Meshed
Graphics Properties	
Visible	Yes
Transparency	1
Definition	
Suppressed	No
Stiffness Behavior	Flexible
Coordinate System	Default Coordinate System
Reference Temperature	By Environment
Material	
Assignment	R4 Grade Llink
Nonlinear Effects	No
Thermal Strain Effects	No
Bounding Box	
Length X	301, mm
Length Y	355, mm
Length Z	226, mm
Properties	
Volume	1,4905e+007 mm³
Mass	117, kg
Centroid X	150,5 mm
Centroid Y	133,67 mm
Centroid Z	113, mm
Moment of Inertia Ip1	1,5682e+006 kg·mm²
Moment of Inertia Ip2	1,6437e+006 kg·mm²
Moment of Inertia Ip3	2,1697e+006 kg·mm²
Statistics	
Nodes	23123

Elements	13189
Mesh Metric	None

TABLE 4
Model (B4) > Geometry > Body Groups

Object Name	*Pin*
State	Meshed
Graphics Properties	
Visible	Yes
Definition	
Suppressed	No
Assignment	R4 Grade Llink
Coordinate System	Default Coordinate System
Bounding Box	
Length X	344, mm
Length Y	132, mm
Length Z	132, mm
Properties	
Volume	3,135e+006 mm³
Mass	24,61 kg
Centroid X	161,76 mm
Centroid Y	244,18 mm
Centroid Z	113, mm
Moment of Inertia Ip1	36603 kg·mm²
Moment of Inertia Ip2	2,8679e+005 kg·mm²
Moment of Inertia Ip3	2,8684e+005 kg·mm²
Statistics	
Nodes	6762
Elements	3787
Mesh Metric	None

TABLE 5
Model (B4) > Geometry > Pin > Parts

Object Name	*Solid*	*Solid*	*Solid*	*Solid*	*Solid*	*Solid*
State	Meshed					
Graphics Properties						
Visible	Yes					
Transparency	1					
Definition						
Suppressed	No					
Stiffness Behavior	Flexible					
Coordinate System	Default Coordinate System					
Reference Temperature	By Environment					
Material						
Assignment	R4 Grade Llink					
Nonlinear Effects	No				Yes	
Thermal Strain Effects	No				Yes	
Bounding Box						
Length X	303, mm	112,5 mm	76, mm	114,5 mm	13, mm	28, mm
Length Y	51, mm	53, mm			132, mm	
Length Z	103,98 mm	104, mm			132, mm	
Properties						
Volume	1,2555e+006 mm³	4,8954e+005 mm³	3,3071e+005 mm³	4,9824e+005 mm³	1,779e+005 mm³	3,8317e+005 mm³
Mass	9,8554 kg	3,8429 kg	2,5961 kg	3,9112 kg	1,3965 kg	3,0079 kg
Centroid X	150,5 mm	245,75 mm	151,5 mm	56,25 mm	-7,5 mm	316, mm

Centroid Y	266,56 mm	222,52 mm			245, mm	
Centroid Z	113, mm					
Moment of Inertia Ip1	8313,7 kg·mm²	3341,8 kg·mm²	2257,6 kg·mm²	3401,2 kg·mm²	3010,9 kg·mm²	6485, kg·mm²
Moment of Inertia Ip2	81564 kg·mm²	6628,6 kg·mm²	2996,4 kg·mm²	6893,8 kg·mm²	1525, kg·mm²	3438, kg·mm²
Moment of Inertia Ip3	76796 kg·mm²	4781,8 kg·mm²	1748,8 kg·mm²	5014,1 kg·mm²	1525, kg·mm²	3438, kg·mm²
Statistics						
Nodes	2761	1068	627	1105	837	1121
Elements	1444	544	310	560	377	552
Mesh Metric	None					

Coordinate Systems

TABLE 6
Model (B4) > Coordinate Systems > Coordinate System

Object Name	*Global Coordinate System*
State	Fully Defined
Definition	
Type	Cartesian
Coordinate System ID	0,
Origin	
Origin X	0, mm
Origin Y	0, mm
Origin Z	0, mm
Directional Vectors	
X Axis Data	[1, 0, 0,]
Y Axis Data	[0, 1, 0,]
Z Axis Data	[0, 0, 1,]

Connections

TABLE 7
Model (B4) > Connections

Object Name	*Connections*
State	Fully Defined
Auto Detection	
Generate Automatic Connection On Refresh	Yes
Transparency	
Enabled	Yes

TABLE 8
Model (B4) > Connections > Contacts

Object Name	*Contacts*
State	Fully Defined
Definition	
Connection Type	Contact
Scope	
Scoping Method	Geometry Selection
Geometry	All Bodies
Auto Detection	
Tolerance Type	Slider
Tolerance Slider	0,
Tolerance Value	1,3589 mm
Use Range	No
Face/Face	Yes
Face/Edge	No
Edge/Edge	No

Priority	Include All
Group By	Bodies
Search Across	Bodies

TABLE 9
Model (B4) > Connections > Contacts > Contact Regions

Object Name	*Frictional - Padeye To Solid*	*Frictional - Padeye To Solid*	*Frictional - Padeye To Solid*
State	Fully Defined		
Scope			
Scoping Method	Geometry Selection		
Contact	1 Face		2 Faces
Target	1 Face		
Contact Bodies	Padeye		
Target Bodies	Solid		
Definition			
Type	Frictional		
Friction Coefficient	0,2		
Scope Mode	Automatic		
Behavior	Program Controlled		
Trim Contact	Program Controlled		
Trim Tolerance	1,3589 mm		
Suppressed	No		
Advanced			
Formulation	Augmented Lagrange		
Detection Method	Program Controlled		
Penetration Tolerance	Program Controlled		
Elastic Slip Tolerance	Program Controlled		
Normal Stiffness	Program Controlled		
Update Stiffness	Each Iteration		
Stabilization Damping Factor	0,2		
Pinball Region	Program Controlled		
Time Step Controls	Automatic Bisection		
Geometric Modification			
Interface Treatment	Adjust to Touch		Add Offset, No Ramping
Contact Geometry Correction	None		
Offset			0, mm

Mesh

TABLE 10
Model (B4) > Mesh

Object Name	*Mesh*
State	Solved
Defaults	
Physics Preference	Mechanical
Relevance	0
Sizing	
Use Advanced Size Function	Off
Relevance Center	Medium
Element Size	Default
Initial Size Seed	Active Assembly
Smoothing	Medium
Transition	Fast
Span Angle Center	Coarse
Minimum Edge Length	20,420 mm
Inflation	
Use Automatic Inflation	None

Inflation Option	Smooth Transition
Transition Ratio	0,272
Maximum Layers	5
Growth Rate	1,2
Inflation Algorithm	Pre
View Advanced Options	No
Patch Conforming Options	
Triangle Surface Mesher	Program Controlled
Patch Independent Options	
Topology Checking	Yes
Advanced	
Number of CPUs for Parallel Part Meshing	Program Controlled
Shape Checking	Standard Mechanical
Element Midside Nodes	Program Controlled
Straight Sided Elements	No
Number of Retries	Default (4)
Extra Retries For Assembly	Yes
Rigid Body Behavior	Dimensionally Reduced
Mesh Morphing	Disabled
Defeaturing	
Pinch Tolerance	Please Define
Generate Pinch on Refresh	No
Automatic Mesh Based Defeaturing	On
Defeaturing Tolerance	Default
Statistics	
Nodes	29885
Elements	16976
Mesh Metric	None

TABLE 11
Model (B4) > Mesh > Mesh Controls

Object Name	*Face Sizing*	*Patch Conforming Method*	*Face Sizing 2*	*Face Sizing 3*
State	Fully Defined			
Scope				
Scoping Method	Geometry Selection			
Geometry	2 Faces	6 Bodies	2 Faces	4 Faces
Definition				
Suppressed	No			
Type	Element Size		Element Size	
Element Size	10, mm		10, mm	15, mm
Behavior	Hard		Soft	
Method		Tetrahedrons		
Algorithm		Patch Conforming		
Element Midside Nodes		Use Global Setting		

Static Structural (B5)

TABLE 12
Model (B4) > Analysis

Object Name	*Static Structural (B5)*
State	Solved
Definition	
Physics Type	Structural
Analysis Type	Static Structural
Solver Target	Mechanical APDL
Options	

Environment Temperature	22, °C
Generate Input Only	No

TABLE 13
Model (B4) > Static Structural (B5) > Analysis Settings

Object Name	*Analysis Settings*
State	Fully Defined
Step Controls	
Number Of Steps	1,
Current Step Number	1,
Step End Time	1, s
Auto Time Stepping	Program Controlled
Solver Controls	
Solver Type	Program Controlled
Weak Springs	Program Controlled
Large Deflection	Off
Inertia Relief	Off
Restart Controls	
Generate Restart Points	Program Controlled
Retain Files After Full Solve	No
Nonlinear Controls	
Newton-Raphson Option	Program Controlled
Force Convergence	Program Controlled
Moment Convergence	Program Controlled
Displacement Convergence	Program Controlled
Rotation Convergence	Program Controlled
Line Search	Program Controlled
Stabilization	Reduce
--Method	Damping
--Damping Factor	0,2
--Activation For First Substep	Yes
--Stabilization Force Limit	0,2
Output Controls	
Stress	Yes
Strain	Yes
Nodal Forces	No
Contact Miscellaneous	No
General Miscellaneous	No
Store Results At	All Time Points
Analysis Data Management	
Solver Files Directory	F:\Ansys\Workbench\Shackle\Model 2_files\dp0\SYS-1\MECH\
Future Analysis	None
Scratch Solver Files Directory	
Save MAPDL db	No
Delete Unneeded Files	Yes
Nonlinear Solution	Yes
Solver Units	Active System
Solver Unit System	nmm

TABLE 14
Model (B4) > Static Structural (B5) > Loads

Object Name	*Fixed Support*	*Bearing Load*
State	Fully Defined	
Scope		
Scoping Method	Geometry Selection	
Geometry	1 Face	
Definition		

Type	Fixed Support	Bearing Load
Suppressed	No	
Define By		Components
Coordinate System		Global Coordinate System
X Component		0, N
Y Component		8,79e+005 N
Z Component		0, N

FIGURE 1
Model (B4) > Static Structural (B5) > Bearing Load

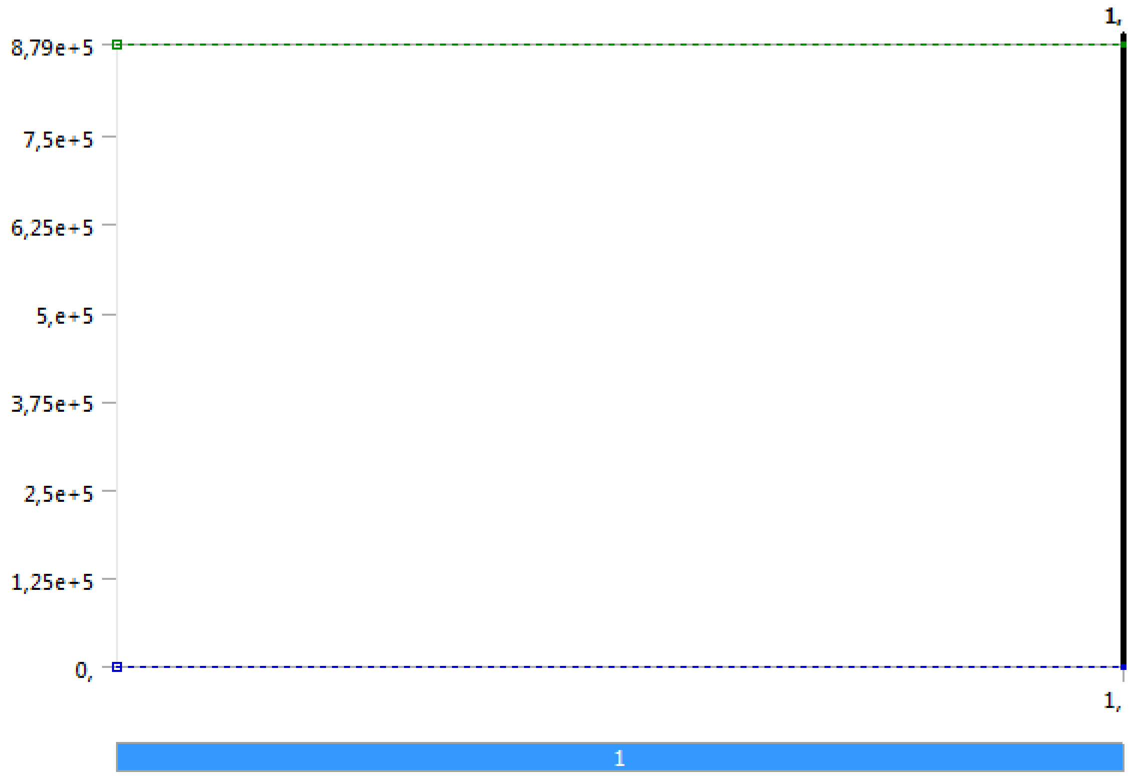

Solution (B6)

TABLE 15
Model (B4) > Static Structural (B5) > Solution

Object Name	*Solution (B6)*
State	Solved
Adaptive Mesh Refinement	
Max Refinement Loops	1,
Refinement Depth	2,
Information	
Status	Done

TABLE 16
Model (B4) > Static Structural (B5) > Solution (B6) > Solution Information

Object Name	*Solution Information*
State	Solved
Solution Information	
Solution Output	Force Convergence
Newton-Raphson Residuals	0
Update Interval	2,5 s
Display Points	All
FE Connection Visibility	

Activate Visibility	Yes
Display	All FE Connectors
Draw Connections Attached To	All Nodes
Line Color	Connection Type
Visible on Results	No
Line Thickness	Single
Display Type	Lines

FIGURE 2
Model (B4) > Static Structural (B5) > Solution (B6) > Solution Information

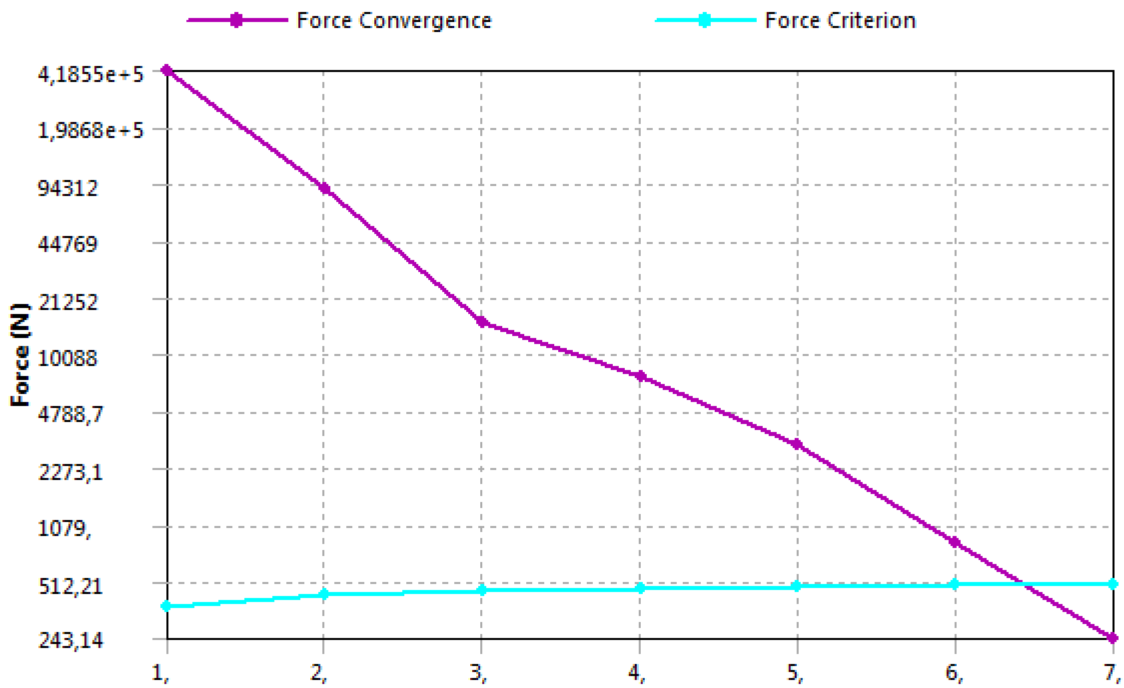

FIGURE 3
Model (B4) > Static Structural (B5) > Solution (B6) > Solution Information

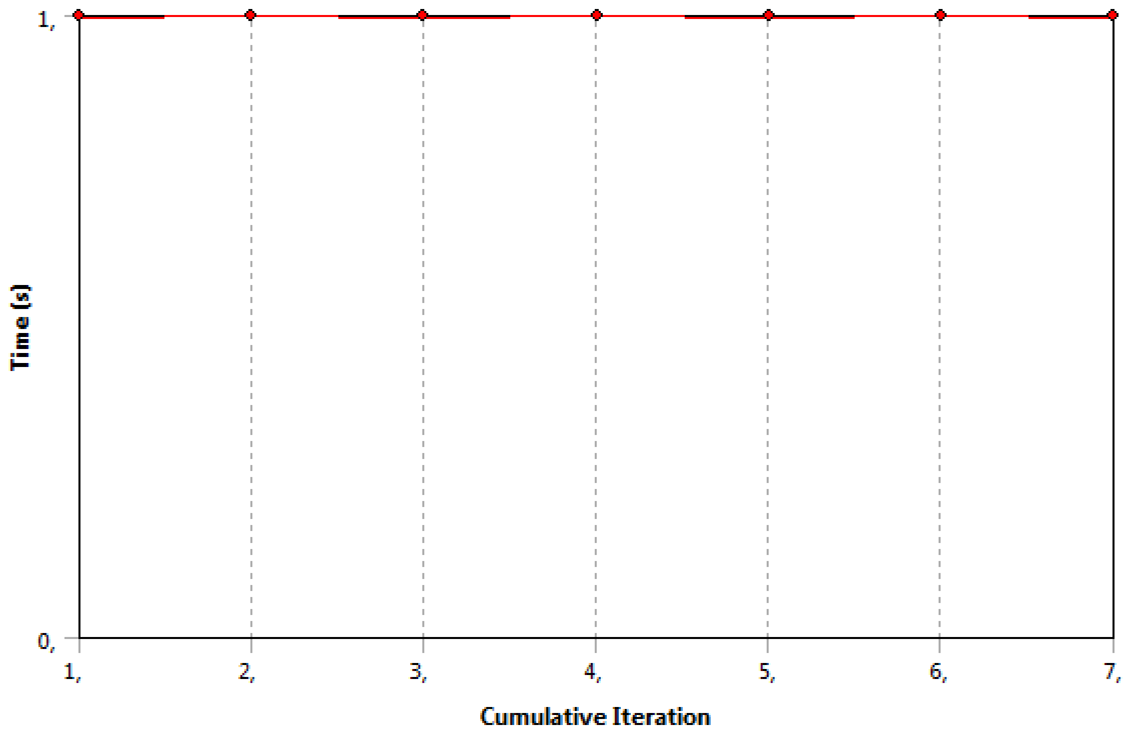

TABLE 17
Model (B4) > Static Structural (B5) > Solution (B6) > Results

Object Name	*Total Deformation*	*Directional Deformation*	*Normal Stress*	*Shear Stress*	*Equivalent Stress*	*Maximum Principal Stress 3*	*Maximum Principal Stress*	*Equivalent Stress 2*	*Normal Stress 2*	*Shear Stress 2*
State	Solved									
Scope										
Scoping Method	Geometry Selection									
Geometry	All Bodies				1 Body		6 Bodies		1 Body	6 Bodies
Definition										
Type	Total Deformation	Directional Deformation	Normal Stress	Shear Stress	Equivalent (von-Mises) Stress	Maximum Principal Stress		Equivalent (von-Mises) Stress	Normal Stress	Shear Stress
By	Time									
Display Time	Last					8,8926e-002 s	Last			
Calculate Time History	Yes									
Identifier										
Suppressed	No									
Orientation		X Axis	Y Axis	XY Plane					Y Axis	XY Plane
Coordinate System		Global Coordinate System		Solution Coordinate System					Global Coordinate System	
Results										
Minimum	0, mm	-9,8029e-003 mm	-1014,3 MPa	-140,19 MPa	0,56513 MPa	-364,35 MPa	-346,58 MPa	0,69621 MPa	-1014,3 MPa	-140,19 MPa
Maximum	4,1324e-	1,1221e-	210,63	127,3 MPa	769,31 MPa	254,57	373,85	521,13 MPa	181,4	127,3

	002 mm	002 mm	MPa			MPa	MPa		MPa	MPa
Minimum Occurs On	Padeye	Solid	Padeye	Solid			Solid			Solid
Maximum Occurs On	Solid						Solid			Solid
Minimum Value Over Time										
Minimum	0, mm	-9,8029e-003 mm	-1014,3 MPa	-140,19 MPa	0,56513 MPa	-364,35 MPa	-346,58 MPa	0,69621 MPa	-1014,3 MPa	-140,19 MPa
Maximum	0, mm	-9,8029e-003 mm	-1014,3 MPa	-140,19 MPa	0,56513 MPa	-364,35 MPa	-346,58 MPa	0,69621 MPa	-1014,3 MPa	-140,19 MPa
Maximum Value Over Time										
Minimum	4,1324e-002 mm	1,1221e-002 mm	210,63 MPa	127,3 MPa	769,31 MPa	254,57 MPa	373,85 MPa	521,13 MPa	181,4 MPa	127,3 MPa
Maximum	4,1324e-002 mm	1,1221e-002 mm	210,63 MPa	127,3 MPa	769,31 MPa	254,57 MPa	373,85 MPa	521,13 MPa	181,4 MPa	127,3 MPa
Information										
Time	1, s									
Load Step	1									
Substep	1									
Iteration Number	7									
Integration Point Results										
Display Option			Averaged							
Average Across Bodies			No							

TABLE 18
Model (B4) > Static Structural (B5) > Solution (B6) > Stress Safety Tools

Object Name	*Stress Tool*
State	Solved
Definition	
Theory	Max Shear Stress
Factor	0,5
Stress Limit Type	Tensile Yield Per Material

TABLE 19
Model (B4) > Static Structural (B5) > Solution (B6) > Stress Tool > Results

Object Name	*Safety Factor*	*Stress Ratio*
State	Solved	
Scope		
Scoping Method	Geometry Selection	
Geometry	All Bodies	6 Bodies
Definition		
Type	Safety Factor	Stress Ratio
By	Time	
Display Time	Last	
Calculate Time History	Yes	
Identifier		
Suppressed	No	
Integration Point Results		
Display Option	Averaged	
Average Across Bodies	No	
Results		
Minimum	0,6781	1,3184e-003

Minimum Occurs On	Padeye	Solid
Maximum		0,98118
Maximum Occurs On		Solid
Minimum Value Over Time		
Minimum	0,6781	1,3184e-003
Maximum	0,6781	1,3184e-003
Maximum Value Over Time		
Minimum	15,	0,98118
Maximum	15,	0,98118
Information		
Time	1, s	
Load Step	1	
Substep	1	
Iteration Number	7	

TABLE 20
Model (B4) > Static Structural (B5) > Solution (B6) > Stress Safety Tools

Object Name	*Stress Tool 2*
State	Solved
Definition	
Theory	Max Equivalent Stress
Stress Limit Type	Tensile Yield Per Material

TABLE 21
Model (B4) > Static Structural (B5) > Solution (B6) > Stress Tool 2 > Results

Object Name	*Safety Factor*	*Stress Ratio*
State	Solved	
Scope		
Scoping Method	Geometry Selection	
Geometry	All Bodies	
Definition		
Type	Safety Factor	Stress Ratio
By	Time	
Display Time	Last	
Calculate Time History	Yes	
Identifier		
Suppressed	No	
Integration Point Results		
Display Option	Averaged	
Average Across Bodies	No	
Results		
Minimum	0,75392	9,7436e-004
Minimum Occurs On	Padeye	
Maximum		1,3264
Maximum Occurs On		Padeye
Minimum Value Over Time		
Minimum	0,75392	9,7436e-004
Maximum	0,75392	9,7436e-004
Maximum Value Over Time		
Minimum	15,	1,3264
Maximum	15,	1,3264
Information		
Time	1, s	
Load Step	1	
Substep	1	
Iteration Number	7	

TABLE 22

Model (B4) > Static Structural (B5) > Solution (B6) > Contact Tools

Object Name	*Contact Tool*
State	Solved
Scope	
Scoping Method	Geometry Selection
Geometry	2 Faces

Model (B4) > Static Structural (B5) > Solution (B6) > Contact Tool

Name	Contact Side

TABLE 23
Model (B4) > Static Structural (B5) > Solution (B6) > Contact Tool > Results

Object Name	*Status*	*Sliding Distance*	*Pressure*
State	Solved		
Definition			
Type	Status	Sliding Distance	Pressure
By	Time		
Display Time	Last		
Calculate Time History	Yes		
Identifier			
Suppressed	No		
Integration Point Results			
Display Option	Averaged		
Information			
Time	1, s		
Load Step	1		
Substep	1		
Iteration Number	7		
Results			
Minimum		0, mm	0, MPa
Maximum		1,5006e-002 mm	939,14 MPa
Minimum Value Over Time			
Minimum		0, mm	0, MPa
Maximum		0, mm	0, MPa
Maximum Value Over Time			
Minimum		1,5006e-002 mm	939,14 MPa
Maximum		1,5006e-002 mm	939,14 MPa

TABLE 24
Model (B4) > Static Structural (B5) > Solution (B6) > Probes

Object Name	*Force Reaction 3*
State	Solved
Definition	
Type	Force Reaction
Location Method	Boundary Condition
Boundary Condition	Fixed Support
Orientation	Global Coordinate System
Suppressed	No
Options	
Result Selection	All
Display Time	End Time
Results	
X Axis	-2,0621e-002 N
Y Axis	-8,79e+005 N
Z Axis	8,5744e-003 N
Total	8,79e+005 N
Maximum Value Over Time	
X Axis	-2,0621e-002 N

Y Axis	-8,79e+005 N
Z Axis	8,5744e-003 N
Total	8,79e+005 N
Minimum Value Over Time	
X Axis	-2,0621e-002 N
Y Axis	-8,79e+005 N
Z Axis	8,5744e-003 N
Total	8,79e+005 N
Information	
Time	1, s
Load Step	1
Substep	1
Iteration Number	7

FIGURE 4
Model (B4) > Static Structural (B5) > Solution (B6) > Force Reaction 3

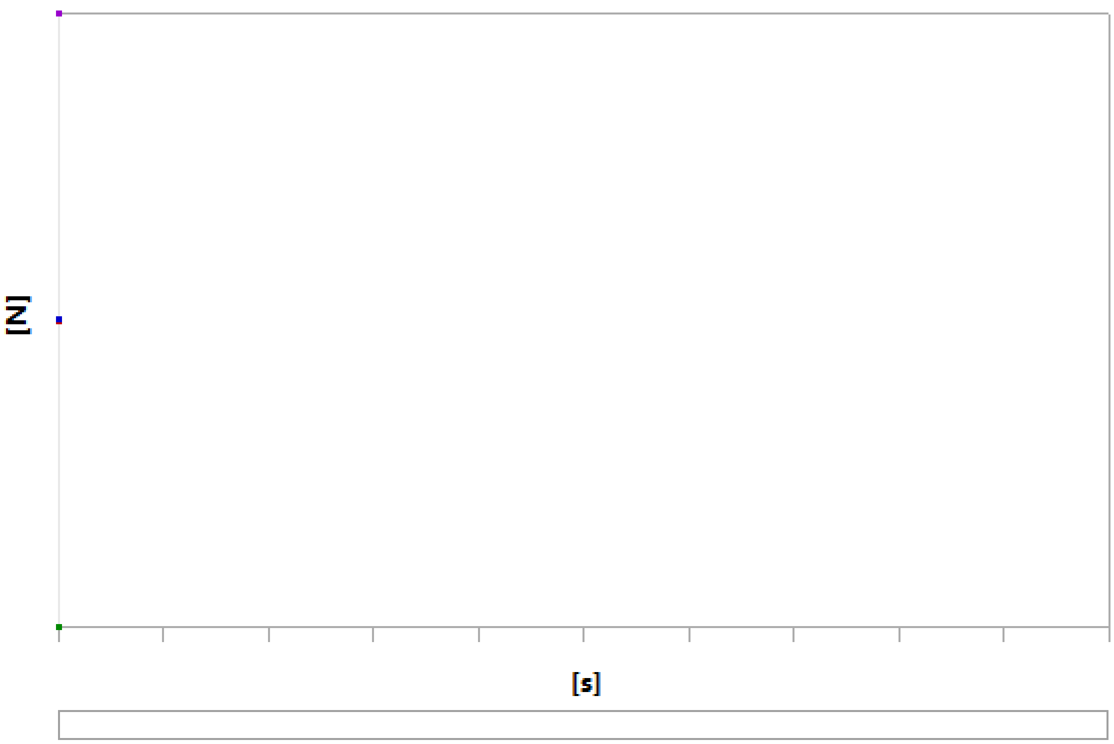

TABLE 25
Model (B4) > Static Structural (B5) > Solution (B6) > Force Reaction 3

Time [s]	Force Reaction 3 (X) [N]	Force Reaction 3 (Y) [N]	Force Reaction 3 (Z) [N]	Force Reaction 3 (Total) [N]
1,	-2,0621e-002	-8,79e+005	8,5744e-003	8,79e+005

Material Data

R4 Grade Llink

TABLE 26
R4 Grade Llink > Constants

Density	7,85e-006 kg mm^-3
Coefficient of Thermal Expansion	1,2e-005 C^-1

TABLE 27
R4 Grade Llink > Tensile Yield Strength

Tensile Yield Strength MPa
580,

TABLE 28
R4 Grade Llink > Compressive Yield Strength

Compressive Yield Strength MPa
580,

TABLE 29
R4 Grade Llink > Tensile Ultimate Strength

Tensile Ultimate Strength MPa
860,

TABLE 30
R4 Grade Llink > Compressive Ultimate Strength

Compressive Ultimate Strength MPa
860,

TABLE 31
R4 Grade Llink > Isotropic Elasticity

Temperature C	Young's Modulus MPa	Poisson's Ratio	Bulk Modulus MPa	Shear Modulus MPa
	2,017e+006	0,3	1,6808e+006	7,7577e+005

TABLE 32
R4 Grade Llink > Isotropic Secant Coefficient of Thermal Expansion

Reference Temperature C
20,

C3 MODEL 3

Project

First Saved	Friday, February 20, 2015
Last Saved	Friday, June 12, 2015
Product Version	15.0 Release
Save Project Before Solution	No
Save Project After Solution	No

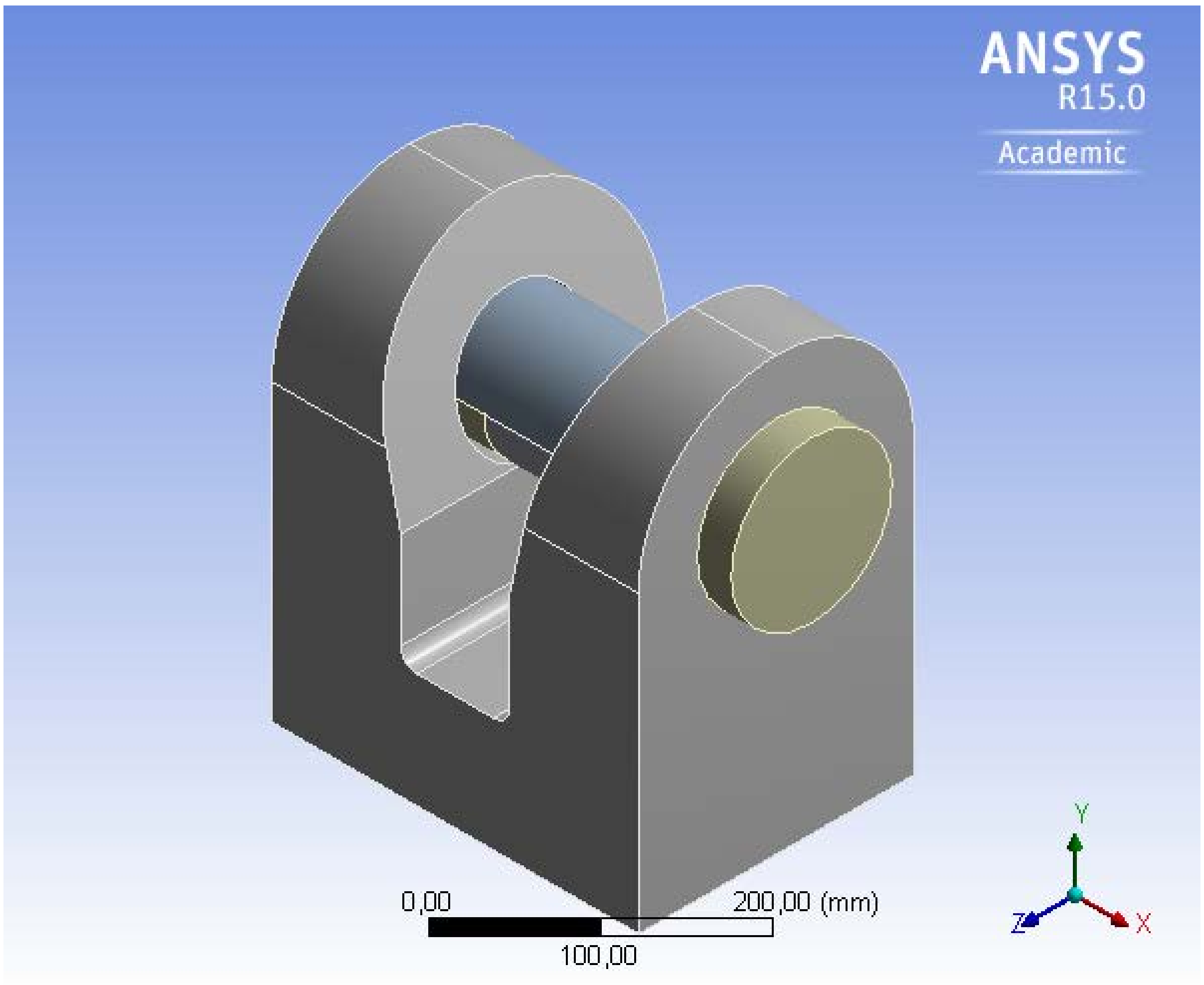

Contents

- **Units**
- **Model (B4)**
  - Geometry
    - Padeye
    - Pin

- Parts
- Coordinate Systems
- Connections
  - Contacts
    - Contact Regions
- Mesh
  - Mesh Controls
- **Static Structural (B5)**
  - Analysis Settings
  - Loads
  - Solution (B6)
    - Solution Information
    - Results
    - Contact Tool
      - Results
    - Force Reaction 3

- **Material Data**
  - R4 Grade Llink

Units

TABLE 1

Unit System	Metric (mm, kg, N, s, mV, mA) Degrees rad/s Celsius
Angle	Degrees
Rotational Velocity	rad/s
Temperature	Celsius

Model (B4)

Geometry

TABLE 2
Model (B4) > Geometry

Object Name	*Geometry*
State	Fully Defined
Definition	
Source	F:\Ansys\Workbench\Shackle\Model 4_files\dp0\Geom\DM\Geom.agdb
Type	DesignModeler
Length Unit	Millimeters
Element Control	Program Controlled
Display Style	Body Color
Bounding Box	
Length X	344, mm
Length Y	355, mm
Length Z	226, mm
Properties	
Volume	1,8039e+007 mm³
Mass	141,61 kg
Scale Factor Value	1,
Statistics	
Bodies	7
Active Bodies	7
Nodes	30016

Elements	17152
Mesh Metric	None
Basic Geometry Options	
Parameters	Yes
Parameter Key	DS
Attributes	No
Named Selections	No
Material Properties	No
Advanced Geometry Options	
Use Associativity	Yes
Coordinate Systems	No
Reader Mode Saves Updated File	No
Use Instances	Yes
Smart CAD Update	No
Compare Parts On Update	No
Attach File Via Temp File	Yes
Temporary Directory	C:\Users\213010\AppData\Roaming\Ansys\v150
Analysis Type	3-D
Decompose Disjoint Geometry	No
Enclosure and Symmetry Processing	Yes

TABLE 3
Model (B4) > Geometry > Parts

Object Name	*Padeye*
State	Meshed
Graphics Properties	
Visible	Yes
Transparency	1
Definition	
Suppressed	No
Stiffness Behavior	Flexible
Coordinate System	Default Coordinate System
Reference Temperature	By Environment
Material	
Assignment	R4 Grade Llink
Nonlinear Effects	No
Thermal Strain Effects	No
Bounding Box	
Length X	301, mm
Length Y	355, mm
Length Z	226, mm
Properties	
Volume	1,4905e+007 mm^3
Mass	117, kg
Centroid X	150,5 mm
Centroid Y	133,62 mm
Centroid Z	113, mm
Moment of Inertia Ip1	1,5673e+006 $kg \cdot mm^2$
Moment of Inertia Ip2	1,6425e+006 $kg \cdot mm^2$
Moment of Inertia Ip3	2,1685e+006 $kg \cdot mm^2$
Statistics	
Nodes	23123
Elements	13189
Mesh Metric	None

TABLE 4
Model (B4) > Geometry > Body Groups

Object Name	*Pin*
State	Meshed
Graphics Properties	
Visible	Yes
Definition	
Suppressed	No
Assignment	R4 Grade Llink
Coordinate System	Default Coordinate System
Bounding Box	
Length X	344, mm
Length Y	132, mm
Length Z	132, mm
Properties	
Volume	3,1344e+006 mm³
Mass	24,605 kg
Centroid X	161,76 mm
Centroid Y	244,18 mm
Centroid Z	113, mm
Moment of Inertia Ip1	36605 kg·mm²
Moment of Inertia Ip2	2,868e+005 kg·mm²
Moment of Inertia Ip3	2,8685e+005 kg·mm²
Statistics	
Nodes	6893
Elements	3963
Mesh Metric	None

TABLE 5
Model (B4) > Geometry > Pin > Parts

<table>
<tr><td>Object Name</td><td>Solid</td><td>Solid</td><td>Solid</td><td>Solid</td><td>Solid</td><td>Solid</td></tr>
<tr><td>State</td><td colspan="6">Meshed</td></tr>
<tr><td colspan="7">Graphics Properties</td></tr>
<tr><td>Visible</td><td colspan="6">Yes</td></tr>
<tr><td>Transparency</td><td colspan="6">1</td></tr>
<tr><td colspan="7">Definition</td></tr>
<tr><td>Suppressed</td><td colspan="6">No</td></tr>
<tr><td>Stiffness Behavior</td><td colspan="6">Flexible</td></tr>
<tr><td>Coordinate System</td><td colspan="6">Default Coordinate System</td></tr>
<tr><td>Reference Temperature</td><td colspan="6">By Environment</td></tr>
<tr><td colspan="7">Material</td></tr>
<tr><td>Assignment</td><td colspan="6">R4 Grade Llink</td></tr>
<tr><td>Nonlinear Effects</td><td colspan="4">No</td><td colspan="2">Yes</td></tr>
<tr><td>Thermal Strain Effects</td><td colspan="4">No</td><td colspan="2">Yes</td></tr>
<tr><td colspan="7">Bounding Box</td></tr>
<tr><td>Length X</td><td>303, mm</td><td>112,5 mm</td><td>76, mm</td><td>114,5 mm</td><td>13, mm</td><td>28, mm</td></tr>
<tr><td>Length Y</td><td>51, mm</td><td colspan="3">53, mm</td><td colspan="2">132, mm</td></tr>
<tr><td>Length Z</td><td>103,98 mm</td><td colspan="3">104, mm</td><td colspan="2">132, mm</td></tr>
<tr><td colspan="7">Properties</td></tr>
<tr><td>Volume</td><td>1,2549e+006 mm³</td><td>4,8954e+005 mm³</td><td>3,3071e+005 mm³</td><td>4,9824e+005 mm³</td><td>1,779e+005 mm³</td><td>3,8317e+005 mm³</td></tr>
<tr><td>Mass</td><td>9,8506 kg</td><td>3,8429 kg</td><td>2,5961 kg</td><td>3,9112 kg</td><td>1,3965 kg</td><td>3,0079 kg</td></tr>
<tr><td>Centroid X</td><td>150,48 mm</td><td>245,75 mm</td><td>151,5 mm</td><td>56,25 mm</td><td>-7,5 mm</td><td>316, mm</td></tr>
<tr><td>Centroid Y</td><td>266,56 mm</td><td colspan="3">222,52 mm</td><td colspan="2">245, mm</td></tr>
<tr><td>Centroid Z</td><td colspan="6">113, mm</td></tr>
<tr><td>Moment of Inertia Ip1</td><td>8316,3 kg·mm²</td><td>3341,8 kg·mm²</td><td>2257,6 kg·mm²</td><td>3401,2 kg·mm²</td><td>3010,9 kg·mm²</td><td>6485, kg·mm²</td></tr>
<tr><td>Moment of Inertia Ip2</td><td>81572 kg·mm²</td><td>6628,6 kg·mm²</td><td>2996,4 kg·mm²</td><td>6893,8 kg·mm²</td><td>1525, kg·mm²</td><td>3438, kg·mm²</td></tr>
</table>

Moment of Inertia Ip3	76804 kg·mm²	4781,8 kg·mm²	1748,8 kg·mm²	5014,1 kg·mm²	1525, kg·mm²	3438, kg·mm²
Statistics						
Nodes	2957	1090	855	1091	735	1024
Elements	1592	559	433	557	321	501
Mesh Metric	None					

Coordinate Systems

TABLE 6
Model (B4) > Coordinate Systems > Coordinate System

Object Name	*Global Coordinate System*
State	Fully Defined
Definition	
Type	Cartesian
Coordinate System ID	0,
Origin	
Origin X	0, mm
Origin Y	0, mm
Origin Z	0, mm
Directional Vectors	
X Axis Data	[1, 0, 0,]
Y Axis Data	[0, 1, 0,]
Z Axis Data	[0, 0, 1,]

Connections

TABLE 7
Model (B4) > Connections

Object Name	*Connections*
State	Fully Defined
Auto Detection	
Generate Automatic Connection On Refresh	Yes
Transparency	
Enabled	Yes

TABLE 8
Model (B4) > Connections > Contacts

Object Name	*Contacts*
State	Fully Defined
Definition	
Connection Type	Contact
Scope	
Scoping Method	Geometry Selection
Geometry	All Bodies
Auto Detection	
Tolerance Type	Slider
Tolerance Slider	0,
Tolerance Value	1,3589 mm
Use Range	No
Face/Face	Yes
Face/Edge	No
Edge/Edge	No
Priority	Include All
Group By	Bodies
Search Across	Bodies

TABLE 9
Model (B4) > Connections > Contacts > Contact Regions

Object Name	*Frictional - Padeye To Solid*	*Frictional - Padeye To Solid*	*Frictional - Padeye To Solid*
State	Fully Defined		
Scope			
Scoping Method	Geometry Selection		
Contact	1 Face		2 Faces
Target	1 Face		
Contact Bodies	Padeye		
Target Bodies	Solid		
Definition			
Type	Frictional		
Friction Coefficient	0,2		
Scope Mode	Automatic		
Behavior	Program Controlled		
Trim Contact	Program Controlled		
Trim Tolerance	1,3589 mm		
Suppressed	No		
Advanced			
Formulation	Augmented Lagrange		
Detection Method	Program Controlled		
Penetration Tolerance	Program Controlled		
Elastic Slip Tolerance	Program Controlled		
Normal Stiffness	Program Controlled		
Update Stiffness	Each Iteration		
Stabilization Damping Factor	0,2		
Pinball Region	Program Controlled		
Time Step Controls	Automatic Bisection		
Geometric Modification			
Interface Treatment	Adjust to Touch		Add Offset, No Ramping
Contact Geometry Correction	None		
Offset			0, mm

Mesh

TABLE 10
Model (B4) > Mesh

Object Name	*Mesh*
State	Solved
Defaults	
Physics Preference	Mechanical
Relevance	0
Sizing	
Use Advanced Size Function	Off
Relevance Center	Medium
Element Size	Default
Initial Size Seed	Active Assembly
Smoothing	Medium
Transition	Fast
Span Angle Center	Coarse
Minimum Edge Length	5,44390 mm
Inflation	
Use Automatic Inflation	None
Inflation Option	Smooth Transition
Transition Ratio	0,272
Maximum Layers	5

Growth Rate	1,2
Inflation Algorithm	Pre
View Advanced Options	No
Patch Conforming Options	
Triangle Surface Mesher	Program Controlled
Patch Independent Options	
Topology Checking	Yes
Advanced	
Number of CPUs for Parallel Part Meshing	Program Controlled
Shape Checking	Standard Mechanical
Element Midside Nodes	Program Controlled
Straight Sided Elements	No
Number of Retries	Default (4)
Extra Retries For Assembly	Yes
Rigid Body Behavior	Dimensionally Reduced
Mesh Morphing	Disabled
Defeaturing	
Pinch Tolerance	Please Define
Generate Pinch on Refresh	No
Automatic Mesh Based Defeaturing	On
Defeaturing Tolerance	Default
Statistics	
Nodes	30016
Elements	17152
Mesh Metric	None

TABLE 11
Model (B4) > Mesh > Mesh Controls

Object Name	*Face Sizing*	*Patch Conforming Method*	*Face Sizing 2*	*Face Sizing 3*
State	Fully Defined			
Scope				
Scoping Method	Geometry Selection			
Geometry	2 Faces	6 Bodies	2 Faces	4 Faces
Definition				
Suppressed	No			
Type	Element Size		Element Size	
Element Size	10, mm		10, mm	15, mm
Behavior	Hard		Soft	
Method		Tetrahedrons		
Algorithm		Patch Conforming		
Element Midside Nodes		Use Global Setting		

Static Structural (B5)

TABLE 12
Model (B4) > Analysis

Object Name	*Static Structural (B5)*
State	Solved
Definition	
Physics Type	Structural
Analysis Type	Static Structural
Solver Target	Mechanical APDL
Options	
Environment Temperature	22, °C
Generate Input Only	No

TABLE 13

Model (B4) > Static Structural (B5) > Analysis Settings

Object Name	*Analysis Settings*
State	Fully Defined
Step Controls	
Number Of Steps	1,
Current Step Number	1,
Step End Time	1, s
Auto Time Stepping	Program Controlled
Solver Controls	
Solver Type	Program Controlled
Weak Springs	Program Controlled
Large Deflection	Off
Inertia Relief	Off
Restart Controls	
Generate Restart Points	Program Controlled
Retain Files After Full Solve	No
Nonlinear Controls	
Newton-Raphson Option	Program Controlled
Force Convergence	Program Controlled
Moment Convergence	Program Controlled
Displacement Convergence	Program Controlled
Rotation Convergence	Program Controlled
Line Search	Program Controlled
Stabilization	Reduce
--Method	Damping
--Damping Factor	0,2
--Activation For First Substep	Yes
--Stabilization Force Limit	0,2
Output Controls	
Stress	Yes
Strain	Yes
Nodal Forces	No
Contact Miscellaneous	No
General Miscellaneous	No
Store Results At	All Time Points
Analysis Data Management	
Solver Files Directory	F:\Ansys\Workbench\Shackle\Model 4_files\dp0\SYS-1\MECH\
Future Analysis	None
Scratch Solver Files Directory	
Save MAPDL db	No
Delete Unneeded Files	Yes
Nonlinear Solution	Yes
Solver Units	Active System
Solver Unit System	nmm

TABLE 14
Model (B4) > Static Structural (B5) > Loads

Object Name	*Fixed Support*	*Bearing Load*
State	Fully Defined	
Scope		
Scoping Method	Geometry Selection	
Geometry	1 Face	
Definition		
Type	Fixed Support	Bearing Load
Suppressed	No	
Define By		Components
Coordinate System		Global Coordinate System

X Component		0, N
Y Component		8,79e+005 N
Z Component		0, N

FIGURE 1
Model (B4) > Static Structural (B5) > Bearing Load

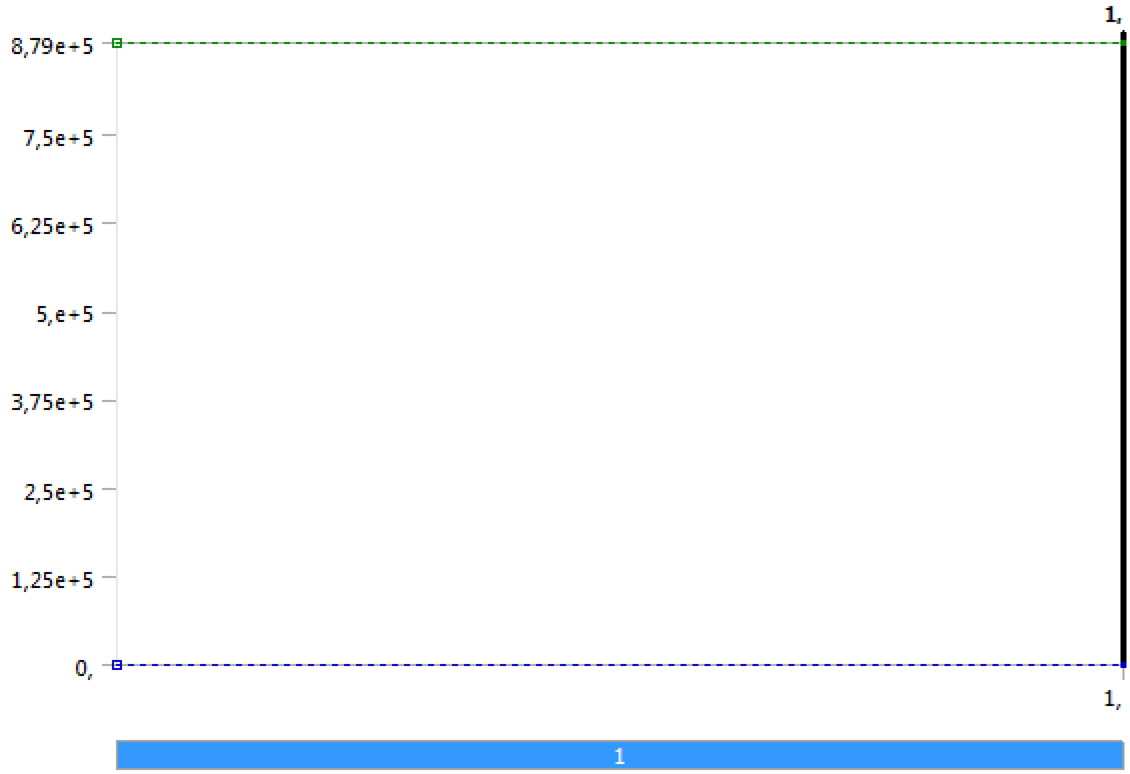

Solution (B6)

TABLE 15
Model (B4) > Static Structural (B5) > Solution

Object Name	*Solution (B6)*
State	Solved
Adaptive Mesh Refinement	
Max Refinement Loops	1,
Refinement Depth	2,
Information	
Status	Done

TABLE 16
Model (B4) > Static Structural (B5) > Solution (B6) > Solution Information

Object Name	*Solution Information*
State	Solved
Solution Information	
Solution Output	Force Convergence
Newton-Raphson Residuals	0
Update Interval	2,5 s
Display Points	All
FE Connection Visibility	
Activate Visibility	Yes
Display	All FE Connectors
Draw Connections Attached To	All Nodes
Line Color	Connection Type

Visible on Results	No
Line Thickness	Single
Display Type	Lines

FIGURE 2
Model (B4) > Static Structural (B5) > Solution (B6) > Solution Information

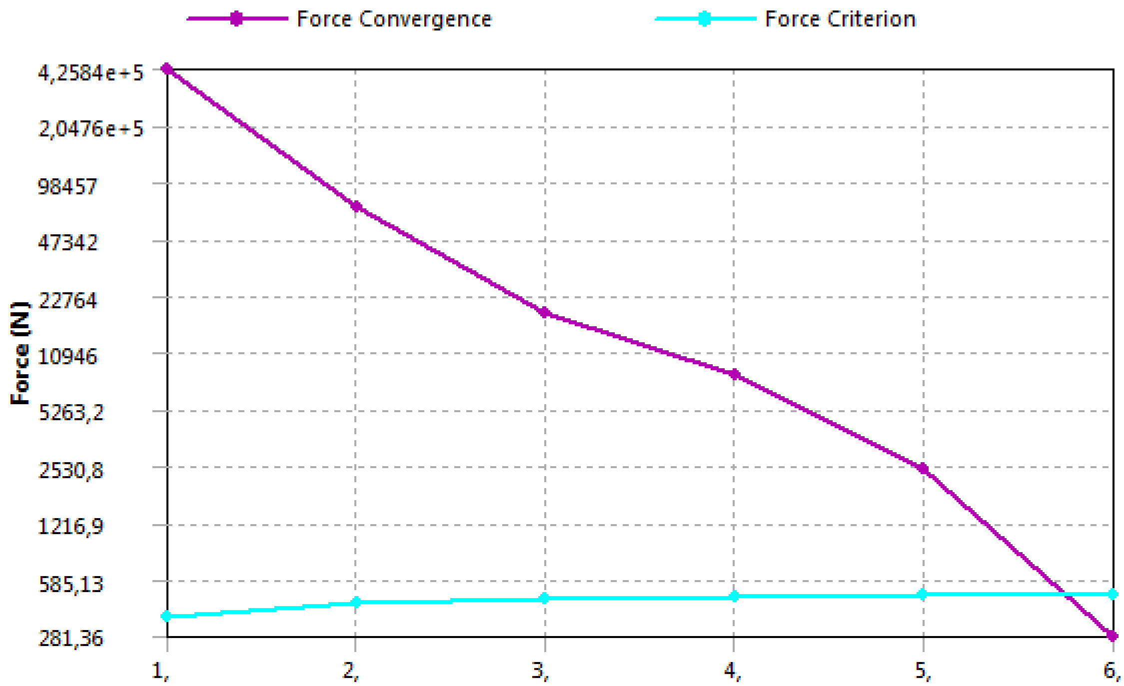

FIGURE 3
Model (B4) > Static Structural (B5) > Solution (B6) > Solution Information

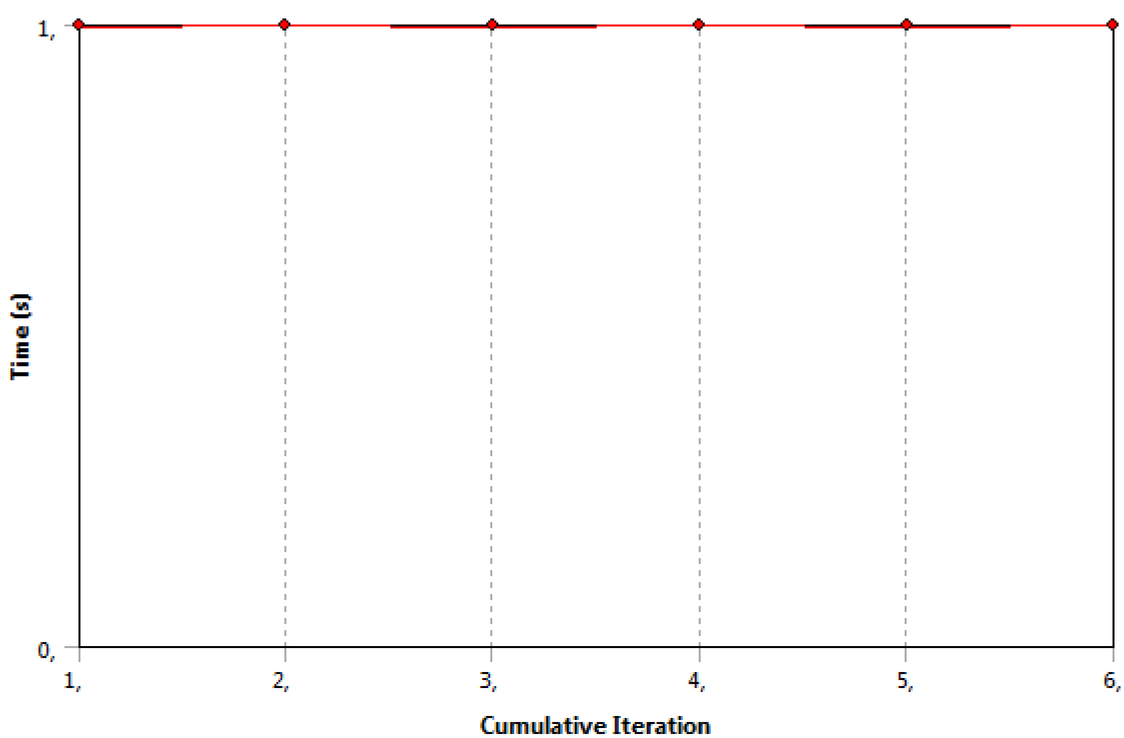

TABLE 17
Model (B4) > Static Structural (B5) > Solution (B6) > Results

Object Name	*Total Deformation*	*Directional Deformation*	*Normal Stress*	*Shear Stress*	*Equivalent Stress 3*	*Equivalent Stress*	*Maximum Principal Stress 3*	*Maximum Principal Stress*	*Maximum Principal Stress 4*	*Shear Stress 2*
State	Solved									
Scope										
Scoping Method	Geometry Selection									
Geometry	All Bodies				5 Bodies	1 Body		6 Bodies	All Bodies	4 Bodies
Definition										
Type	Total Deformation	Directional Deformation	Normal Stress	Shear Stress	Equivalent (von-Mises) Stress		Maximum Principal Stress			Shear Stress
By	Time									
Display Time	Last						8,8926e-002 s	0,60561 s	Last	
Calculate Time History	Yes									
Identifier										
Suppressed	No									
Orientation		X Axis		XY Plane						XY Plane
Coordinate System		Global Coordinate System		Solution Coordinate System						Global Coordinate System
Results										
Minimum	0, mm	-1,0071e-002 mm	-430,28 MPa	-238,79 MPa	0,81007 MPa	0,44405 MPa	-357,28 MPa	-371,97 MPa		-238,79 MPa
Maximum	4,1842e-002 mm	1,1283e-002 mm	295,58 MPa	102,01 MPa	872,62 MPa	769,98 MPa	258,69 MPa	332,45 MPa		102,01 MPa
Minimum Occurs On	Padeye	Solid						Solid		
Maximum Occurs On	Solid							Solid		
Minimum Value Over Time										
Minimum	0, mm	-1,0071e-002 mm	-430,28 MPa	-238,79 MPa	0,81007 MPa	0,44405 MPa	-357,28 MPa	-371,97 MPa		-238,79 MPa
Maximum	0, mm	-1,0071e-002 mm	-430,28 MPa	-238,79 MPa	0,81007 MPa	0,44405 MPa	-357,28 MPa	-371,97 MPa		-238,79 MPa
Maximum Value Over Time										
Minimum	4,1842e-002 mm	1,1283e-002 mm	295,58 MPa	102,01 MPa	872,62 MPa	769,98 MPa	258,69 MPa	332,45 MPa		102,01 MPa
Maximum	4,1842e-002 mm	1,1283e-002 mm	295,58 MPa	102,01 MPa	872,62 MPa	769,98 MPa	258,69 MPa	332,45 MPa		102,01 MPa
Information										
Time	1, s									
Load Step	1									
Substep	1									
Iteration Number	6									
Integration Point Results										
Display Option			Averaged							
Average Across			No							

Bodies		

TABLE 18
Model (B4) > Static Structural (B5) > Solution (B6) > Contact Tools

Object Name	*Contact Tool*
State	Solved
Scope	
Scoping Method	Geometry Selection
Geometry	2 Faces

Model (B4) > Static Structural (B5) > Solution (B6) > Contact Tool

Name	Contact Side

TABLE 19
Model (B4) > Static Structural (B5) > Solution (B6) > Contact Tool > Results

Object Name	*Status*	*Sliding Distance*	*Pressure*
State	Solved		
Definition			
Type	Status	Sliding Distance	Pressure
By	Time		
Display Time	Last		
Calculate Time History	Yes		
Identifier			
Suppressed	No		
Integration Point Results			
Display Option	Averaged		
Information			
Time	1, s		
Load Step	1		
Substep	1		
Iteration Number	6		
Results			
Minimum		0, mm	0, MPa
Maximum		1,4119e-002 mm	1029,9 MPa
Minimum Value Over Time			
Minimum		0, mm	0, MPa
Maximum		0, mm	0, MPa
Maximum Value Over Time			
Minimum		1,4119e-002 mm	1029,9 MPa
Maximum		1,4119e-002 mm	1029,9 MPa

TABLE 20
Model (B4) > Static Structural (B5) > Solution (B6) > Probes

Object Name	*Force Reaction 3*
State	Solved
Definition	
Type	Force Reaction
Location Method	Boundary Condition
Boundary Condition	Fixed Support
Orientation	Global Coordinate System
Suppressed	No
Options	
Result Selection	All
Display Time	End Time
Results	
X Axis	-2,0273e-002 N
Y Axis	-8,79e+005 N
Z Axis	8,0295e-003 N

Total	8,79e+005 N
Maximum Value Over Time	
X Axis	-2,0273e-002 N
Y Axis	-8,79e+005 N
Z Axis	8,0295e-003 N
Total	8,79e+005 N
Minimum Value Over Time	
X Axis	-2,0273e-002 N
Y Axis	-8,79e+005 N
Z Axis	8,0295e-003 N
Total	8,79e+005 N
Information	
Time	1, s
Load Step	1
Substep	1
Iteration Number	6

FIGURE 4
Model (B4) > Static Structural (B5) > Solution (B6) > Force Reaction 3

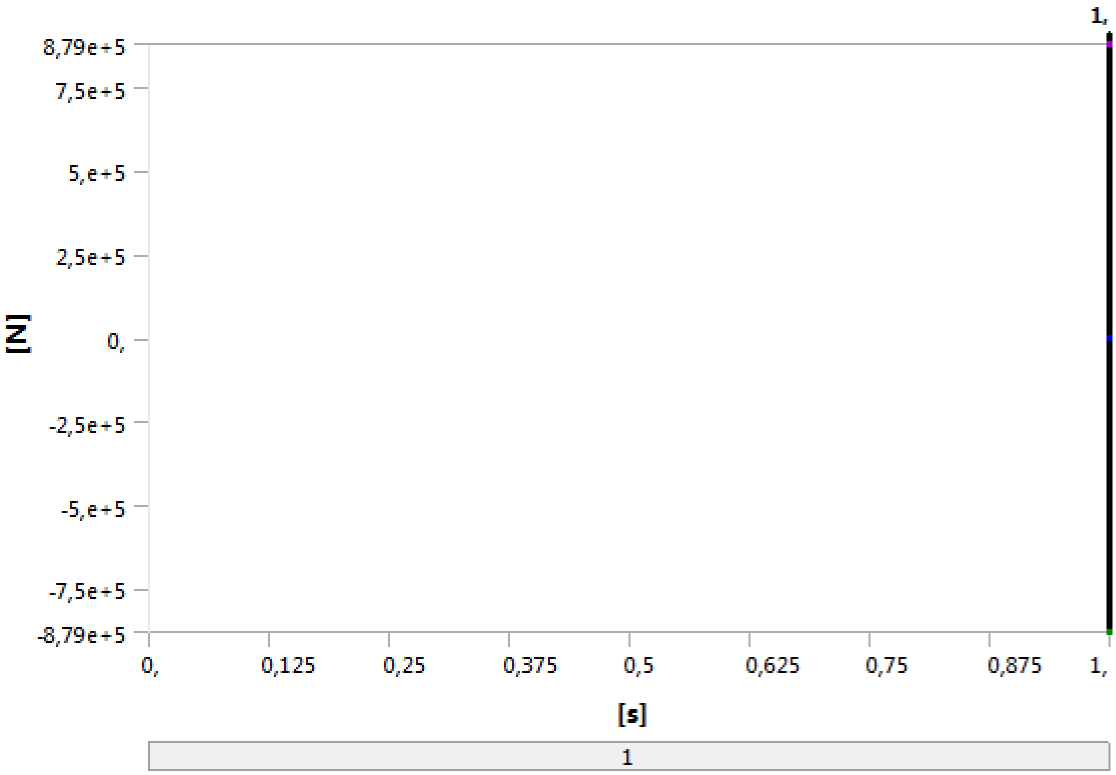

TABLE 21
Model (B4) > Static Structural (B5) > Solution (B6) > Force Reaction 3

Time [s]	Force Reaction 3 (X) [N]	Force Reaction 3 (Y) [N]	Force Reaction 3 (Z) [N]	Force Reaction 3 (Total) [N]
1,	-2,0273e-002	-8,79e+005	8,0295e-003	8,79e+005

Material Data

R4 Grade Llink

TABLE 22
R4 Grade Llink > Constants

Density	7,85e-006 kg mm^-3

Coefficient of Thermal Expansion	1,2e-005 C^-1

TABLE 23
R4 Grade Llink > Tensile Yield Strength

Tensile Yield Strength MPa
580,

TABLE 24
R4 Grade Llink > Compressive Yield Strength

Compressive Yield Strength MPa
580,

TABLE 25
R4 Grade Llink > Tensile Ultimate Strength

Tensile Ultimate Strength MPa
860,

TABLE 26
R4 Grade Llink > Compressive Ultimate Strength

Compressive Ultimate Strength MPa
860,

TABLE 27
R4 Grade Llink > Isotropic Elasticity

Temperature C	Young's Modulus MPa	Poisson's Ratio	Bulk Modulus MPa	Shear Modulus MPa
	2,017e+006	0,3	1,6808e+006	7,7577e+005

TABLE 28
R4 Grade Llink > Isotropic Secant Coefficient of Thermal Expansion

Reference Temperature C
20,